

Improved Gram-Scale Procedure for MIBA-Catalyzed Direct Amidation and Its
Application to the Preparation of alpha and beta Peptides
by

Solmaz Fatemi

A thesis submitted in partial fulfillment of the requirements for the degree of

Master of Science

Department of Chemistry
University of Alberta

© Solmaz Fatemi, 2015

Abstract

Direct condensation between a carboxylic acid and amine must overcome the initial formation of a thermodynamically stable and unreactive carboxylate-ammonium salt, providing the amide product only at very high temperatures (over 160 °C) that are incompatible with many functionalized molecules. Currently, the most popular industrial methods of amide synthesis rely on activation of a carboxylic acid (using a coupling reagent such as a carbodiimide) and subsequent coupling of the activated species with an amine. These methodologies suffer from inherent drawbacks such as low yields, racemization, degradation and difficult purification, thus making them expensive and wasteful. To address these challenges, numerous mild coupling reagents and methods have been developed that not only are high yielding, but that potentially help to prevent racemization of neighbouring stereogenic centres.

The development of a mild and general direct amidation reaction is of great interest in organic synthesis and process chemistry. In the past decade, the use of boronic acids has emerged as a very useful and versatile tool for direct amidation at low temperatures. Driven by this goal, Hall and coworkers discovered the exceptional ability of *ortho*-iodophenylboronic acid as a recoverable catalyst for direct amidations under mild and waste-free conditions at room temperature. A drawback of the initial optimal procedure is

that the reactant concentrations must be low and a fairly large amount of molecular sieves is required to drive the reaction, which limits large-scale applications.

The objectives of this research are firstly, to optimize the direct amidation reaction conditions to develop a scalable and “greener” process, secondly, to explore superior catalysts in order to expand the reaction scope, thirdly, to investigate proper additives to improve the efficiency of this direct amidation reaction. Chapter Two describes the details of optimization of this methodology and the applications in multigram syntheses of amides and dipeptides. As a result, the E factor in the newly optimized conditions is almost 10 times higher.

Currently, there are no general catalytic methods to access dipeptides directly from amino acids in a simple, green, and atom-economical fashion at low temperature. The subsequent application of our methodology in dipeptide syntheses was also investigated and discussed in Chapter Three. The optimization of the catalytic direct dipeptide synthesis and the substrate scope is discussed in detail. Both catalysts and substrates were optimized to perform direct peptide synthesis catalytically using doubly protected amino acids (α -phthalimido amino acids or α -azido carboxylic acids) as *C*-terminal amino acids with *C*-protected α -amino esters as *N*-terminal amino acids.

DEDICATION

To Felora, my mother. Her support, encouragement, quiet patience and endless love were undeniably the bedrock upon which this dream was built. Her tolerance during my bad moments and long nights is the biggest testimony of her unyielding devotion and love for me.

To Jalal, my father. He always taught me to never give up and showed me that smiling is possible despite of the biggest suffering.

To Saman, my brother. Because during my whole life he always has taught me the power of faith and love.

To my lovely friends. They are my greatest pride and reason to live. Their smiles, little details, pampering and even their noises brighten each of my days.

ACKNOWLEDGMENTS

I would like to express my immense gratitude to Professor Dennis Hall for all his support during this fantastic journey through science, his guidance, understanding, patience, support and also for having given me the opportunity to be here.

Special thanks to Professor Jeffrey Stryker, I definitely do not have the exact words to quantify how much I am grateful to him. He is always available to help me out at any time I am in need of his expert opinion. I also see him as a father.

I would like to thank all of the Hall Group members, past and present, for their support. I am particularly thankful to Carolynne L. Ricardo, Taras Rybak, Burcin Akgun and other nice labmates for their friendship and help on a personal level.

Table of Contents

Chapter 1: Introduction: Direct Amide Bond Formation and Peptide Synthesis

1.1 Introduction	1
1.2 Methods and Strategies for Amide Bond Formation	2
1.2.1 Non-Boron Reagents for Direct Amide Bond Formation	3
1.2.1.1 Stoichiometric Activation of Carboxylic Acids	3
1.2.1.2 Recent Developments	5
1.2.1.3 Catalyzed and Uncatalyzed Direct Amidation Reaction	10
1.2.1.3.1 Thermal Uncatalyzed	10
1.2.1.4 Microwave Irradiation	12
1.2.1.5 Metal Catalysis	13
1.2.1.5.1 Homogeneous Metal Protocols	14
1.2.1.5.2 Heterogeneous Metal Protocols	15
1.2.2 Boron Reagents For Direct Amide Bond Formation	15
1.2.2.1 Stoichiometric Activation of Carboxylic Acids	16
1.2.2.1.1 Trisdialkylaminoborane $[B(NR_3)_3]$	16
1.2.2.1.2 Tridialkylboranes $[BR_3]$, Trialkoxyboranes $[B(OR)_3]$ & Chlorodialkoxyboranes $[ClB(OR')_2]$	17
1.2.2.1.3 Borane and Catecholborane	20
1.2.2.2 Catalytic Activation of Carboxylic Acids	21
1.2.2.2.1 Boric Acid	21
1.2.2.2.2 Electron-Poor Arylboronic Acids	22
1.2.2.2.3 Aminoarylboronic Acids	28
1.3 Conclusion	34
1.4 Project Objectives	35
1.5 References	36

Chapter 2: Search for An Improved Catalytic System for the Direct Amide-Bond Formation and Scale-up Studies

2.1 Introduction	41
2.2 Results	42
2.2.1 Design of Third Generation Catalysts for Direct Amide Bond Formation	42
2.2.1.1 Synthesis of 4-Iodo-3-Furanboronic Acid (2-3)	44
2.2.1.2 Synthesis of 3-Bromo-2-Thienylboronic Acid (2-5)	44
2.2.1.3 Attempts to Synthesize other Designated Boronic Acids	45
2.2.1.3.1 Attempted Synthesis of 2-4	46
2.2.1.3.2 Attempted Synthesis of <i>Ortho</i> -Iodo-Phenanthreneboronic Acids (2-12)	46
2.2.1.3.2.1 Diiodo Approach	46
2.2.1.3.2.2 Directed <i>Ortho</i> -Iodination of Boronic Acids or Esters	49
2.2.1.4 Screening of the Heteroareneboronic Acids	51
2.2.2 Effect of Additives	54
2.2.2.1 Lewis Acids	55
2.2.2.2 Protic Acid Additives	56
2.2.2.3 Nucleophilic Additive	57
2.2.3 Plans To Replace Molecular Sieves As a Drying Agent:	
Implication of Staudinger Reaction	58
2.2.3.1 Introduction	59
2.2.3.2 Results	64
2.3 Scalability Study of the Direct Amidation of Carboxylic Acids Catalyzed by Arylboronic Acid	67
2.3.1 Optimization of Reaction Parameters	68
2.3.2 Optimization of Reaction Solvent and Temperature	71
2.3.3 Multigram-Scale Results	72
2.4 Conclusion	73

2.5 Experimental	74
2.5.1 General Information	74
2.5.1.1 Preparation and Characterization Data of 4-Iodofuran-3-yl-3-Boronic Acid (2-3)	75
2.5.1.2 Preparation and Characterization Data of 3,4-Diiodofuran (Scheme 2-6, step 2)	75
2.5.1.3 Preparation and Characterization Data of (E)-2,3-Diiodobut- 2-ene-1,4-Diol (Scheme 2-6, step 1)	76
2.5.1.4 Preparation and Characterization Data of 2,3-Diiodo-4- methoxy-4,5,6,7-tetrahydrobenzofuran (2-11)	76
2.5.1.5 Preparation and Analytical Data of 3-Bromo-2- Thienylboronic Acid (2-5)	76
2.5.1.6 Preparation and Analytical Data of Phenanthreneboronic Acid (2-16)	77
2.5.1.7 Preparation and Analytical Data of Phenanthreneboronic Ester (2-17)	77
2.5.2 General Procedure for Organocatalytic Direct Amidation	78
2.5.2.1 Preparation and Characterization Data of N-Benzyl-2- Phenyl-Acetamide (2-31)	78
2.5.2.2 Preparation and Characterization Data of Phenyl-1- Pyrrolidin-1-yl- Ethanone (2-32)	79
2.5.2.3 Preparation and Characterization Data of 2-33	79
2.6 References	79

Chapter 3: Application of Catalytic System for the Direct Amide-Bond Formation in Dipeptide Synthesis

3.1 Introduction	84
3.1.1 Properties of Amino Acids	85
3.2 Results	91
3.2.1 Initial Screening of <i>Ortho</i> -Functionalized Arylboronic Acids	91
3.2.2 Direct Amide Formation of Amino Acid Derivatives	93
3.2.2.1 The Effect of Drying Agents on Catalyst Reactivity	93
3.2.2.2 Evaluation of Whiting's Catalyst Versus <i>Ortho</i> -Iodoarylboronic Acid Catalysts in Direct Amide Formation of Amino Acid Derivatives	95
3.3 Optimization of Reaction Parameters	97
3.3.1 Optimization of Reaction Solvent	97
3.3.2 Optimization of Reaction Concentration and Time	99
3.3.3 Optimization of Amine Stoichiometry	99
3.4 Design of New Substrates to Optimize the Catalytic Direct Dipeptide Synthesis	100
3.5 Substrate Scope for Catalytic Direct Amide Bond Formation Between Amino Acids Derivatives	102
3.5.1 Peptide Synthesis from Protected α -Amino acid	102
3.5.2 Peptide Synthesis Using α -Azido Carboxylic Acids	105
3.5.2.1 Optimization of the Reaction Solvent	105
3.5.3 Dipeptide Synthesis Using <i>N</i> -Boc Protected β -Amino acids	109
3.6 Investigation of Possible Racemization in Catalytic Direct Dipeptide Synthesis	110
3.7 Conclusion	112
3.8 Experimental	113
3.8.1 General Information	113
3.8.2 Preparation and Characterization Data for <i>Ortho</i> -Iodophenylboronic Acid (1- 30)	114

3.8.3	Preparation and Characterization Data of 5-Methoxy-2-Iodophenylboronic Acid (1-31)	114
3.8.4	General Procedure for Table 3-2: Comparison in product yields for different dehydrating agents and catalysts 1-30 , 1-31 , 3-2 and solvents in a direct amidation reaction between (Boc)-proline and benzylamine	116
3.8.5	General Procedure for Preparation of <i>N</i> -Protected Amino Acids	116
3.8.5.1	General Procedure for Preparation of L-N-Phthaloyl Amino Acids	116
3.8.5.2	General Procedure of Azide Derivatives of L-Amino Acid	117
3.8.6	General Procedure for Dipeptide Synthesis by Direct Amidation	118
3.8.6.1	Preparation and Characterization Data of 3-14	118
3.8.6.2	Preparation and Characterization Data of 3-15	119
3.8.6.3	Preparation and Characterization Data of 3-16	119
3.8.6.4	Preparation and Characterization Data of 3-17	119
3.8.6.5	Preparation and Characterization Data of 3-18	120
3.8.6.6	Preparation and Characterization Data of 3-19	120
3.8.6.7	Preparation and Characterization Data of 3-20	121
3.8.6.8	Preparation and Characterization Data of 3-21	121
3.8.6.9	Preparation and Characterization Data of 3-24	122
3.8.6.10	Preparation and Characterization Data of 3-25	122
3.8.6.11	Preparation and Characterization Data of 3-26	122
3.8.6.12	Preparation and Characterization Data of 3-27	123
3.8.6.13	Preparation and Characterization Data of 3-28	123
3.8.6.14	Preparation and Characterization Data of 3-29	123
3.8.6.15	Preparation and Characterization Data of 3-30	124
3.8.6.16	Preparation and Characterization Data of 3-31	124
3.8.6.17	Preparation and Characterization Data of 3-32	125
3.8.7	General Procedure for Preparation of epimerization scope studies in direct	

peptide synthesis methodology (Scheme 3-10)	125
3.9 References	126
 Chapter 4: Conclusions and Future Directions	
Conclusions and Future Directions	129
Bibliography of All Sources	132
Appendix 1: Copies of Selected NMR Spectra	133
Appendix 2: Chromatograms for Enantiomeric Excess Measurement	150

List of Tables

Table 2-1: Effect of Lewis acids as additives on catalytic direct amide bond formation	56
Table 2-2: Effect of protic acids as additives on direct amide bond formation	57
Table 2-3: Effect of nucleophilic additives on catalytic direct amide bond formation	58
Table 2-4: Optimization of reactant concentration and amount of molecular sieves in the amidation reaction	70
Table 2-5: Optimization of amidation reaction solvent	71
Table 2-6: Scale up result for the direct amidation reaction using 5 g of carboxylic acid	72
Table 3-1: Direct dipeptide synthesis using boronic acids 3-2 or mixed catalyst system 3-2 and 3-3 (1:1)	90
Table 3-2: Comparison in product yields for different dehydrating agents and catalysts 1-30 and 1-31 in a direct amidation reaction between double <i>N</i> -protected amino acids and benzylamine	94
Table 3-3: Comparison in product yields for different dehydrating agents and catalysts 1-30 , 1-31 , 3-2 and solvents in a direct amidation reaction between (Boc)-proline and benzylamine	96
Table 3-4: Optimization of solvent for amidation of doubly protected α -amino acids	98
Table 3-5: Optimization of solvent for amidation of a monoprotected β -amino acid	98
Table 3-6: Optimization of reactant concentration with catalyst 1-31	99
Table 3-7: Solvent optimization in dipeptide synthesis	106

List of Figures

Figure 1-1: Structures of pharmaceutical drugs containing amide bonds	2
Figure 1-2: Common coupling reagents and an example mechanism with HBTU	5
Figure 1-3: A hypervalent iodine (III) reagent, iodosodilactone (2)	7
Figure 1-4: Electrophilic assistance to nucleophilic attack	13
Figure 1-5: 3,4,5-Trifluorophenylboronic (1-12) and 3,5-bis(trifluoromethyl)phenylboronic acid (1-13)	23
Figure 1-6: 3,5-Bis(perfluorodecyl)phenylboronic acid (1-15) and 4-(perfluorodecyl)phenylboronic acid (1-16)	25
Figure 1-7: Structure of <i>N</i> -alkyl-4-boronopyridinium iodide (1-17) and <i>N</i> -polystyrene resin-bound 4-boronopyridinium salts (1-18a-d)	26
Figure 1-8: 4,5,6,7-Tetrachlorobenzo[<i>d</i>][1,2,3]dioxaborole	27
Figure 1-9: Structure of known boron catalysts in the literature	28
Figure 1-10: Tetraacyldiborate (1-23) intermediate	29
Figure 1-11: Proposed transition state for the enantioselectivity in amidation using catalyst	32
Figure 1-12: New generation of boronic acid catalyst for direct amidation at room temperature	33
Figure 2-1: Evolution of catalysts in the direct ambient amidation	42
Figure 2-2: Proposed <i>ortho</i> -functionalized heterocyclic boronic acids	43
Figure 2-3: Electrophilic iodinating reagents	48
Figure 2-4: Other proposed thiophene boronic acids	54
Figure 3-1: Neutral and zwitterion structures of amino acids	85
Figure 3-2: The effect of pH on the equilibrium of amino acids	86
Figure 3-3: Resonance structures in amides	86

Figure 3-4: Direct amidations between fully *N*-phthaloyl α -amino acids and *C*-protected α -amino esters catalyzed by boronic acids **1-31** at 50 °C 104

Figure 3-5: Direct amidations between protected α -azido carboxylic acids and *C*-protected α -amino acids catalyzed by boronic acid **1-31** at 50 °C 108

Figure 3-6: Direct amidations between *N*-protected β -amino acids and *C*-protected β -amino acids (as free amines) catalyzed by boronic acids **1-31** at 50 °C 109

List of Schemes

Scheme 1-1: Amidation with BBDI without bases	6
Scheme 1-2: A plausible mechanism for the amidation reaction	6
Scheme 1-3: Proposed AlMe ₃ -mediated amidation mechanism	7
Scheme 1-4: Proposed amidation mechanism with hypervalent iodine (III) reagent 1-2	8
Scheme 1-5: Reaction scheme and mechanism using XtalFluor-E as an activator	9
Scheme 1-6: Preparation of amides by direct condensation	10
Scheme 1-7: The proposed mechanism for direct amide formation supported by DFT calculations	11
Scheme 1-8: Examples of solvent-free amidation under microwave heating	12
Scheme 1-9: Examples of ZrCl ₄ -catalyzed amidation reactions	14
Scheme 1-10: Proposed carboxylic activation modes using a Zr catalyst	15
Scheme 1-11: Proposed mechanism for direct amide bond formation from mixing carboxylic acids with trisdialkylaminoboranes	16
Scheme 1-12: Formation of acyloxydialkylborane 1-5 and the corresponding amide product	17
Scheme 1-13: (a) Liberation of alcohol from acyloxyborate 1-5 ; (b) Formation of an unreactive carboxylate ammonium salt	18
Scheme 1-14: Formation of an aminodialkylborate species	19
Scheme 1-15: Borate-mediated direct amidation	19
Scheme 1-16: Borate promoted amidation	19
Scheme 1-17: Ganem's amide bond formation using catecholborane	20
Scheme 1-18: Wang's solid-supported catecholborane for direct amide bond formation	21
Scheme 1-19: Proposed catalytic cycle for the direct amide bond formation with boric acid	22

Scheme 1-20: Proposed catalytic cycle for direct boronic acid-catalyzed amide formation	23
Scheme 1-21: Proposed catalytic cycle for direct amide bond formation using 4,5,6,7-tetrachlorobenzo[<i>d</i>][1,2,3]dioxaborol 1-19b	27
Scheme 1-22: Proposed overall mechanism for amide formation involving either boric or arylboronic acid catalysis	30
Scheme 1-23: Whiting's bifunctional catalysts for direct amide bond formation	31
Scheme 1-24: Reaction scheme and proposed catalytic cycle for direct ambient amidation catalyzed by MIBA (1-31)	34
Scheme 2-1: Synthesis of 4-iodo-3-furanboronic acid (FIBA)	44
Scheme 2-2: Synthesis of 3-bromo-2-thienylboronic acid (2-5)	45
Scheme 2-3: Three potential ways to synthesize <i>ortho</i> -iodoarylboronic acid	45
Scheme 2-4: Retrosynthetic analysis and reaction scheme for boronic acid 2-4	46
Scheme 2-5: Retrosynthetic pathway for catalyst 2-12	47
Scheme 2-6: A possible alternate route for synthesizing <i>ortho</i> -iodo-phenanthreneboronic acids (2-6)	48
Scheme 2-7: Reverse retrosynthetic pathway for catalyst 2-12	49
Scheme 2-8: Preparation of phenanthrene 9-boronic acid (2-16)	49
Scheme 2-9: Proposed mechanism for <i>ipso</i> displacement of boron	50
Scheme 2-10: <i>Ips</i> <i>o</i> -displacement of boron	50
Scheme 2-11: Preparation of pinacolboronate and regioselective iodination	51
Scheme 2-12: General mechanism of boron ipso displacement	51
Scheme 2-13: Examining the catalytic reactivity of MIBA (1-31) and FIBA (2-3) on direct amide bond formation	52
Scheme 2-14: Comparison of product yields of catalysts MIBA (1-31) and electron-rich heteroareneboronic acids in a direct amidation reaction	53

Scheme 2-15: Screening of <i>ortho</i> -bromoheteroarylboronic acids as catalysts in direct amide bond formation	54
Scheme 2-16: The Staudinger reaction	59
Scheme 2-17: Non-traceless Staudinger ligation according to Saxon and Bertozzi	60
Scheme 2-18: The “traceless” Staudinger ligation according to Raines and Bertozzi	61
Scheme 2-19: Putative mechanism of the traceless Staudinger ligation	62
Scheme 2-20: Plausible mechanism and reaction scheme for Staudinger reaction and the effect of the activator	63
Scheme 2-21: The design of intermolecular direct amidation reaction combined with the Staudinger reaction	64
Scheme 2-22: A typical Staudinger reaction	64
Scheme 2-23: Mechanistic steps in the Staudinger ligation	65
Scheme 2-24: Staudinger reaction in direct amidation	66
Scheme 2-25: Proposed mechanism for the role of phosphine in Staudinger coupling	66
Scheme 2-26: Control Staudinger experiment	67
Scheme 2-27: Scale up result for the direct amidation reaction in dipeptide synthesis using 5 g of Boc- β -Ala-OH	73
Scheme 3-1: Oxazolone-mediated racemization occurring during peptide coupling	88
Scheme 3-2: Comparison of different catalysts in the amidation of Boc-proline by Whiting and co-workers	88
Scheme 3-3: Comparison of different catalysts in the amidation of C-protected amino acids by Whiting and co-workers	89
Scheme 3-4: Effect of different catalysts on the model amidation reaction	93
Scheme 3-5: In situ neutralization using Hünig’s base	100
Scheme 3-6: General reaction scheme for the reaction of arylboronic acids with malic acid	100

Scheme 3-7: Substrate modification to avoid irreversible complexation with a boronic acid catalyst	101
Scheme 3-8: Synthesis of double <i>N</i> -phthalamido α -amino acid (A) and neutralization of α -amino ester salt (B)	103
Scheme 3-9: Synthesis of α -azido acid (A) and neutralization of α -amino ester salt (B)	107
Scheme 3-10: Summary of the epimerization scope in direct peptide synthesis methodology	112

List of Equations

Equation 1-1: Direct coupling of metal carboxylate salts with amines	10
Equation 1-2: Direct high-temperature thermal amidation	12
Equation 1-3: Direct high-temperature thermal amidation	13
Equation 1-4: Direct polycondensation of amines and carboxylic acids	24
Equation 1-5: Direct condensation of urea with 4-phenylbutyric acid	25
Equation 1-6: Asymmetric direct amide formation	31

List of Abbreviations

AC	Acetyl
ACS	American Chemical Society
Ar	Aryl group
BBDI	1- <i>tert</i> -Butoxy-2- <i>tert</i> -butoxycarbonyl-1,2-dihydroisoquinoline
Bn	Benzyl
<i>t</i> -Boc	<i>tert</i> -Butyloxycarbonyl
BOP	benzotriazol-1-yloxy)tris(dimethylamino)phosphonium hexafluorophosphate
br	Broad
cm ⁻¹	Wavenumbers
dd	Doublet of doublets
ddd	Doublet of doublet of doublets
DCC	<i>N,N'</i> -dicyclohexylcarbodiimide
DFT	Density functional theory
DIC	3-Diisopropylcarbodiimide
DMAP	4-Dimethylaminopyridine
DMSO	Dimethyl sulfoxide
dq	Doublet of quartets
dt	Doublet of triplets
ee	Enantiomeric excess
EI	Electron impact

eq	Equation
equiv	Equivalents
ESI	Electron ionization
Et	Ethyl
Et ₂ O	Diethyl ether
EtOAc	Ethyl acetate
EtOH	Ethanol
FIBA	4-Iodo-3-furanboronic acid
GCI	Green Chemistry Institute
h	Hour
HATU	1-Bis(dimethylamino)methylene]-1 <i>H</i> -1,2,3-triazolo[4,5- <i>b</i>]pyridinium 3-oxid hexafluorophosphate, <i>N</i> -[(dimethylamino)-1 <i>H</i> -1,2,3-triazolo-[4,5- <i>b</i>]pyridin-1-ylmethylene]- <i>N</i> -methylmethanaminium hexafluorophosphate <i>N</i> -oxide
HBTU	<i>N,N,N',N'</i> -tetramethyl- <i>O</i> -(1 <i>H</i> -benzotriazol-1-yl)uroniumhexafluorophosphate, <i>O</i> -(benzotriazol-1-yl)- <i>N,N,N',N'</i> -tetramethyluronium hexafluorophosphate
HOAt	1-Hydroxy-7-azabenzotriazole
HOBt	Hydroxybenzotriazole
HPLC	High performance liquid chromatography
HRMS	High resolution mass spectrometry
IBA	<i>ortho</i> -Iodophenylboronic acid
IR	Infrared spectroscopy

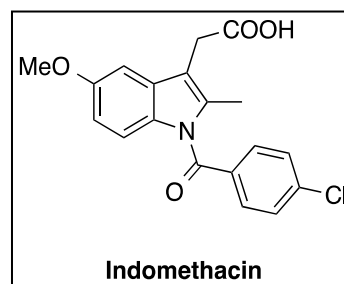
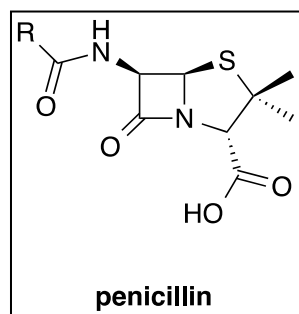
LDA	Lithium diisopropylamide
m	Multiplet
Me	Methyl
MIBA	5-Methoxy-2-iodophenylboronic acid
MS	Molecular sieves
<i>N</i> -Boc	<i>N</i> - <i>tert</i> -Butyl carbamate
<i>N</i> -Ac	<i>N</i> -acetyl
NHC	<i>N</i> -Heterocyclic carbene
NIS	<i>N</i> -Iodosuccinimide
NMP	<i>N</i> -methylpyrrolidinone
NMR	Nuclear magnetic resonance
Nu	Nucleophile
<i>o</i> -NPBA	<i>o</i> -Nitrophenyl- boronic acids
PyBrop	Bromo(tri-1-pyrrolidiny)phosphonium hexafluorophosphate
<i>i</i> -Pr	Isopropyl
q	Quartet
qd	Quartet of doublet
qt	Quartet of doublet
PMe ₃	Trimethylphosphane
PPh ₃	Triphenylphosphane
PySeSePy	2,2'-Dipyridyl diselenide
t	Triplet
td	Triplet of doublets

TFA	Trifluoroacetic acid
TFPBA	3,4,5-Trifluorophenylboronic
THF	Tetrahydrofuran
TICA	Triiodoisocyanuric acid

Direct Amide Bond Formation and Peptide Synthesis

1.1 Introduction

The amide functionality is one of the most fundamental chemical building blocks found in nature. It constitutes the backbone of the biologically crucial proteins, and it is present in a vast number of synthetic structures. Amide bonds are also present in a vast array of useful molecules including numerous industrially important compounds, as well as a wide selection of bioactive natural products. The synthesis of amides is hugely important in the pharmaceutical industry, where amides are present in about 25% of top-selling pharmaceuticals and in many other medicinally important compounds.^{1a,b} For example, Penicillin is known to destroy bacterial infections, Indomethacin is commonly used as a prescription medication to reduce fever, pain, stiffness, and swelling, Prazosin is a sympatholytic drug used to treat high blood pressure, anxiety and panic disorder, Terazosin is used for treatment of symptoms of an enlarged prostate (BPH) and Doxazosin is used to treat high blood pressure and urinary retention associated with benign prostatic hyperplasia (**Figure 1-1**).



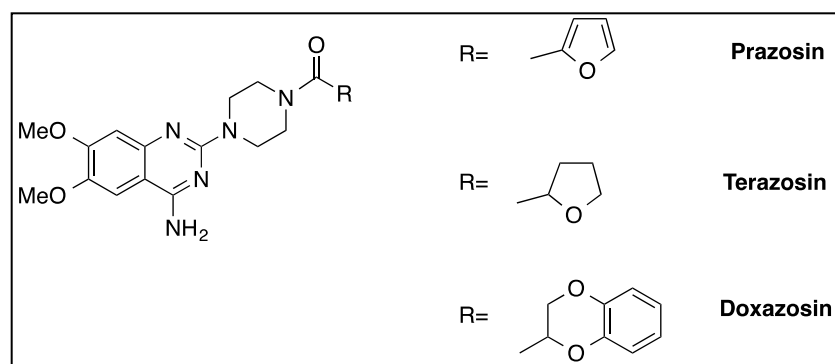


Figure 1-1: Structures of pharmaceutical drugs containing amide bonds.

In this introductory chapter, a delineated background about the importance of the amide bond and the challenge of forming this bond from carboxylic acids and amines is presented, and the objectives of this thesis are outlined. The first section focuses on using non-boron reagents for direct amide bond formation, which are stoichiometric in all use of coupling reagents or catalytic in all use of multimetal salts and additives. In the second section, the use of boron reagents for direct amide bond formation, currently the attractive approach for the activation of carboxylic acids, is described. The detailed mechanisms for the use of catalytic and stoichiometric boron reagents are outlined. Lastly, the conclusion and project objectives are presented.

1.2 Methods and Strategies for Amide Bond Formation

A survey in 2007 revealed that amide bond formation was not only one of the top 15 reactions currently used in drug discovery industry, but was also identified as a priority research area by the American Chemical Society (ACS) Green Chemistry Institute (GCI) and several leading global pharmaceutical corporations.^{2a,b} Consequently, the development of efficient amidation methods targeting high atom economy continues to be an important scientific pursuit. More recently, boron reagents and, especially, boronic acids and boric acid have provided a possible benign alternative and one of the most attractive approaches for this long-standing problem.

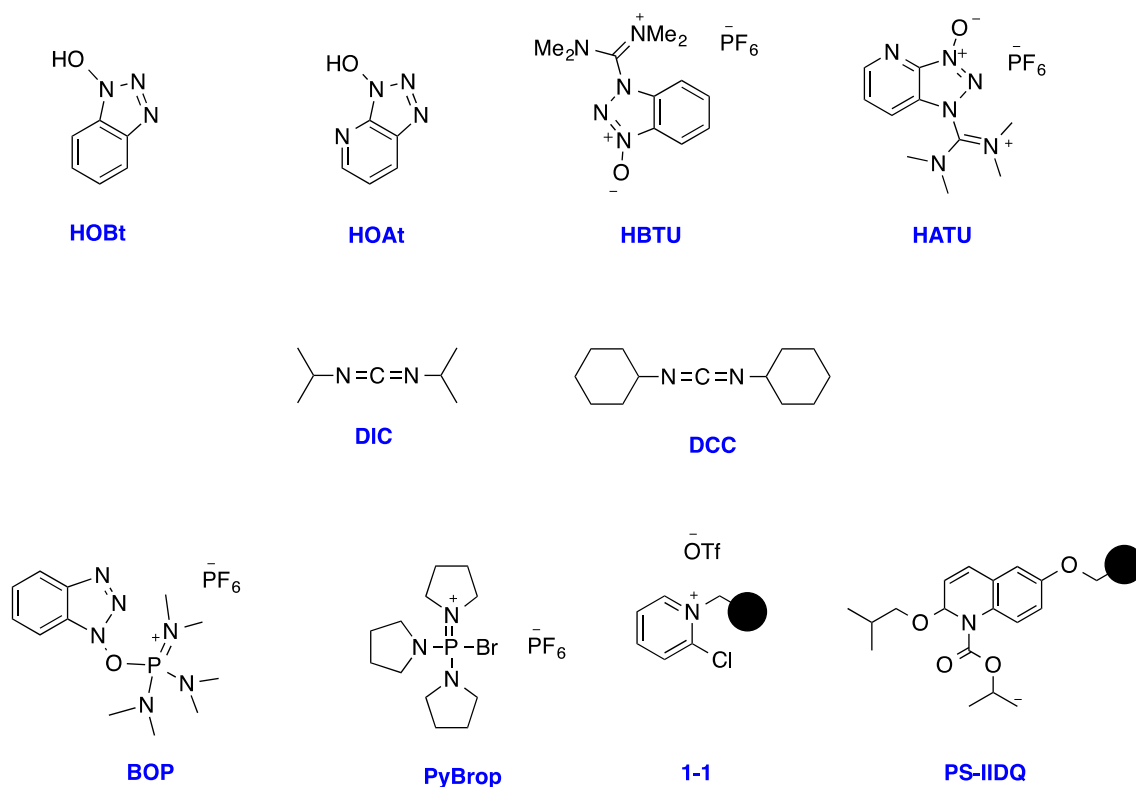
1.2.1 Non-Boron Reagents for Direct Amide Bond Formation

For the direct amide bond formation between a carboxylic acid and an amine, the carboxylic acid moiety needs to be pre-activated before adding the amine. Several stoichiometric and catalytic methods have been developed for activating the carboxylic acid moiety.

1.2.1.1 Stoichiometric Activation of Carboxylic Acids

Carboxyl groups can be activated as acyl halides, acyl azides, acylimidazoles, anhydrides, esters, etc.³ The predominance of carbodiimide and active ester techniques has been gradually replaced with the so-called ‘onium salts’. Among these reagents, HOBt [hydroxybenzotriazole]- and HOAt [1-hydroxy-7-azabenzotriazole] - based uronium, phosphonium and immonium salts are proving to be very efficient. For example, during the synthesis of ACP decapeptides (H-Val-Gln-Ala-Ala-Ile-Asp-Tyr-Ile-Asn-Gly-NH₂), HBTU [*N,N,N',N'*-tetramethyl-*O*-(1*H*-benzotriazol-1-yl)uroniumhexafluorophosphate, *O*-(benzotriazol-1-yl)-*N,N,N',N'*-tetramethyluronium hexafluorophosphate] (**Figure 1-2**), was the fastest reagent after two minutes while almost none of the expected amide was formed using DIC [1,3-diisopropylcarbodiimide] (**Figure 1-2**) after this time. However, after eight minutes, DIC was comparable to HBTU. In addition very few side-reactions were observed with DIC compared to BOP [benzotriazol-1-yloxy)tris(dimethylamino)phosphonium hexafluorophosphate] or HATU [1-bis(dimethylamino)methylene]-1*H*-1,2,3-triazolo[4,5-*b*]pyridinium3-oxid hexafluorophosphate, *N*-[(dimethylamino)-1*H*-1,2,3-triazolo-[4,5-*b*]pyridin-1-ylmethylene]-*N*-methylmethanaminium hexafluorophosphate *N*-oxide] (**Figure 1-2**). This study demonstrated that a simple reagent like DIC performs well in many cases, and a compromise of speed/purity/by-products needs to be sought.⁴ Overall, keeping in mind all possible issues (side-reactions), HATU and HBTU offer generally excellent reactivity. If quick coupling times are required, HATU probably represents the reagent of choice, providing the substrates are not hindered. Otherwise, the traditional method DCC [*N,N'*-

dicyclohexylcarbodiimide], DIC/HOBt remains an excellent choice for many substrates. For difficult couplings (*e.g.* secondary amines), PyBrop [bromo(tri-1-pyrrolidinyl)phosphonium hexafluorophosphate] is generally reliable.³ Triazines can be an alternative for difficult couplings, although the most reactive reagents tend to give side-products. Recent developments by Kaminski, however, are bringing new applications to this class of coupling reagents. Finally, for library synthesis either the polymer-supported Mukaiyama reagent (**1-1**) or polymer-supported IIDQ are clearly the most suitable reagents,⁴ and their efficiency has been confirmed by many laboratories. These reagents have the advantage of simplifying purification as the consumed reagent is separated *via* simple filtration. In conclusion, selecting suitable coupling reagents can be summarized by “keeping it simple” as most reagents appear to be merely fancy and costly alternatives. It is generally wise to avoid “exotic” reagents and not be misled by “fast” coupling reagents. Efficiency is the key, with high conversions, low levels of epimerization and limited by-products all being essential criteria.



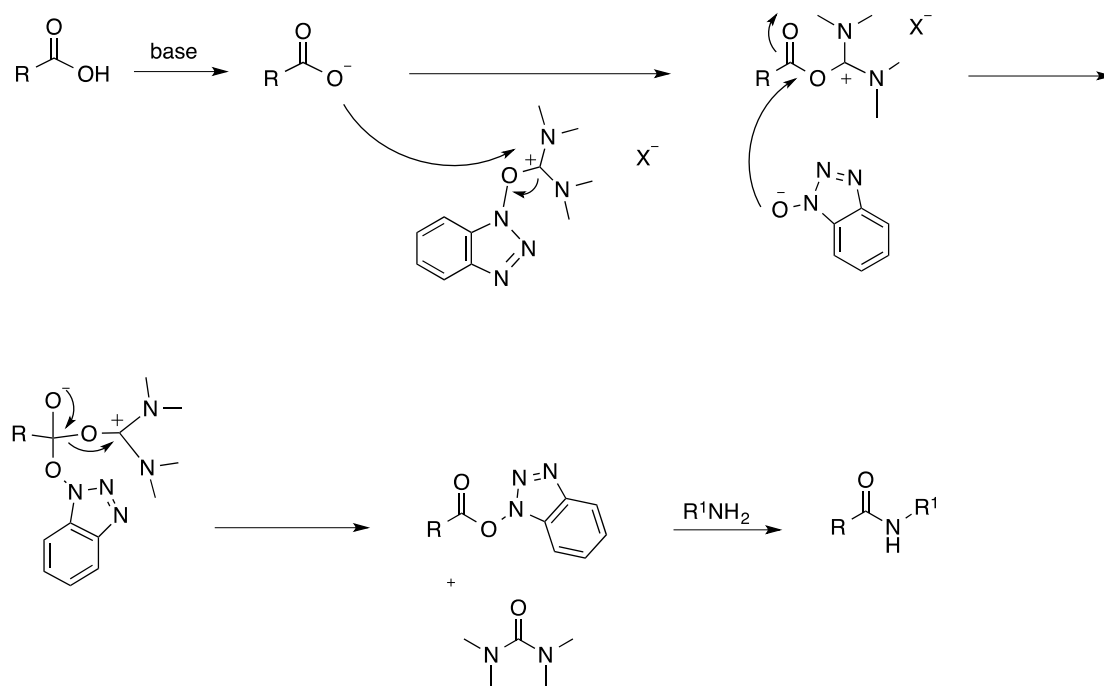
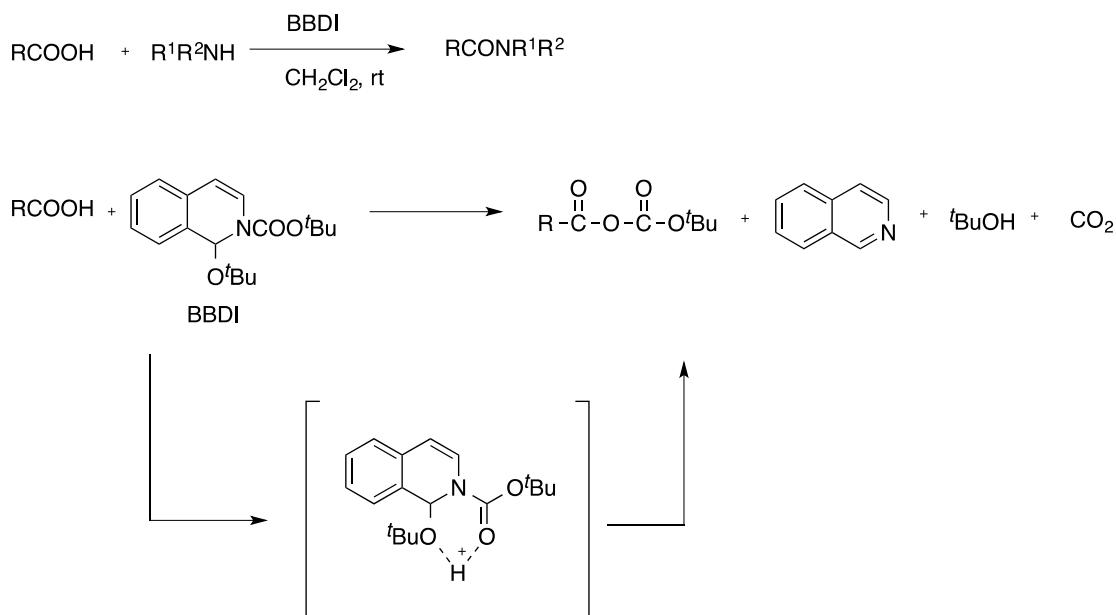


Figure 1-2: Common coupling reagents and an example mechanism with HBTU.

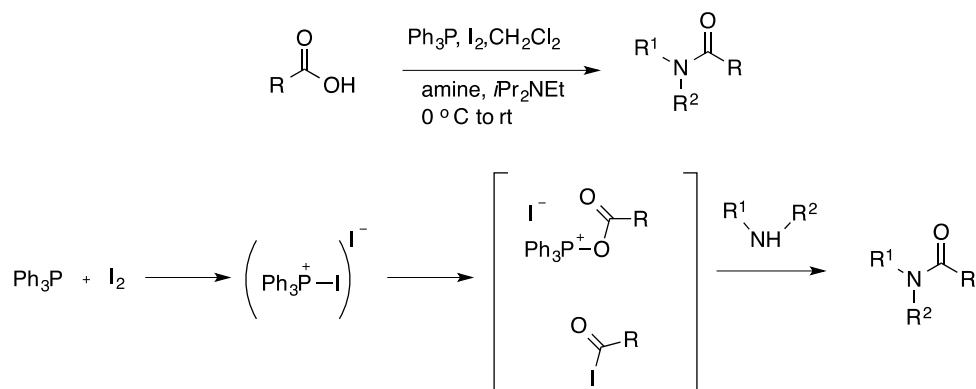
1.2.1.2 Recent Developments

A simple and mild carboxamination of carboxylic acids using a *tert*-butoxycarbonylation reagent, 1-*tert*-butoxy-2-*tert*-butoxycarbonyl-1,2-dihydroisoquinoline (BBDI), was reported in 2008.⁵ This procedure has several advantages including removal of reagent-derived byproducts by simple work-up and no requirement for any bases (**Scheme 1-1**).⁶



Scheme 1-1: Amidation with BBDI without bases.

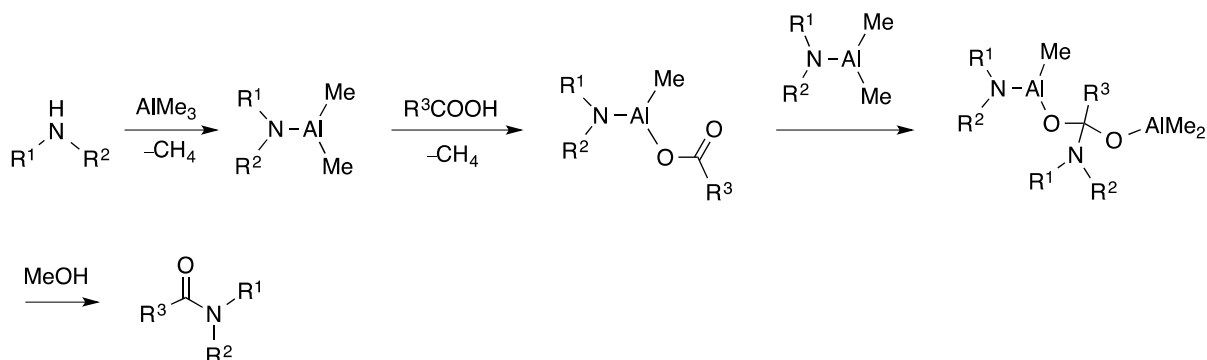
The advantage of the PPh_3/I_2 combination is that the reagents are inexpensive and easy-to-handle, and the reactions are straightforward to conduct.



Scheme 1-2: A plausible mechanism for the amidation reaction.

Because Ph_3PO is a byproduct in this reaction, polymer supported PPh_3 (Pol- PPh_3) can be used instead. In 2012, Bang-Chi Chen reported an efficient AlMe_3 -promoted coupling

reaction between acids and amines to give amides. The dimethylaluminium amide must be pre-formed before the acid can be added to the reaction mixture (**Scheme 1-3**).⁷



Scheme 1-3: Proposed AlMe₃-mediated amidation mechanism.

This method is noteworthy, because activation of both the carboxylic acid and of the amine occurs during the reaction mechanism, leading to more effective acylation of poorly nucleophilic amines. This is in contrast to most other methods, which proceed solely through activation of the carboxylic acid component. In 2012, Chi Zhang reported a system based on the hypervalent iodine **1-2**, DMAP and PPh₃ (**Figure 1-3**) to construct amide bonds from carboxylic acids and amines.⁸

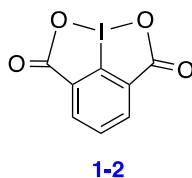
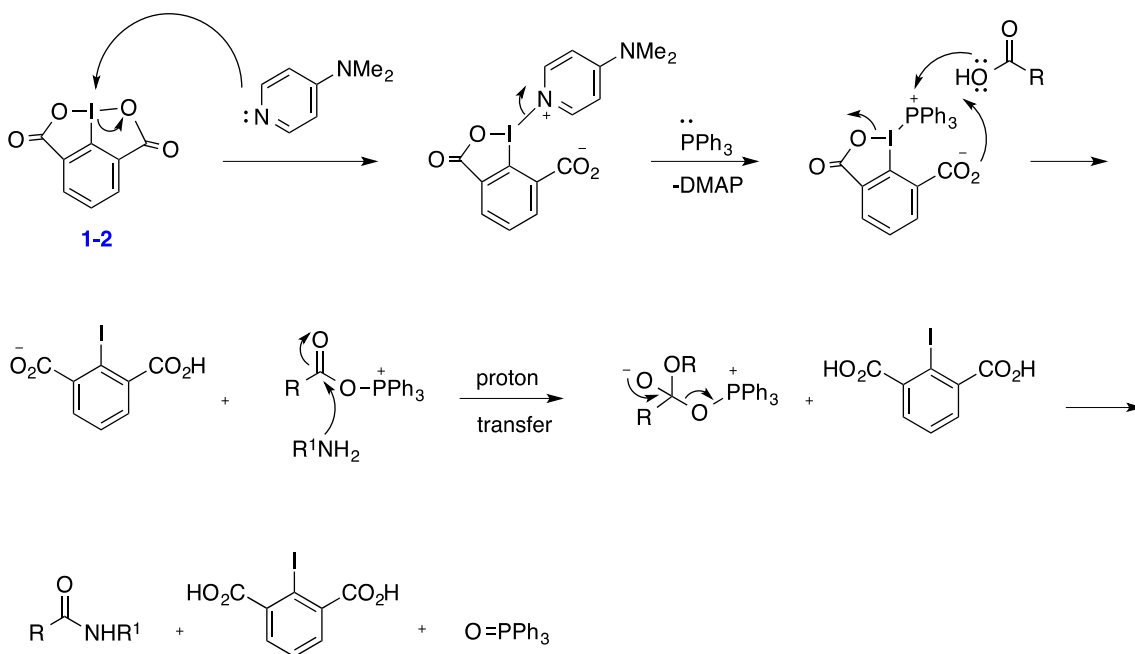


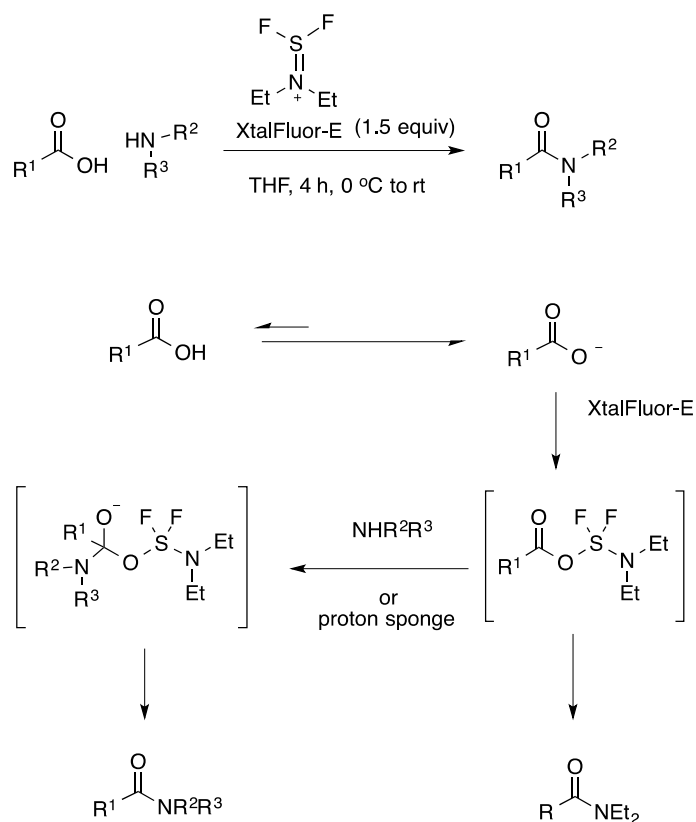
Figure 1-3: A hypervalent iodine (III) reagent, iodosodilactone (1-2).

The proposed mechanism is shown in **Scheme 1-4**.



Scheme 1-4: Proposed amidation mechanism with hypervalent iodine (III) reagent 1-2.

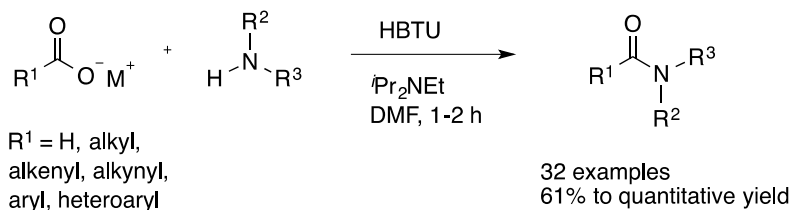
In 2013, XtalFluor-E was shown to be an efficient coupling reagent for the synthesis of amides from carboxylic acids and amines without epimerization/racemization of the substrates (**Scheme 1-5**).⁹



Scheme 1-5: Reaction scheme and mechanism using XtalFluor-E as an activator.

Even poorly reactive carboxylic acids can be transformed to amides using this method. There was no epimerization/racemization during the process.

In 2014, Batey and coworkers developed the direct coupling of alkali metal carboxylate salts with amines using HBTU (**Figure 1-1**) as a coupling agent in combination with Hünig's base. When the corresponding acyl chlorides or carboxylic acids are unstable or the system is acid-sensitive, amidation of a carboxylate salts with either free amines or their ammonium hydrochloride salts can be achieved using this method (**Equation 1-1**).¹⁰



Equation 1-1: Direct coupling of metal carboxylate salts with amines.

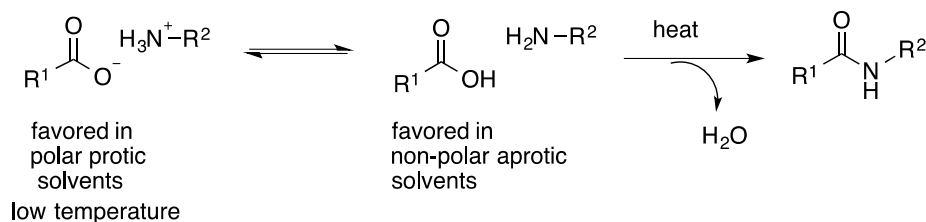
The main drawbacks of all the above strategies using stoichiometric reagents are the formation of toxic/corrosive by-products, poor atom economy and costly waste streams that clearly mark them out as non-sustainable processes.

1.2.1.3 Catalyzed and Uncatalyzed Direct Amidation Reaction

In recent times, the direct amidation of non-activated carboxylic acids has attracted more attention, with an increasing number of laboratories focusing on this area of research.

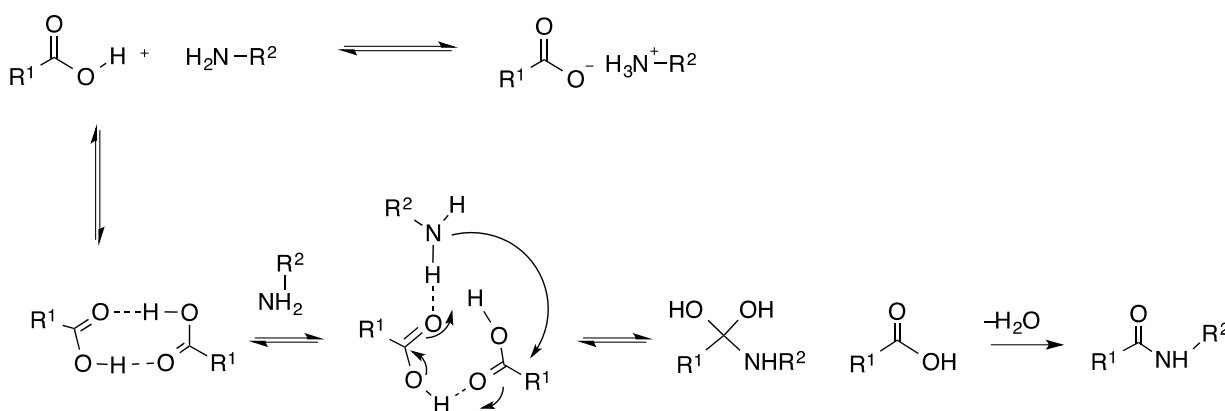
1.2.1.3.1 Thermal Uncatalyzed Amidation

A direct conversion of carboxylic acids involving nucleophilic substitution of the hydroxy group by an amine is very desirable but intrinsically difficult (**Scheme 1-6**).¹¹ A dehydration of the resulting ammonium carboxylates usually requires drastic conditions that this approach can be applied only to particularly reactive and otherwise unfunctionalized derivatives.



Scheme 1-6: Preparation of amides by direct condensation.

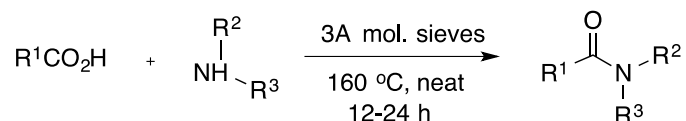
Indeed, the degree of ammonium carboxylate salt formation is strongly dependent both on the substrates employed and on the reaction conditions.¹¹ With more acidic systems, a high degree of ammonium carboxylate salt formation was observed. However, the reactivity of the amine component were much more difficult to evaluate, and amine reactivity was thought to be regulated by a complex balance of steric and electronic effects.¹² On the basis of a recent computational study it was proposed that the key step of the reaction mechanism is nucleophilic attack of the amine on a hydrogen-bonded carboxylic acid dimer (**Scheme 1-7**).¹²



Scheme 1-7: The proposed mechanism for direct amide formation supported by DFT calculations.

Intermolecular direct amide formation proceeds through the existence of carboxylic acid hydrogen-bonded dimers, which are not only known to persist even at elevated temperatures but are likely to be highly favourable in non-polar solvents. The role of such hydrogen-bonded dimers is to enable both carboxylic acid activation towards nucleophilic attack by the amine and to allow the reaction to proceed through a neutral intermediate. It was also rationalized that efficient water removal is necessary since small amounts of water caused hydration of mutually H-bonded cyclic carboxylic acid dimer. In 2012, Williams and co-workers reported the direct thermal uncatalyzed amidation reaction in non-polar solvents particularly in toluene at 110 °C without the need to remove water.¹³ Increasing the concentration of the reaction to 2.0 M allowed complete conversion into product after 20 h. Several simple Lewis acids catalyzed the reaction and

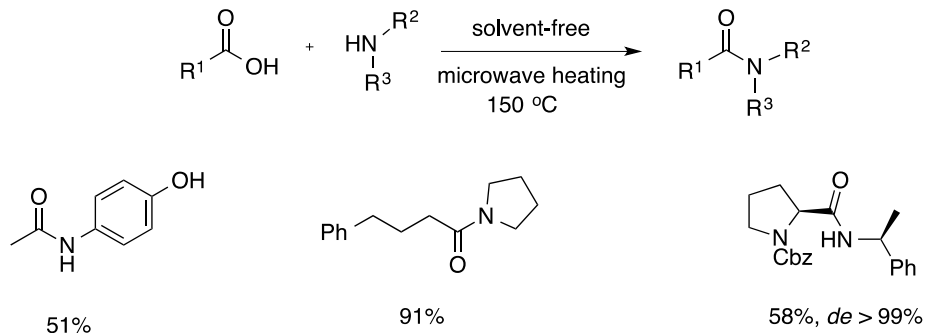
two zirconium catalysts [ZrCl_4 , ZrCp_2Cl_2 (5 mol%)] were particularly effective for the process.¹⁵ Gooßen *et al.* reported direct thermal condensations at 160 °C under neat conditions in the presence of 3A molecular sieves (**Equation 1-2**).¹⁴



Equation 1-2: Direct high-temperature thermal amidation.

1.2.1.4 Microwave Irradiation

Pyrolysis of salts obtained by mixing neat amines and carboxylic acids were realized under solvent-free conditions within short times and appreciable yields with microwave promoted heating (**Scheme 1-8**).¹⁶



Scheme 1-8: Examples of solvent-free amidation under microwave heating.

It was claimed that having either the amine or carboxylic acid in excess was favourable with this method. The simplest explanation was that the excess carboxylic acid or amine can complex the carboxylic acid by hydrogen bonding to the carbonyl group. This interaction results in electronic assistance to nucleophilic attack by the amine nitrogen atom shown in **Figure 1-4 (A)**, **(B)**. If this is indeed occurring, the protonated amine could also provide assistance shown in **Figure 1-4 (C)**.

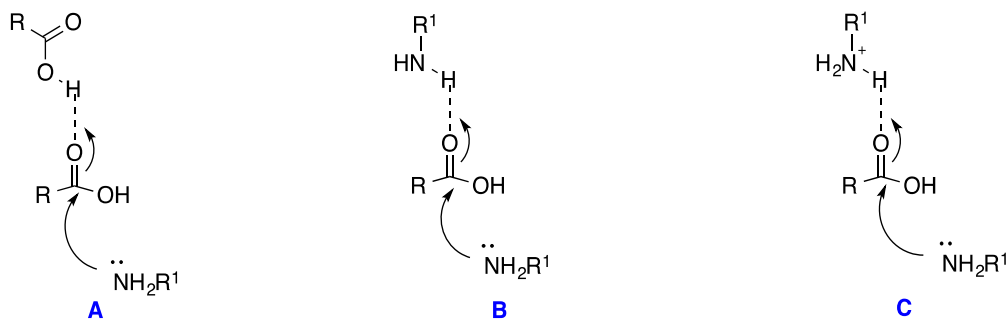
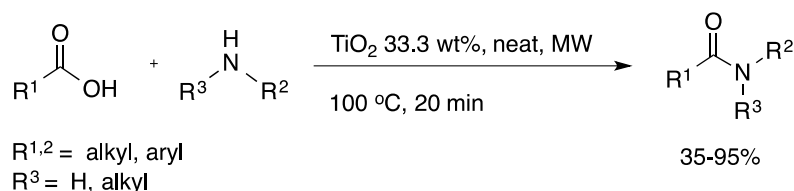


Figure 1-4: Electrophilic assistance to nucleophilic attack.

However, this explanation fails to take into account that pK_a s between (A), (B) and (C) would be quite different. Another plausible theory is that the addition of an excess of either the carboxylic acids or amine starting material would help to drive the reaction towards product formation (Le Chatelier's Principle). It has also been claimed that the addition of one equivalent of imidazole facilitates the amide formation.¹⁷ Recently, TiO_2 was reported to facilitate the solvent-free conversion of benzoic acid to amides at 100 °C (**Equation 1-3**).¹⁸



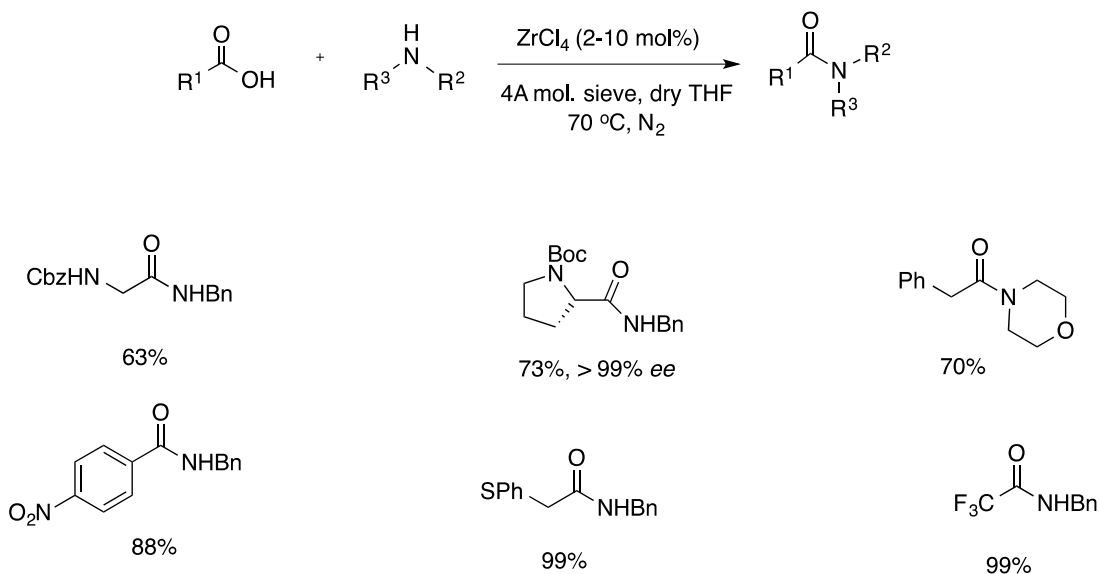
Equation 1-3: Direct high-temperature thermal amidation.

1.2.1.5 Metal Catalysis

The use of metal-based catalysts for the direct amidation of carboxylic acids and amines has mainly received attention in the last few years, and remains an underdeveloped area.

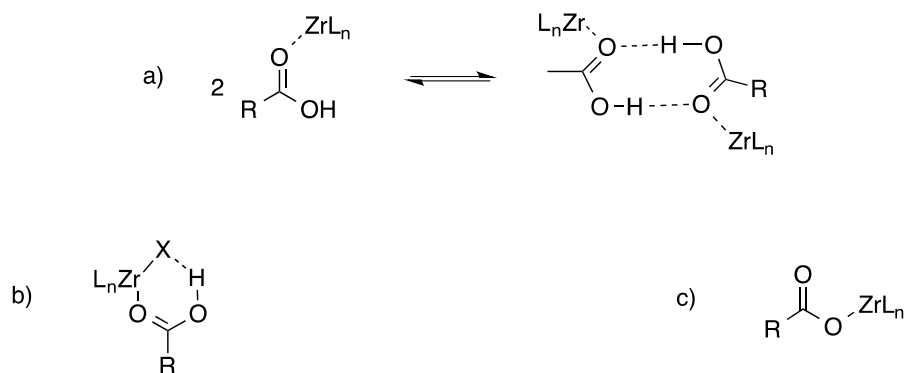
1.2.1.5.1 Homogeneous Metal Protocols

In 2012, Hans Adolfsson and co-workers demonstrated that several early transition-metal complexes such as titanium (IV) isopropoxide¹⁹ and zirconium (IV) chloride^{20,21} are efficient catalysts for the direct amidation of nonactivated carboxylic acids with amines (**Scheme 1-9**). No racemization was observed in the coupling of two *N*-protected amino acids, and this simple and high-yielding method tolerates a wide range of functionalities, including acid labile groups. For the formation of amides using this protocol, the use of an excess of the amine component was highly beneficial.



Scheme 1-9: Examples of $ZrCl_4$ -catalyzed amidation reactions.

It has been proposed that zirconium catalysts activate the carboxylic acid through several different coordination modes (**Scheme 1-10**), including: a) Lewis acid activation of the carbonyl group either in the acid or in the hydrogen-bonded dimer, b) Lewis acid activation of the carbonyl group with simultaneous activation of the leaving group by hydrogen bonding, and c) zirconium activation of the carboxylate oxygen as a leaving group.



Scheme 1-10: Proposed carboxylic activation modes using a Zr catalyst.

1.2.1.5.2 Heterogeneous Metal Protocols

A number of heterogeneous metal-containing catalysts such as $\text{ZrOCl}_2 \cdot 8\text{H}_2\text{O}$,²¹ metal doped zeolites,²² ZnO ,²³ macroporous ZnO ,²⁴ ZnO -nanofuid,²⁴ nanocrystalline- MgO ,²⁵ sulfated tungstate,^{26,27} $\text{FeCl}_3 \cdot 6\text{H}_2\text{O}$,²⁸ Fe^{+3} exchanged K-10 montmorillonite,²⁹ elemental zinc,³⁰ K60 silica,³¹ have been developed. Recently, Hosseini-Sarvari reported a nano-sulfated TiO_2 catalyst.³² The main advantage of heterogeneous catalysis is the possibility of facile separation of the catalyst from the reaction medium and the potential recyclability, overall leading to a better atom economy. Generally, the metal catalysts that are presented in the literature require high to fairly high reaction temperatures in order to work, which can be a drawback for sensitive substrates. The majority of the catalytic systems are inhibited by coordinating groups in the substrates. Removal of the formed water is also required in order to reach high conversions.

1.2.2 Boron Reagents For Direct Amide Bond Formation

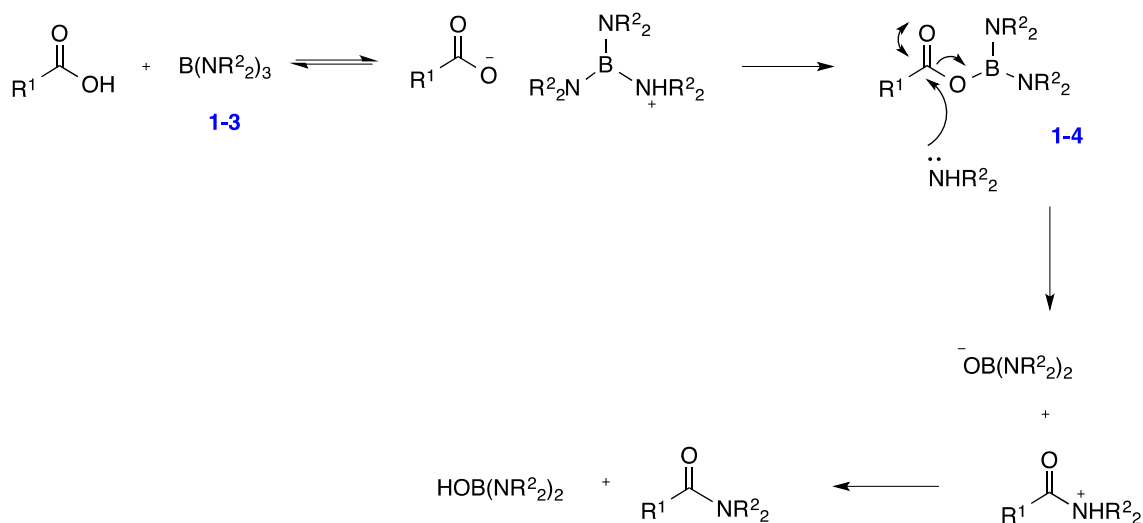
In the last few decades, the use of boron-based compounds as catalysts has gained considerable interest.³³ The Lewis acidity of boron-based catalysts can be fine-tuned by substituent effects.

1.2.2.1 Stoichiometric Activation of Carboxylic Acids

In 1965, Pelter and co-workers reported boron-containing compounds could be used as reactive entities with certain functional groups, in particular for converting carboxylic acids to amides.^{33a, b}

1.2.2.1.1 Trisdialkylaminoborane [B(NR₂)₃]

The mixing of carboxylic acids with trisdialkylaminoboranes [B(NR₂)₃] (**1-3**) in inert conditions was found to be exothermic.³³ Depending on the carboxylic acid used, the reaction might need cooling or refluxing at 120 °C for several hours to provide the desired amide product. In the proposed mechanism (**Scheme 1-11**), only one of the dialkylamino reagents was consumed for the conversion of the carboxylic acid to the amide. The reaction proceeds *via* initial salt formation followed by the production of mixed anhydrides. The mixed anhydride **1-4** is formed following nucleophilic attack by the carboxylate group on the protonated trisdialkylaminoborane.

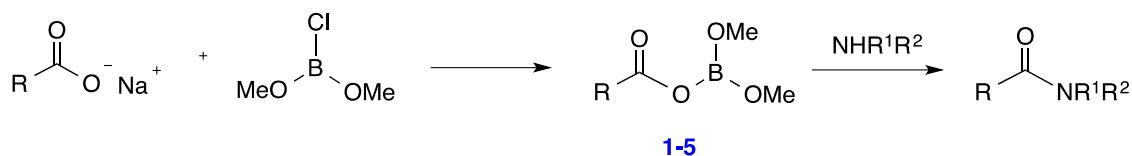


Scheme 1-11: Proposed mechanism for direct amide bond formation from mixing carboxylic acids with trisdialkylaminoboranes.

The limitations of this methodology are: only one of the amino groups is utilized, there is potential for racemization, and it features a limited substrate scope since aminoboranes are reactive reagents and few organic functional groups are tolerant of these reaction conditions.³⁴

1.2.2.1.2 Trialkylboranes [BR₃], Trialkyloxyboranes [B(OR)₃] & Chlorodialkoxymboranes [ClB(OR')₂]

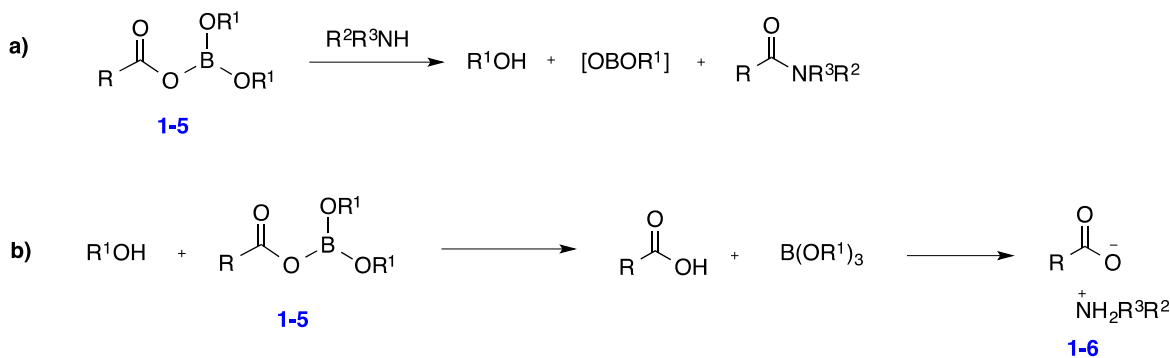
Trialkylboranes [BR₃] was found to be less active than the borane **1-3** in direct amidation reaction.³⁵ High excess of trialkyloxyboranes [B(OR)₃], and elevated temperature, however, are necessary in order to provide the amide product alongside trace amounts of ester.³⁵ Notably, acyloxydialkylborate [RCO₂B(OR)₂] were suggested to be good candidates for direct amide formation via intermediate **1-5**.³⁵ These intermediates can be formed by the reaction between chlorodimethoxyborate [ClB(OMe)₂] and the sodium salt of carboxylic acids, as outlined in **Scheme 1-12**. This reaction proceeds rapidly at reflux temperature in benzene and there was infrared spectroscopic evidence for formation of the corresponding acyloxydialkylborane species **1-5**.^{34, 35}



Scheme 1-12: Formation of acyloxydialkylborane 1-5 and the corresponding amide product.

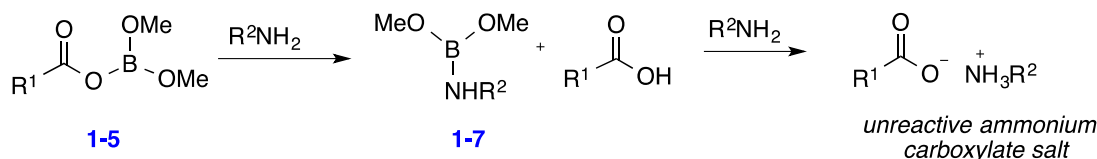
Interestingly, the addition of methanol to the mixed intermediate **1-5** at room temperature gave no ester. In contrast, the addition of amine at room temperature rapidly gave the amide product in 44% yield. This yield was increased to 70% by heating the reaction mixture.³⁴ The reaction conditions were mild, and when applied to peptide synthesis, racemization was low. Further investigations were performed to establish why low conversions were obtained at room temperature. Possible reasons were proposed as follows: firstly, the dialkyloxyborane species was not being formed efficiently or was

undergoing further reaction before the addition of the carboxylic acid; secondly, the mixed anhydride of type **1-5** may be susceptible to decomposition or reduction; thirdly, the reaction of the mixed anhydride with an amine occurred at the boron atom or resulted in products that could not participate further in the reaction.³⁵ Investigations into each of these options showed that the third possibility was most likely. One mole of alcohol can be liberated in the attack of an amine upon the mixed anhydride species **1-5** [Scheme 1-13(a)]. This liberated alcohol can also go on to compete with the amine for the mixed anhydride and result in the formation of an unreactive salt (**1-6**), *i.e.* as outlined in Scheme 1-13(b).



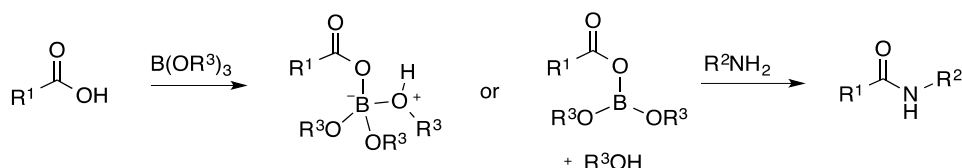
Scheme 1-13: (a) Liberation of alcohol from acyloxyborane 1-5; (b) Formation of an unreactive carboxylate ammonium salt.

Since alcohols can attack acyloxydialkyloxyborane **1-5** at boron, it is possible that nucleophiles such as amines will also attack at boron, although less selectively. This means that as well as the amide being produced as in Scheme 1-13(a), the aminodialkyloxyborane species **1-7** could also be produced along with an unreactive carboxylate ammonium salt (Scheme 1-14). This rationale presents a likely explanation for the low conversion to amide at room temperature by this method, since it is a competitive reaction with the amide formation.



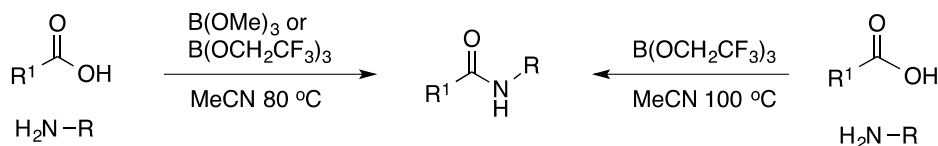
Scheme 1-14: Formation of an aminodialkyloxyborane species.

Sheppard and co-workers, reported the use of simple borates $[\text{B}(\text{OCH}_2\text{CF}_3)]$ as promoters for amide bond formation and conversion of primary amides to secondary amides *via* transamidation.^{36a} Activation of the carboxylic acid presumably occurs *via in situ* generation of a three or four-coordinate boron species (**Scheme 1-15**).



Scheme 1-15: Borate-mediated direct amidation.

The above mentioned boron reagent is a practical reagent for direct amide bond formation under both thermal and microwave conditions. Unlike many other coupling methods, this approach exhibits good functional group tolerance, purification is extremely straightforward and do not require anhydrous reaction conditions. $\text{B}(\text{OCH}_2\text{CF}_3)_3$ was also shown to activate amides toward transamidation albeit, at high temperature (**Scheme 1-16**).



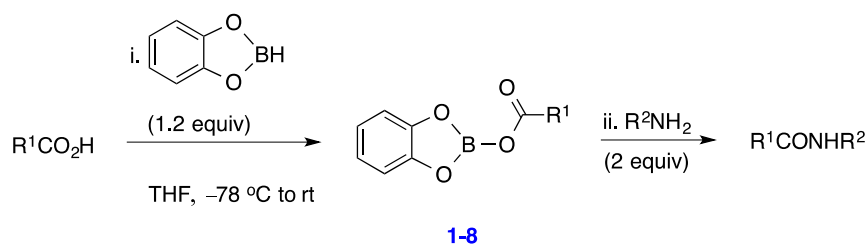
Scheme 1-16: Borate promoted amidation.

Recently, the same group studied the full scope of these reagents application and a wide range of acids and amines containing various functionalities could be successfully used in $B(OCH_2CF_3)_3$ -mediated amidation reactions. In addition, the pure amide products can be isolated following an operationally simple solid-phase work-up procedure using commercially available resins, avoiding the need for aqueous work-up or chromatographic purification.^{36b}

1.2.2.1.3 Borane and Catecholborane

Trapani and coworkers employed borane-trimethylamine as the coupling reagent in a 1:1:3 molar ratio (for the amine:borane:carboxylic acid), resulting in good to high amide yields under refluxing xylene conditions.³⁷ It was claimed that triacyloxyborane species are the activated acylating species involved in the reaction.

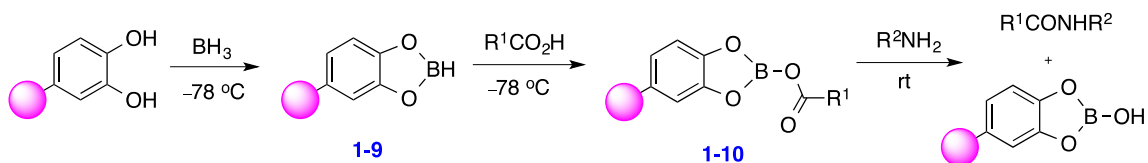
Closely related to this work, Ganem and coworkers reported that carboxylic acids and amines condense readily to form amides in the presence of the stoichiometric amount of catecholborane, but under milder conditions, *i.e.* THF, $-78\text{ }^{\circ}\text{C}$ to room temperature as outlined in **Scheme 1-17**.³⁸ The mixing of carboxylic acid and catecholborane gave the active intermediate **1-8** [1740 cm^{-1} carbonyl absorption). The aromatic ring in this system enhances the reactivity of the active ester and can reduce side reactions.



Scheme 1-17: Ganem's amide bond formation using catecholborane.

Resin-bound catecholborane (**1-9**) can also be used for direct amide formation as a solid phase reagent (**Scheme 1-18**).³⁹ After forming the solid-phase catecholborane by reacting the catechol with BH_3 , the carboxylic acid was added and the mixture was shaken to form

the activated mixed anhydride (**1-10**). The amine was taken added at ambient temperature to form the desired amide product in moderate yields.



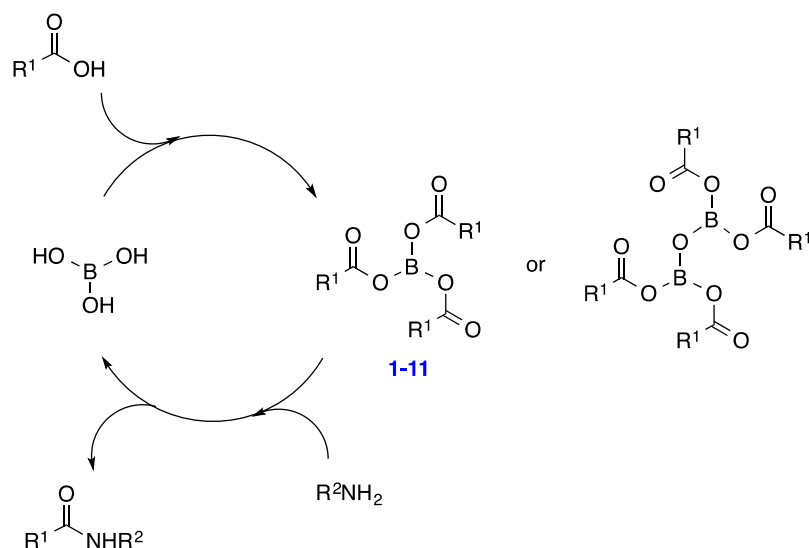
Scheme 1-18: Wang's solid-supported catecholborane for direct amide bond formation.

1.2.2.2 Catalytic Activation of Carboxylic Acids

Due to the advantages of atom-economy and reduced costs, in the last few decades, the use of boron-based compounds as catalysts has gained considerable interest.

1.2.2.2.1 Boric Acid

In 2005, Tang and co-workers reported that the cheap and readily available, non-toxic compound, boric acid $[B(OH)_3]$, also constitutes a highly effective catalyst for direct amide formation.⁴⁰ In most cases, the use of 5 mol% of $B(OH)_3$ is sufficient for obtaining excellent yields in toluene at reflux temperature. It was proposed that boric acid reacts with the carboxylic acid to form a mixed anhydride **1-11** as the actual acylating agent.^{41,42} Upon reaction with an amine, this intermediate forms the desired carboxamide and regenerates the catalytically active boric acid (**Scheme 1-19**).

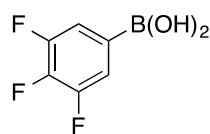


Scheme 1-19: Proposed catalytic cycle for the direct amide bond formation with boric acid.

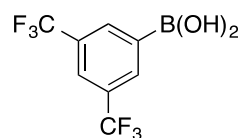
The present method is successfully applicable to aromatic amines, which are less nucleophilic compared to aliphatic amines. In 2007, this amidation procedure has been tested in the synthesis of several active pharmaceutical ingredients.^{43, 44}

1.2.2.2.2 Electron-Poor Arylboronic Acids

In 1996, Yamamoto and co-workers found that arylboronic acids bearing electron-withdrawing groups at the *meta*- or *para*- position are highly efficient catalysts for direct amide bond formation at reflux temperature in toluene.⁴⁵ Unlike the previous stoichiometric boron-mediated amidation (Section 1.2.2.1), arylboronic acids with electron-withdrawing groups can overcome the problem of transformation into an inactive species (without decomposition of acyloxyboronate intermediate) or it is possible that they are in equilibrium with these species. These catalysts are water-, acid- and base-tolerant Lewis acids that can generate acyloxyboron species, resulting in an increased reactivity with amines. Both 3,4,5-trifluorophenylboronic (**1-12**) and 3,5-bis(trifluoromethyl)phenylboronic acid (**1-13**) catalyzed amide bond formation in refluxing toluene.



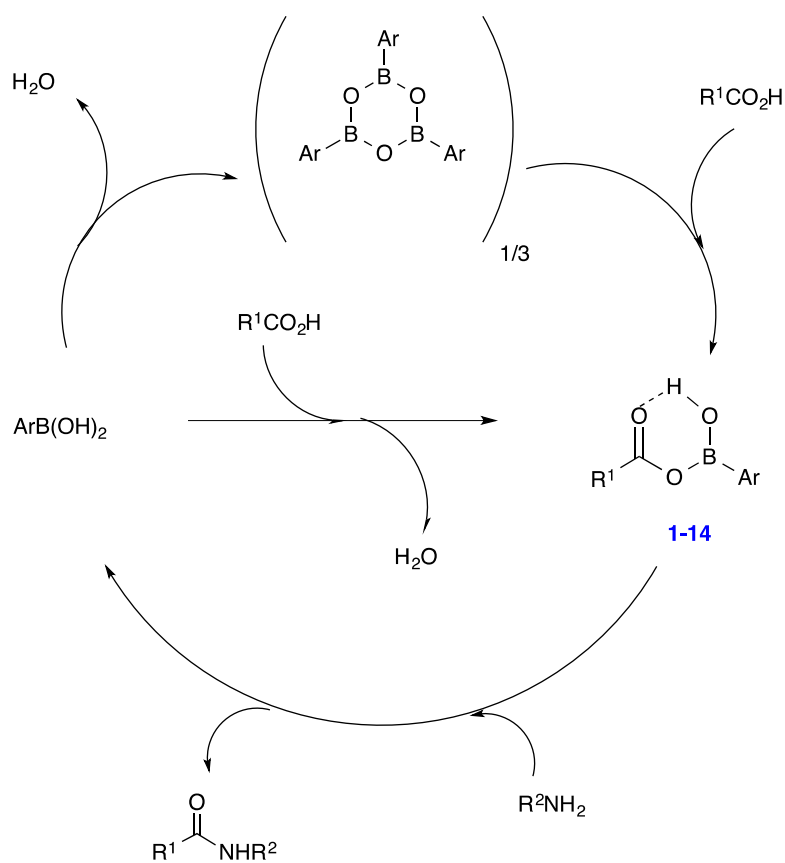
1-12



1-13

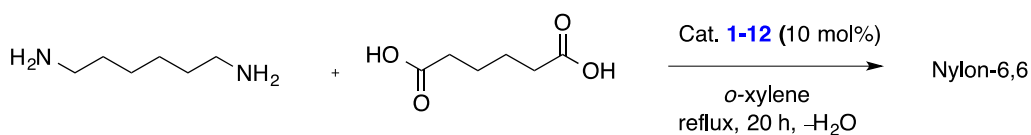
Figure 1-5: 3,4,5-Trifluorophenylboronic (12) and 3,5-bis(trifluoromethyl)phenylboronic acid (13).

Catalyst **1-12** was found to be the most active, and a proposed mechanism is shown in **Scheme 1-20**.⁴⁵ For more demanding substrates, like aniline instead of benzylamine, more forcing conditions were employed and the reaction required refluxing in mesitylene (163-166 °C) for several hours to provide the amide product in 99% yield.⁴⁵



Scheme 1-20: Proposed catalytic cycle for direct boronic acid-catalyzed amide formation.

The authors claimed that monoacyloxyboronate **1-14**, the mixed anhydride, is produced, which is then attacked by the amine to form the amide product. The reported ^1H -NMR and IR data for the active intermediate are inconclusive without any ^{11}B -NMR data. It was claimed that the absorption bond at 1586 cm^{-1} in the IR spectrum is for the monoacylboronate **1-14**. According to Ganem's work, the monoacylboronate was observed at 1740 cm^{-1} by IR and free acid at 1709 cm^{-1} . No evidence for the detection of diacyloxyboronate derivatives was reported. Indeed, further investigations are required to determine whether the monoacylboronate (**1-14**) is the active species or whether other species are involved. Furthermore, upon addition of benzyl amine to a toluene solution of (**1-14**), the corresponding amide was produced at room temperature, with up to 50% conversion achieved. It was suggested that the reaction stopped because the intermediate (**1-14**) can be decomposed by hydrolysis. It is believed that the rate-determining step for this catalyzed reaction was the formation of monoacylboronate intermediate (**1-14**),^{45,46} though the intervention and requirement for more activated species can not be ruled out. 3,4,5-Trifluorophenylboronic (**1-12**) is also an effective catalyst for the polycondensation of dicarboxylic acids and diamines.⁴⁷ Direct polycondensation is desirable both environmentally and industrially. The direct condensation between adipic acid and hexamethylenediamine was achieved with 10 mol% of the catalyst (**1-12**) at reflux in *o*-xylene with the presence of 4A molecular sieves in Soxhlet thimble (**Equation 1-4**).⁴⁷ The polyamide product was isolated in 89% yield after 20 h and the average molecular weight number was estimated to be 2680. This result can be increased to 4690 with the use of a 1:3 mixture of *m*-cresol and *o*-xylene.⁴⁷



Equation 1-4: Direct polycondensation of amines and carboxylic acids.

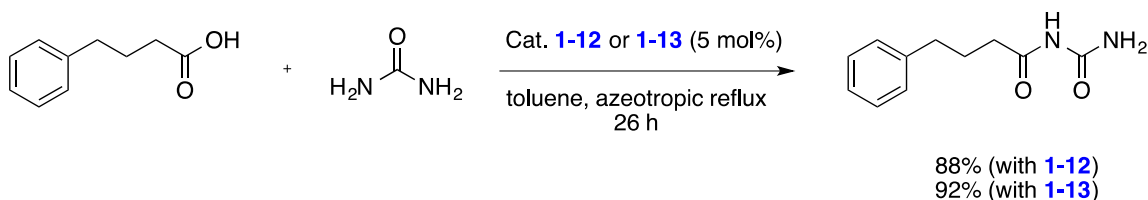
In 2001, the catalytic reactivity of 3,5-bis(perfluorodecyl)phenylboronic acid (**1-15**) and 4-(perfluorodecyl)phenylboronic acid (**1-16**), **Figure 1-6**, was tested in the model

reaction between 4-phenylbutyric acid (1 equiv) and 3,5-dimethylpiperidine (1 equiv) in toluene with removal of water (4A molecular sieves in a Soxhlet thimble) for one hour with a catalyst loading of 5 mol%. Even though the catalytic activity of catalyst **(1-15)** was found to be less active than both **(1-12)** and **(1-13)**, it can be fully recovered by extraction with fluoruous phase and reused with no loss of activity.⁴⁸



Figure 1-6: 3,5-Bis(perfluorodecyl)phenylboronic acid (1-15) and (perfluorodecyl)phenylboronic acid (1-16).

Yamamoto and co-workers have also found that catalysts **1-12** and **1-13** are also effective for the amidation of *N*-acylurea with 4-phenylbutyric acid, which is less nucleophilic than the amines previously screened (**Equation 1-5**).⁴⁹



Equation 1-5: Direct condensation of urea with 4-phenylbutyric acid.

The major disadvantage of these catalysts is the use of elevated temperature, which is not compatible with many functionalized substrates and drugs.⁵⁰ Moreover, their activity is reduced in polar solvents, which restricts the scope of substrates that can be used in this process. In 2000, a polar-solvent-tolerable-catalyst [*N*-alkyl-4-boronopyridinium iodide (**1-17**)] has been demonstrated to be successful for direct amide formation. This compound is much more active than the neutral arylboronic acid catalysts when direct

amidation is achieved in solvents such as anisole, acetonitrile and *N*-methylpyrrolidinone (NMP).⁵¹

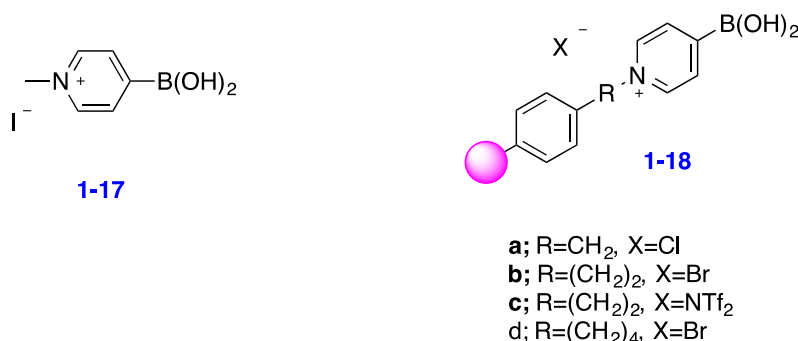
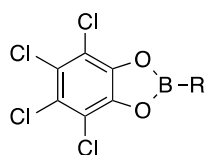


Figure 1-7: Structure of *N*-alkyl-4-boronopyridinium iodide (1-17) and *N*-polystyrene resin-bound 4-boronopyridinium salts (1-18a-d).

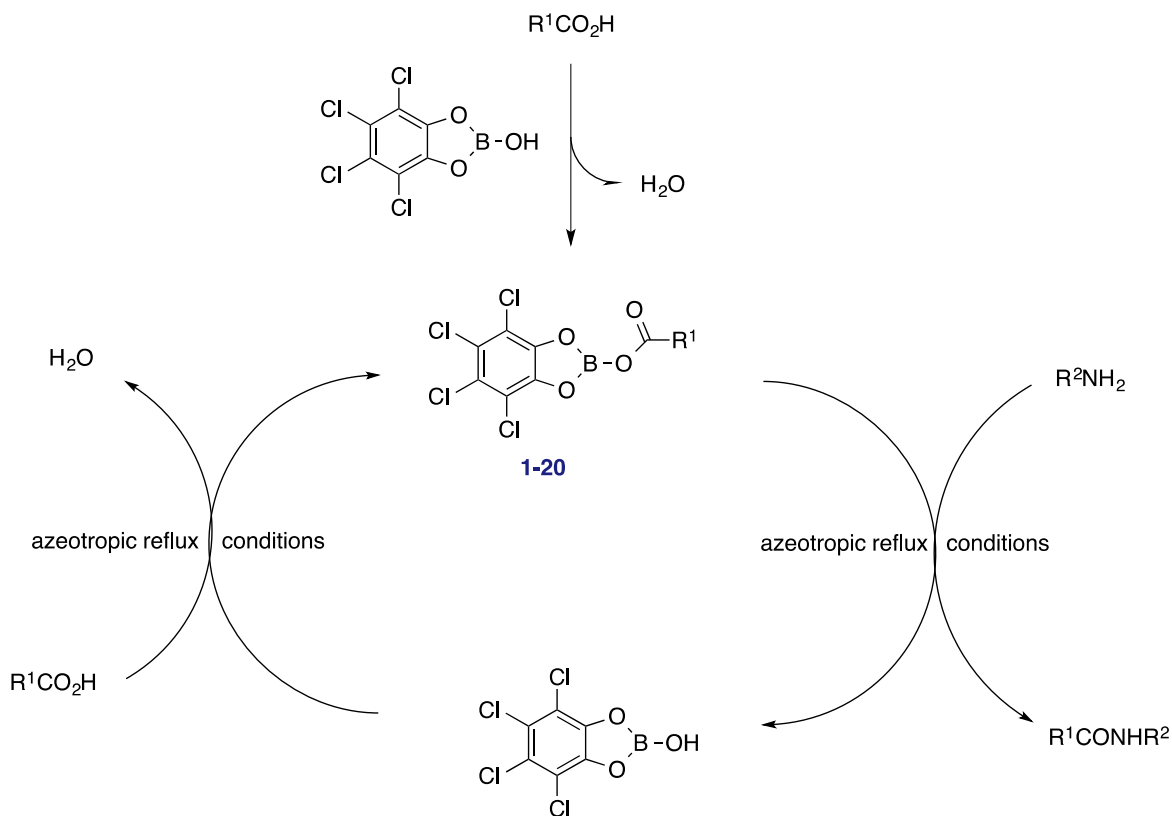
Catalyst **1-17** can be recycled through the use of ionic liquid-toluene biphasic solvents. A resin-bound version of the catalyst has also been developed. *N*-Polystyrene resin-bound 4-boronopyridinium salts (**1-18a-d**) have been produced as heterogeneous catalysts for direct amidation without the need for ionic liquids.^{51,52} Under azeotropic-reflux conditions, the required reaction conditions, a protodeboronation reaction was found to be one of the problems when using these heterogeneous catalysts. Under these harsh conditions, it is expectable that decomposition is taking place to give boric acid and *N*-polystyrene-bound pyridinium salts which indeed limits the long term use of these solid phase catalyst.^{51,52,53} For more sterically demanding carboxylic acids, 4,5,6,7-tetrachlorobenzo[*d*][1,2,3]dioxaborol-2-ol (**1-19b**) was effective as a catalyst for the direct amidation reaction. Yamamoto and co-workers found that compound (**1-19b**) could be used to catalyze direct amidations between equimolar mixtures of carboxylic acids and amines with 5 mol% catalyst loading in refluxing toluene or *o*-xylene (**Figure 1-8**).⁴⁴ The proposed mechanism is shown in **Scheme 1-21**, through formation of **1-20**. It was claimed that catalyst **1-19b** is superior to boric acid for the direct amide formation between aliphatic and aromatic carboxylic acids.⁵³



1-19

a; R= H
b; R= OH

Figure 1-8: 4,5,6,7-Tetrachlorobenzo[*d*][1,2,3]dioxaborole.



Scheme 1-21: Proposed catalytic cycle for direct amide bond formation using 4,5,6,7-tetrachlorobenzo[*d*][1,2,3]dioxaborol **1-19b.**

4,5,6,7-Tetrachlorobenzo[*d*][1,2,3]dioxaborol-2-ol (**1-19b**) displays a similar catalytic activity to 3,5(trifluoromethyl)benzeneboronic acid (**1-13**).^{53, 44} Both catalysts (**1-19a-b**) were effective catalysts for amide condensation.

1.2.2.2.3 Bifunctional Catalysts

Kinetic studies published in 2006 showed that the direct formation of amides from amines and carboxylic acids may occur in the absence of a catalyst under relatively low temperature conditions, but was highly substrate dependent.^{54a} For less reactive carboxylic acids, the presence of a boronic acid (such as **1-12**, **1-21** or **1-22**) or boric acid catalyst greatly improved the yield of amide produced. Initial results indicated that bifunctional catalysts such as **1-22** showed even greater potential (**Figure 1-9**).

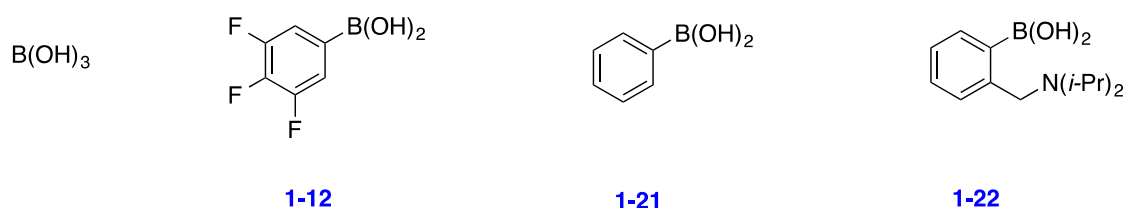


Figure 1-9: Structure of known boron catalysts in the literature.

The bifunctional activity of catalyst **1-22** in assisting certain substrate-dependent reaction was proven in their study.¹⁵ The performance of the catalyzed reactions showed only a slight improvement, with boric acid, **1-12** and **1-22** being close to identical at elevated temperature. To study only the catalytic effects, conditions that minimized the thermal reaction were employed (refluxing fluorobenzene, 85 °C), and showed noticeable improvement over the thermal reaction. For less reactive substrates, the bifunctional catalyst **1-22** was advantageous.^{54a} On the other hand, the more electron-deficient catalyst **1-12** is an effective catalyst for amide formation reactions, and indeed, similar to boric acid, which is also a good general catalyst under the higher temperature conditions. It may well be the case that the combination of both electron deficiency and an intramolecular base may provide more active and more generally applicable catalysts in the future. These findings highlighted many issues that have not been fully addressed in the literature to date.

- Thermolysis of carboxylate ammonium salts in non-polar solvent conditions alone does produce amide products, however, the efficiency is highly substrate- and temperature-dependent.
- The general reactivity of boric acid at higher temperature raises the question as to why this occurs. It is possible that the formation of tetraacyldiborate (**1-23**) or triacylborane species is essential for the catalytic activity of boric acid and that the higher temperature (refluxing toluene) assists catalytic recycling (**Figure 1-10**).^{33,35}

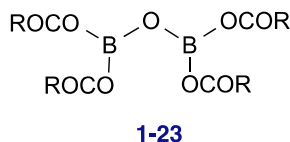
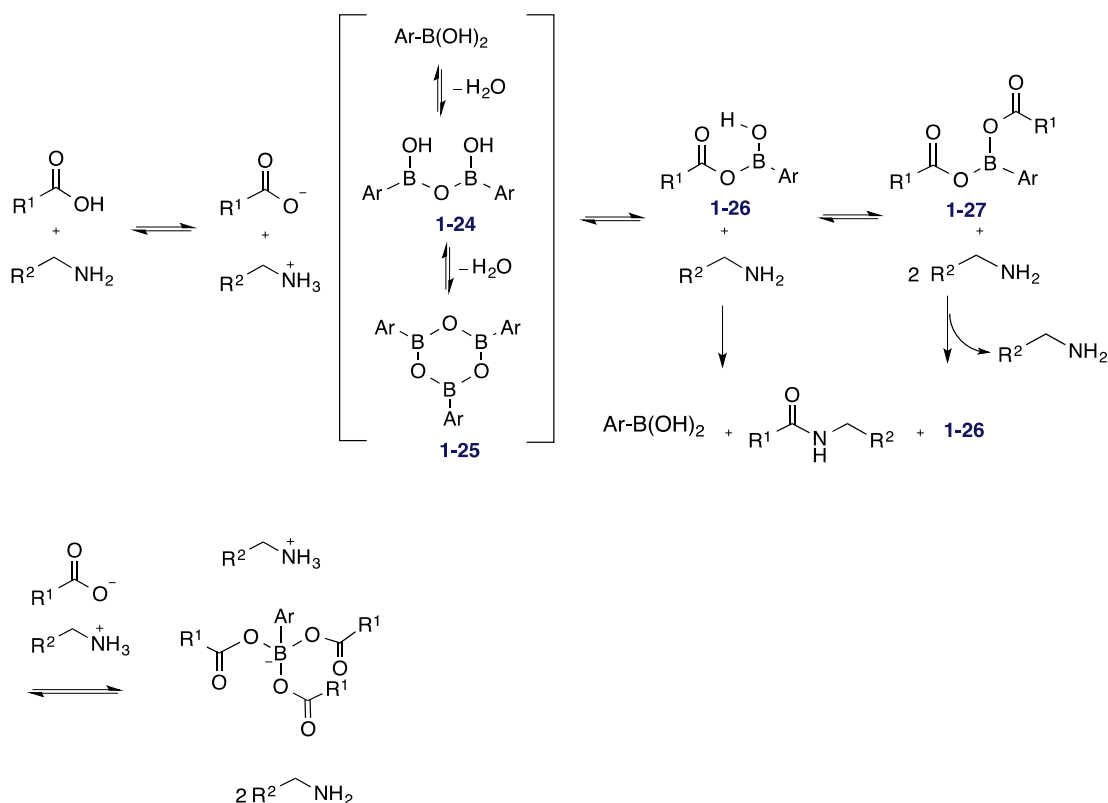


Figure 1-10: Tetraacyldiborate (1-23) intermediate.

- NMR (¹H, ¹³C and ¹¹B) and IR spectroscopic studies are not sufficient to determine exactly which acylating species are produced in these amide formation reactions. However, using ambient, soft ionization electrospray mass spectrometric techniques, several species, including boroxine (**1-25**), diboronate (**1-24**) and monoacyloxyboronate (**1-26**) were detected whereas diacyloxyboronate (**1-27**) was absent (**Scheme 1-22**).^{56,57}

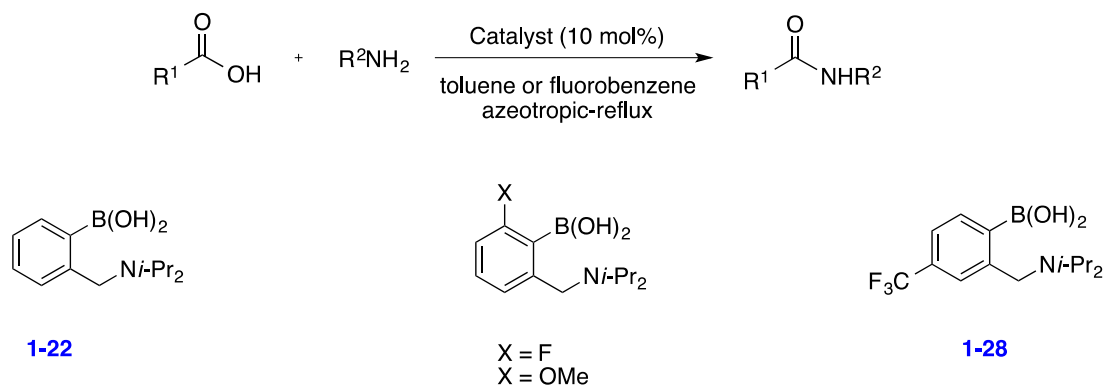


Scheme 1-22: Proposed overall mechanism for amide formation involving either boric or arylboronic acid catalysis.

First-order kinetics for the catalyzed amide formation shows that the reaction proceeds through intermediates. Under catalytic conditions, these are likely to be either **1-26** or **1-27** derived from acylation of the boronic acids. Brown reported the influence of the substituents on the formation of acyloxyboranes from carboxylic acids and boranes, where carboxylic acids with lower pK_a values were shown to slow the formation of acyloxyborane. In other words, the more electron-rich carboxylic acid was inherently more reactive towards formation of the acyloxyboronate, and hence, underwent amide formation more readily.⁵⁵

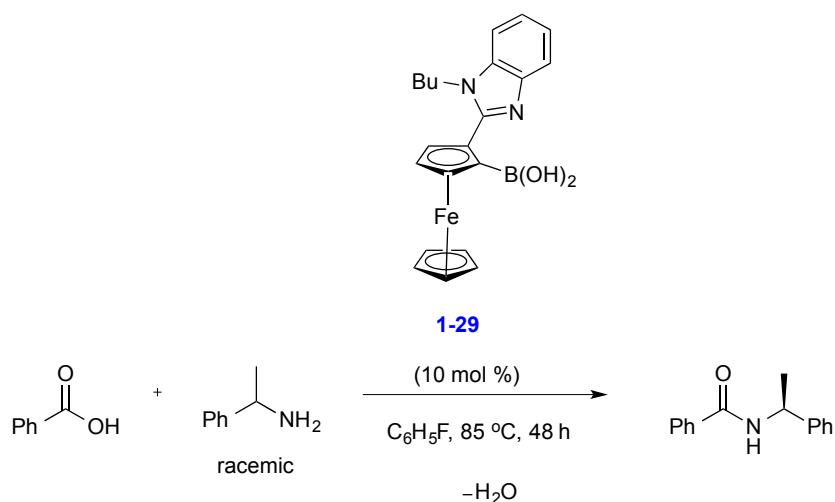
The addition of electron-withdrawing functions to the aryl ring of **1-22**, for example trifluoromethyl derivative **1-28**, certainly results in increased catalytic activity for amide formation, which reinforces the view that such catalysts act by forming mixed

anhydride-type analogues,¹⁵ and the electron withdrawing group increases the leaving group ability during the amide formation step (**Scheme 1-23**).^{54b, 58}



Scheme 1-23: Whiting's bifunctional catalysts for direct amide bond formation.

The first report of an asymmetric direct amide formation *via* kinetic resolution of racemic α -substituted benzylamines with achiral carboxylic acids, using a planar chiral ferrocene based bifunctional amino-boronic acid catalyst, appeared in 2008 (**Equation 1-6**).⁵⁹



Equation 1-6: Asymmetric direct amide formation.

Asymmetric induction is possible under elevated temperature (refluxing fluorobenzene) in the presence of a planar chiral ferrocene based bifunctional amino-boronic acid catalyst (**1-29**). This catalyst is able to select one amine enantiomer of α -chiral benzylamine at the hydrogen bonding stage to provide the desired amide product with low to moderate enantioselectivity, as depicted in (**Figure 1-11**).

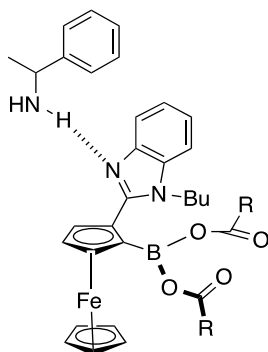


Figure 1-11: Proposed transition state for the enantioselectivity in amidation using catalyst 1-29.

The low enantiomeric excess observed might be explained by the partial degradation of the catalyst by proto-deboronation, coupled with direct background contributions for the more reactive carboxylic acid.⁵⁹

In 2008, Hall and co-workers reported the exceptional ability of *ortho*-bromo- and especially *ortho*-iodophenylboronic acid (**IBA**, **1-30**) to serve as recoverable catalysts for direct amidations under mild conditions at room temperature.⁶⁰ In 2012, the same group found that electron-donating substituents are preferable, in particular, an alkoxy substituent positioned para to the iodide. The optimal new catalyst, 5-methoxy-2-iodophenylboronic acid (**MIBA**, **1-31**), led to a notable increase of product yields for the reactions of a wide variety of carboxylic acids and amines performed under identical reaction times (**Figure 1-12**).⁶¹

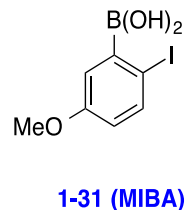
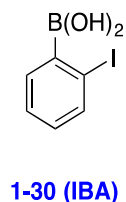
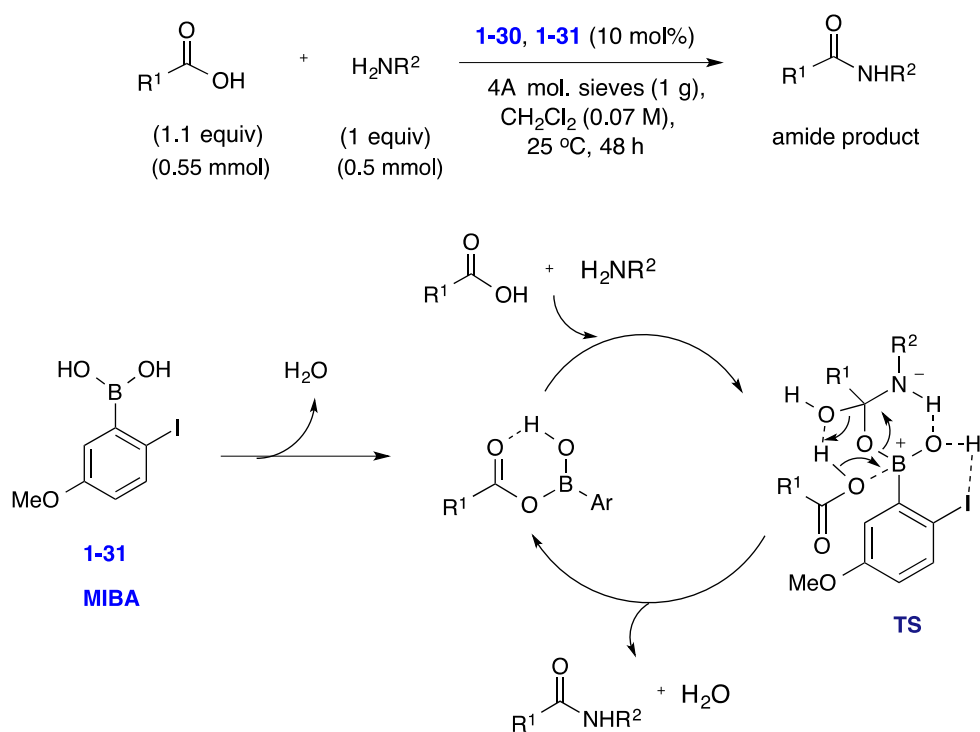


Figure 1-12: New generation of boronic acid catalyst for direct amidation at room temperature.

A mechanistic study confirmed the essential role of molecular sieves and ruled out boronic anhydrides as the active catalyst. It was claimed that the sieves would also exert a second role as a reservoir of water for hydrolyzing boronic anhydrides and maintain a high concentration of free boronic acid.⁶¹ The optimal ring substitution pattern of catalyst **1-30**, with an electron-donating 5-methoxy group (**1-31**), supports a role for the *ortho*-iodo substituent as hydrogen-bond acceptor in the orthoaminal transition structure. According to Marcelli's DFT calculations the remarkable catalytic activity of *ortho*-halophenylboronic acid was rationalized in term of the Lewis basicity of the halogens, that is, their capability to engage in an O-H---X hydrogen bond stabilizing the rate-determining transition state, which is greater for iodine than for chlorine (**Scheme 1-24**).⁶²



Scheme 1-24: Reaction scheme and proposed catalytic cycle for direct ambient amidation catalyzed by MIBA (31).

Because of the reverse trend observed in the *ortho*-halogen series ($I > Br > Cl > F$), inductive effects alone cannot account for the superiority of catalysts (**1-30** and **1-31**) and subtle electronic or structural effects may be at play. The stability order of the intramolecular hydrogen bond might be explained by the geometrical constraints.^{63, 64} A solid-supported version of catalyst of **1-31** was found to be less active than its homogeneous analogue.⁶⁵

1.3 Conclusion

There is a need for simple and effective catalytic methods for amide direct formation from carboxylic acids and amines as a way to avoid the use of coupling reagents. Boron-based catalysts generally work well with a fairly broad substrate scope. The yields are usually high and there are several examples where the catalyst can be recycled without loss of activity. A drawback of many of the boron-based catalysts is that they often

require elevated reaction temperatures, which may result in problems with racemization and limit the substrate scope. There are two notable exceptions of boronic acid catalysts that perform well at room temperature (**IBA, 1-30**) and (**MIBA, 1-31**),^{63, 64} and thus can circumvent the racemization issue. However, in this case, the reactant concentrations must be low and a fairly large amount of molecular sieves is required to drive the reaction, which limits large-scale applications. Although most boronic acids are stable towards water, its removal is crucial to drive the reaction forward for the majority of the methods presented above, which might be troublesome for large-scale applications. Another challenge for the development of new boron-based catalysts includes the catalytic coupling of amino acids and peptides, which to date is limited to dimerization or stoichiometric methods.

1.4 Project Objectives

The objectives of this research are firstly, to develop scalable reaction conditions in a greener fashion and apply this procedure in larger scale preparations. On the other hand, there is a need for superior catalysts to expand the reaction scope. Both of these objectives are discussed in Chapter Two.

One major challenge of amidation methodology is its application in peptide synthesis, which is described in Chapter Three.

1.5 Reference

- (1) (a) Ghose, A. K.; Viswanadhan, V. N.; Wendoloski, J. J. *J. Comb. Chem.* **1999**, *1*, 55. (b) Roughley, S. D.; Jordan, A. M. *J. Med. Chem.* **2011**, *54*, 3451.
- (2) (a) Constable, D. J. C.; Dunn, P. J.; Hayler, J. D.; Humphrey, G. R.; Johnnie L Leazer, J.; Linderman, R. J.; Lorenz, K.; Manley, J.; Pearlman, B. A.; Wells, A.; Zaks, A.; Zhang, T. Y. *Green Chem.* **2007**, *9*, 411.; (b) Carey, J. S.; Laffan, D.; Thomson, C.; Williams, M. T. *Org. Biomol. Chem.* **2006**, *4*, 2337.
- (3) Montalbetti, C. A. G. N.; Falque, V. *Tetrahedron* **2005**, *61*, 10827.
- (4) Valeur, E.; Bradley, M. *Chem. Soc. Rev.* **2009**, *38*, 606.
- (5) Saito, Y.; Ouchi, H.; Takahata, H. *Tetrahedron* **2008**, *64*, 11129.
- (6) Kumar, A.; Akula, H. K.; Lakshman, M. K. *Eur. J. Org. Chem.* **2010**, 2709.
- (7) Li, J.; Subramaniam, K.; Smith, D.; Qiao, J. X.; Li, J. J.; Qian-Cutrone, J.; Kadow, J. F.; Vite, G. D.; Chen, B.-C. *Org. Lett.* **2011**, *14*, 214.
- (8) Tian, J.; Gao, W. C.; Zhou, D. M.; Zhang, C. *Org. Lett.* **2012**, *14*, 3020.
- (9) Orliac, A.; Gomez Pardo, D.; Bombrun, A.; Cossy, J. *Org. Lett.* **2013**, *15*, 902.
- (10) Goodreid, J. D.; Duspara, P. A.; Bosch, C.; Batey, R. A. *J. Org. Chem.* **2014**, *79*, 943.
- (11) Charville, H.; Jackson, D.; Hodges, G.; Whiting, A. *Chem. Commun.* **2010**, *46*, 1813.

- (12) Charville, H.; Jackson, D. A.; Hodges, G.; Whiting, A.; Wilson, M. R. *Eur. J. Org. Chem.* **2011**, 2011, 5981.
- (13) Allen, C. L.; Chhatwal, A. R.; Williams, J. M. J. *Chem. Commun.* **2012**, 48, 666.
- (14) Gooßen, L. J.; Ohlmann, D. M.; Lange, P. P. *Synthesis* **2009**, 1, 160.
- (15) Arnold, K.; Davies, B.; Giles, R. L.; Grosjean, C.; Smith, G. E.; Whiting, A. *Adv. Synth. Catal.* **2006**, 348, 813.
- (16) Perreux, L.; Loupy, A.; Volatron, F. *Tetrahedron* **2002**, 58, 2155.
- (17) Baldwin, B. W.; Hirose, T.; Wang, Z.-H. *Chem. Commun.* **1996**, 2669.
- (18) Gaudino, E. C.; Carnaroglio, D.; Nunes, M. A. G.; Schmidt, L.; Flores, E. M. M.; Deiana, C.; Sakhno, Y.; Martra, G.; Cravotto, G. *Catal. Sci. Technol.* **2014**, 4, 1395.
- (19) Lundberg, H.; Tinnis, F.; Adolfsson, H. *Synlett* **2012**, 23, 2201.
- (20) Lundberg, H.; Tinnis, F.; Adolfsson, H. *Chem. Eur. J.* **2012**, 18, 3822.
- (21) Reddy, C. S.; Nagaraj, A.; Jalapathi, P. *Chin. Chem. Lett.* **2007**, 18, 1213.
- (22) Mohan, K. V. V. K.; Narender, N.; Kulkarni, S. J. *Green Chem.* **2006**, 8, 368.
- (23) Sarvari, M. H.; Sharghi, H. *J. Org. Chem.* **2006**, 71, 6652.
- (24) Thakuria, H.; Borah, B. M.; Das, G. *J. Mol. Catal. A: Chem.* **2007**, 274, 1.
- (25) Reddy, M. B. M.; S.; Ashoka, G. T.; Chandrappa G.T.; Pasha, M. A. *Catal. Lett.*

2010, *138*, 82–87.

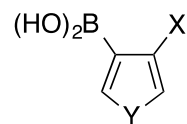
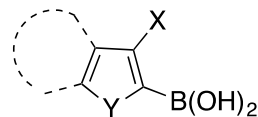
- (26) Pathare, S. P.; Jain, A. K. H.; Akamanchi, K. G. *Green Chem.* **2010**, *12*, 1707.
- (27) Pathare, S. P.; Sawant, R. V.; Akamanchi, K. G. *Tetrahedron Lett.* **2012**, *53*, 3259.
- (28) Terada, Y.; Ieda, N.; Komura, K.; Sugi, Y. *Synthesis* **2008**, *15*, 2318.
- (29) Likhari, P. R.; Arundhati, R.; Ghosh, S.; Kantam, M. L. *J. Mol. Catal. A: Chem.* **2009**, *302*, 142.
- (30) Kim, J. G.; Jang, D. O. *Bull. Korean Chem. Soc.* **2010**, *31*, 2989.
- (31) Comerford, J. W.; Clark, J. H.; Macquarrie, D. J. *Chem. Commun.* **2009**, 2562.
- (32) Hosseini-Sarvari, M.; Sodagar, E.; Doroodmand, M. M. *J. Org. Chem.* **2011**, *76*, 2853.
- (33) (a) Pelter, A.; Levitt, T. E. *Tetrahedron* **1970**, *26*, 1899. (b) Nelson, P.; Pelter, A. *J. Chem. Soc.* **1965**, 5142.
- (34) Pelter, A.; Levitt, T. E.; Nelson, P. *Tetrahedron* **1970**, *26*, 1539.
- (35) A. Pelter, T. E. Levitt, *Tetrahedron* **1970**, *26*, 1545.
- (36) (a) Starkov, P.; Sheppard, T. D. *Org. Biomol. Chem.* **2011**, *9*, 1320; (b) Lanigan, R. M.; Starkov, P. *J. Org. Chem.* **2013**, *78*, 4512.
- (37) Trapani, G.; Reho, A.; Latrofa, A.; *Synthesis* **1983**, 1013.
- (38) Collum, D. B.; Chen, S. C.; Ganem, B. *J. Org. Chem.* **1978**, *43*, 4393.

- (39) Yang, W.; Gao, X.; Springsteen, G.; Wang, B. *Tetrahedron Lett.* **2002**, 43, 6339.
- (40) Tang, P. *Org. Synth.* **2005**, 81, 262.
- (41) Hayter, R. G.; Laubengayer, A. W.; Thompson, P. G. *J. Am. Chem. Soc.* **1957**, 79, 4243.
- (42) Anderson, G. W.; Paul, R. *J. Am. Chem. Soc.* **1958**, 80, 4423.
- (43) Mylavarapu, R. K.; Kondaiah, G. K.; Kolla, N.; Veeramalla, R.; Koilkonda, P.; Bhattacharya, A.; Bandichhor, R. *Org. Process Res. Dev.* **2007**, 11, 1065.
- (44) Toshikatsu Maki; Kazuaki Ishihara, A.; Hisashi Yamamoto. *Org. Lett.* **2006**, 8, 1431.
- (45) Ishihara, K.; Ohara, S.; Yamamoto, H. *J. Org. Chem.* **1996**, 61, 4196.
- (46) Ishihara, K.; Ohara, S.; Yamamoto, H. *Org. Synth.* **2004**, 10, 80.
- (47) Ishihara, K.; Ohara, S.; Yamamoto, H. *Macromolecules* **2000**, 33, 3511.
- (48) Ishihara, K.; Kondo, S.; Yamamoto, H. *Synlett* **2001**, 9, 1371.
- (49) Maki, T.; Ishihara, K.; Yamamoto, H. *Synlett* **2004**, 8, 1355.
- (50) Jursic, B. S.; Zdravkovski, Z. *Synth. Commun.* **1998**, 28, 1093.
- (51) Maki, T.; Ishihara, K.; Yamamoto, H. *Org. Lett.* **2005**, 7, 5043.
- (52) Latta, R.; Springsteen, G.; Wang, B. *Synthesis*, **2001**, 11, 1611.

- (53) Ishihara, K. *Tetrahedron* **2009**, *65*, 1085.
- (54) (a) Arnold, K.; Davies, B.; Giles, R. L.; Grosjean, C.; Smith, G. E.; Whiting, A. *Adv. Synth. Catal.* **2006**, *348*, 813. (b) Arnold, K.; Batsanov, A. S.; Davies, B.; Whiting, A. *Green Chemistry* **2008**, *10*, 124.
- (55) Brown, H. C.; Stocky, T. P. *J. Am. Chem. Soc.* **1977**, *99*, 8218.
- (56) Bruins, A. P.; Covey, T. R.; Henion, J. D. *Anal. Chem.* **1987**, *59*, 2642.
- (57) Whitehouse, C. M.; Dreyer, R. N.; Yamashita, M. *Anal. Chem.* **1985**, *57*, 675.
- (58) Georgiou, I.; Ilyashenko, G.; Whiting, A. *Acc. Chem. Res.* **2009**, *42*, 756.
- (59) Arnold, K.; Davies, B.; Hérault, D.; Whiting, A. *Angew. Chem. Int. Ed.* **2008**, *47*, 2673.
- (60) Al-Zoubi, R. M.; Marion, O.; Hall, D. G. *Angew. Chem. Int. Ed.* **2008**, *47*, 2876.
- (61) Gernigon, N.; Al-Zoubi, R. M.; Hall, D. G. *J. Org. Chem.* **2012**, *77*, 8386.
- (62) Marcelli, T. *Angew. Chem. Int. Ed.* **2010**, *49*, 6840.
- (63) Kovács, A.; Varga, Z. *Coord. Chem. Rev.* **2006**, *250*, 710.
- (64) Brammer, L.; Bruton, E. A.; Sherwood, P. *Cryst. Growth Des.* **2001**, *1*, 277.
- (65) Gernigon, N.; Zheng, H.; Hall, D. G. *Tetrahedron Lett.* **2013**, *54*, 4475.

Search for An Improved Catalytic System for the Direct Amide-Bond Formation and Scale-up Studies

In this chapter, heteroareneboronic acids are examined in order to identify a better catalyst for direct amide bond formation. The first section presents the synthesis and comparative studies of this class of catalysts in the direct amidation reaction. In the second section, the effect of additives is investigated. After which, the implication of the Staudinger reaction towards direct amidation using boronic acid catalysts is examined. Then, the last section reports the results of a scale-up feasibility study, where reactions were achieved at lower dilution and with a lesser amount of molecular sieves.



Y = O, S

2.1 Introduction

Our group is interested in developing a highly efficient boronic acid catalyst that could activate carboxylic acids for reaction with amines to form amides at room temperature. In 2012, it was shown with the MIBA catalyst (**1-31**) that an increased electron density of the iodo substituent by the addition of a methoxy group in the *para* position of the arylboronic acid framework increased both the yield and reaction rate of the amidation (**Figure 2-1**).¹ Based on these results, electron rich heterocycles were designed and tested as potentially more reactive catalysts. In other words, increasing the electron density in the aromatic backbone of the catalyst appeared to increase the nucleophilicity of the iodo substituent without adversely affecting boron's Lewis acidity. It was then rationalized that changing the aromatic backbone using different aromatic rings, such as heteroarenes that are known to be more electron-rich than cyclohexatriene systems, could enhance the

catalytic reactivity. However, this characteristic may impact the stability profile of arylboronic acid catalysts due to the occurrence of *ipso*-deboronation.

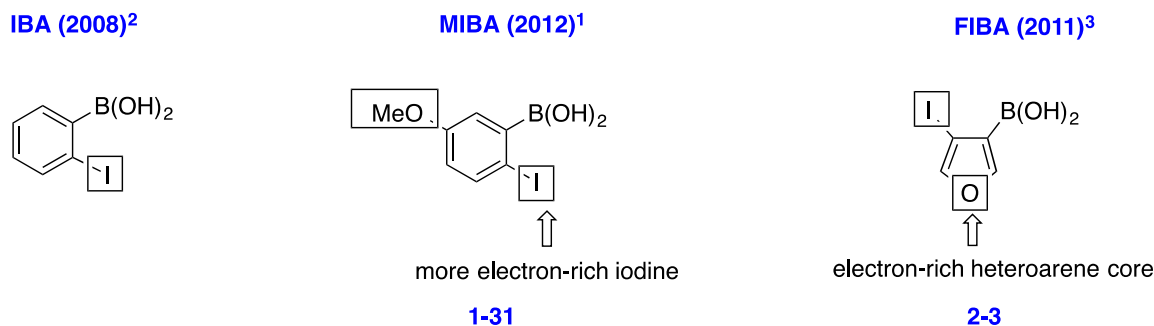


Figure 2-1: Evolution of catalysts in the direct ambient amidation.

2.2 Results

The remarkable catalytic activity of *ortho*-halophenylboronic acids was rationalized in terms of the Lewis basicity of the halogens, that is, their capability to engage in O-H \cdots X hydrogen bonds that can stabilize the rate-determining transition state, an effect that would be greater for iodine than for other halogens.⁴ As explained in Chapter One, electron-rich *ortho*-iodoarylboronic acids were claimed to be more active catalysts than the neutral *ortho*-iodoarylboronic acid (**IBA**) in direct amide bond formation. Following a previous report by Al-Zoubi and Hall,³ it was rationalized that changing the aromatic backbone on these catalysts, and using more electron-rich heteroarenes compared to the cyclohexatriene framework, could enhance the catalytic reactivity in direct amide bond formation. Further electronic and steric modifications may affect the catalytic reactivity of this class of catalysts. On the basis of the above rationale, some additional potential catalysts were designed and their activity was screened in model amidation reactions.

2.2.1 Design of Third Generation Catalysts for Direct Amide Bond Formation

To further investigate and optimize the electronic and steric effects of 4-iodo-3-furanboronic acid, FIBA catalyst (**2-3**), different heterocyclic boronic acids (**Figure 2-2**)

were designed and synthesized. Since different heteroaromatic rings can affect the catalytic activity of this system towards direct amide bond formation, thiophene boronic acids such as **2-5** were considered as well for this purpose.

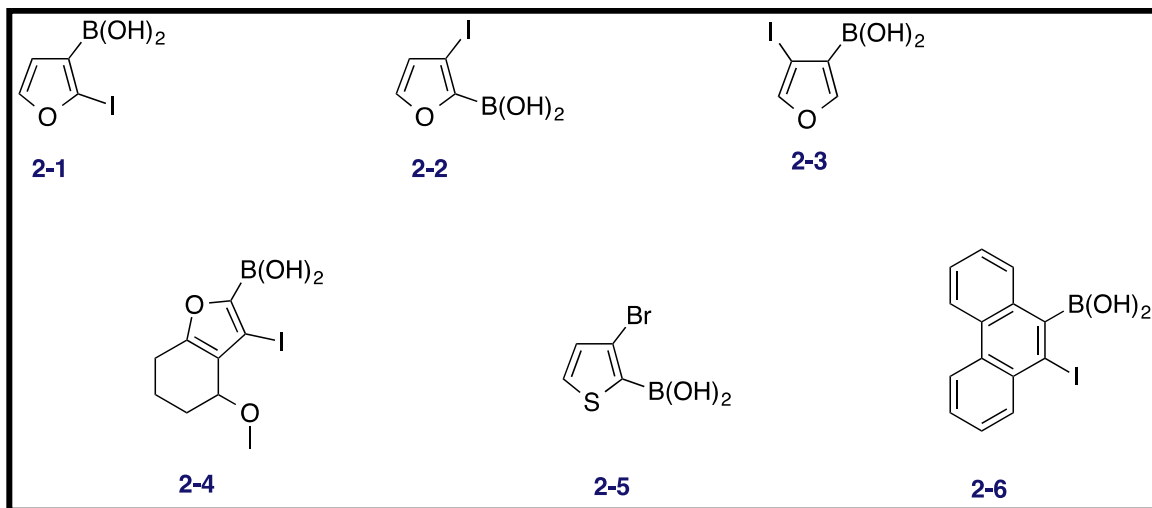
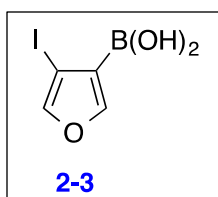


Figure 2-2: Proposed *ortho*-functionalized heterocyclic boronic acids.

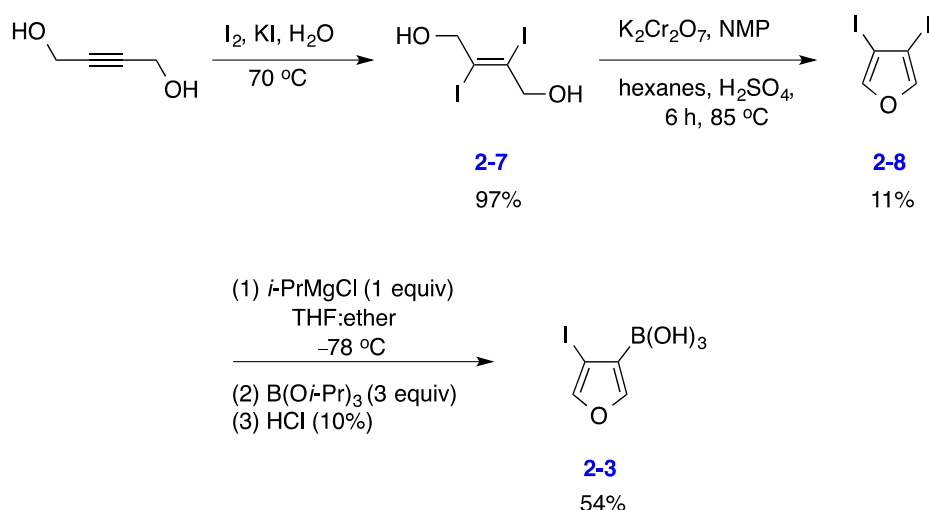
It is believed that the electronic property of various heterocycles influences the Lewis acidity of boron and nucleophilicity of the halogen. In order to confirm this rationale, the synthesis of target catalysts shown in **Figure 2-2** was planned so that they could be subjected to comparative studies of direct amidation reactions. Among the catalysts shown in **Figure 2-2**, only catalysts **2-3** and **2-5** were successfully synthesized.

Previous studies suggest that a precise distance between the iodide atom and the B(OH)_2 group is needed in order to optimize the catalyst's reactivity. A smaller distance did not improve the catalyst reactivity.¹ It can also be envisaged that a farther distance between the iodide and the boron atom may be desirable. To explore this possibility, we hypothesized that a catalyst such as **2-6** may demonstrate improved catalytic reactivity.

2.2.1.1 Synthesis of 4-Iodo-3-Furanboronic Acid (**2-3**)

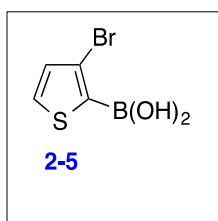


Following the procedure reported by Al-Zoubi,³ catalyst **2-3** was synthesized through a metalation reaction of the diiodo precursor **2-8** using *isopropylmagnesium chloride* followed by trapping with the triisopropyl borate reagent in three steps (**Scheme 2-1**).⁵ The overall yield of the reaction was low (only 11% in the second step). Attempts to improve the reaction yield in the second step were made using mono-protected diol for oxidation.

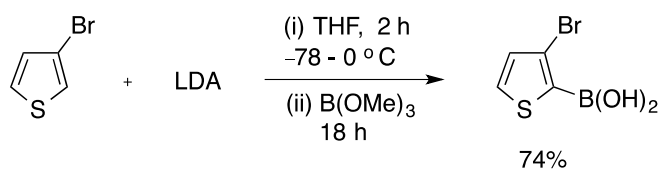


Scheme 2-1: Synthesis of 4-iodo-3-furanboronic acid (FIBA).

2.2.1.2 Synthesis of 3-Bromo-2-Thienylboronic Acid (**2-5**)



The desired boronic acid was obtained by a simple regioselective deprotonation followed by borate trapping as described in **Scheme 2-2**.⁶ The temperature is important to obtain a high regioselectivity. At $-78\text{ }^\circ\text{C}$, deprotonation of 3-bromothiophene occurred at both α -positions of the thiophene ring, but as the temperature increased to $0\text{ }^\circ\text{C}$, the reaction showed greater selectivity for deprotonation at position 2.⁷

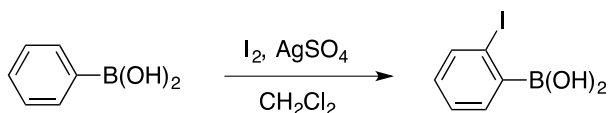


Scheme 2-2: Synthesis of 3-bromo-2-thienylboronic acid (2-5).

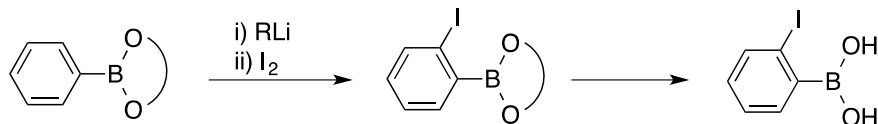
2.2.1.3 Attempts to Synthesize other Designed Boronic Acids

There are three approaches to the synthesis of *ortho*-iodoarylboronic acid: (1) a direct electrophilic iodination of arylboronic acids, (2) a directed *ortho*-metalation followed by iodine trapping and (3) electrophilic borate trapping of an arylmetal intermediate from *ortho*-diiodobenzene (**Scheme 2-3**).

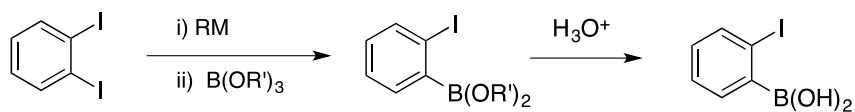
1. Electrophilic iodination of phenylboronic acid.



2. Electrophilic iodine trapping of an arylboronate intermediate from directed *ortho*-lithiation.



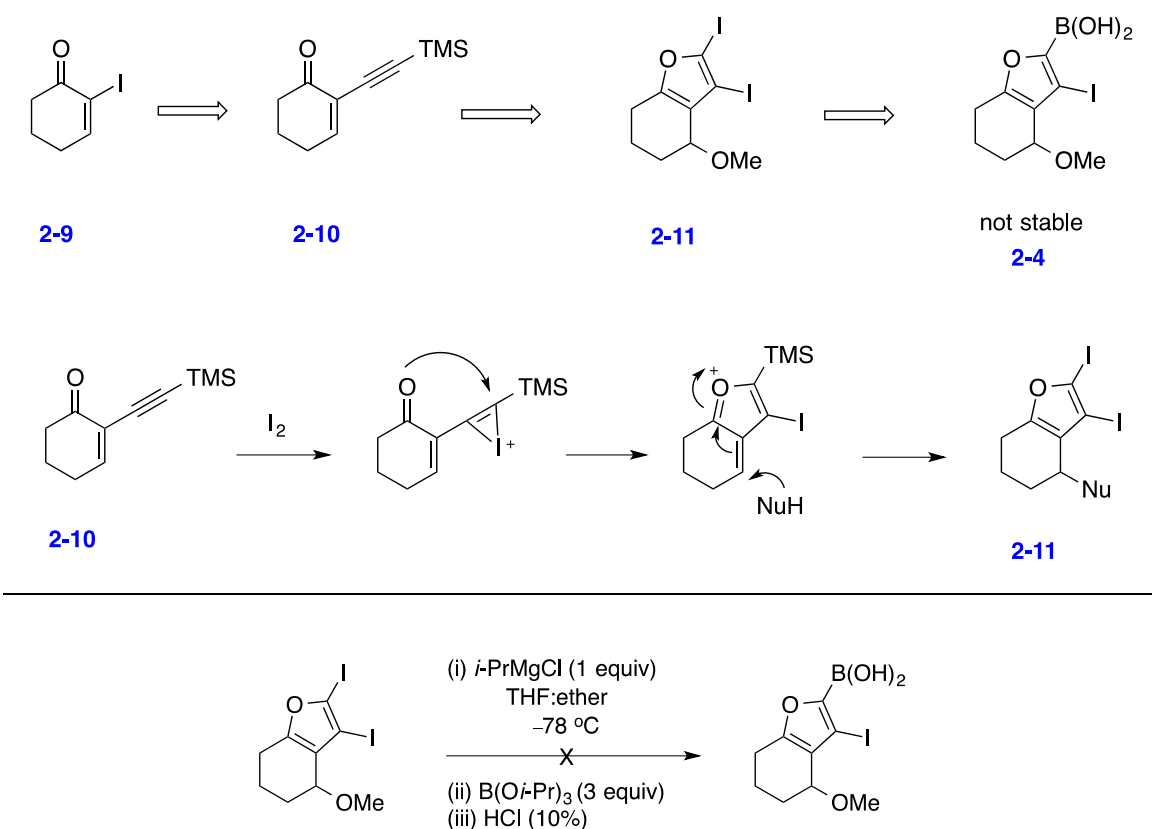
3. Electrophilic borate trapping of an arylmetal intermediate from *ortho*-diiodobenzene.



Scheme 2-3: Three potential ways to synthesize *ortho*-iodoarylboronic acid.

2.2.1.3.1 Attempted Synthesis of 2-4

The synthesis of **2-4** commenced with the commercially available 2-iodo-2-cyclohexen-1-one alkene (**2-9**) followed by Sonogashira coupling, and the resulting product (**2-10**) was then reacted with I_2 to convert it to the diiodo-furan precursor **2-11**. Surprisingly, a selective metalation followed by triisopropyl borate trapping did not provide the arylboronic acid **2-4**.⁸ Decomposition was observed after purification of the reaction mixture using column chromatography in the last step.

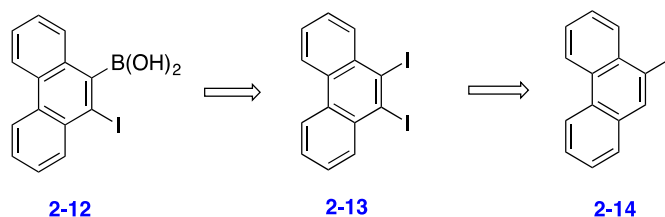


Scheme 2-4: Retrosynthetic analysis and reaction scheme for boronic acid 2-4.

2.2.1.3.2 Attempted Synthesis of *Ortho*-Iodo-Phenanthreneboronic Acids (**2-12**)

2.2.1.3.2.1 Diiodo Approach

The synthesis of **2-12** was based on a selective metalation with Grignard reagent followed by a borate trapping approach (**Scheme 2-5**). Prior to this step, the diiodo compound **2-13** needs to be synthesized from the commercially available monoiodo precursor **2-14**.



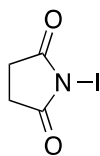
Scheme 2-5: Retrosynthetic pathway for catalyst 2-12.

The preparation of **2-13** can be very challenging and several factors have to be considered. It is generally not possible to perform direct iodination with elemental iodine, even if electron-rich aromatic compounds are utilized under the usual electrophilic iodine trapping conditions. In this case, reactive iodonium ion needs to be employed to synthesize compound **2-13**. It is noteworthy that the monoiodo-phenanthrene is less reactive than phenanthrene towards the electrophile (iodonium ion).

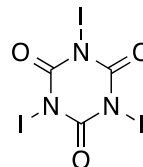
Other reactive iodonium reagents were tested for the formation of 9,10-diiodophenanthrene from mono-iodophenanthrene and are listed below.

1- NIS (*N*-iodosuccinimide) activated by trifluoromethanesulfonic acid in catalytic or stoichiometric quantities has been found to be useful in generating electrophilic iodonium.⁹ This method however, did not provide the desired diiodophenanthrene.

2- A successful iodination reaction afforded the required diiodo intermediate **2-13** using the reactive electrophilic iodonium reagents. Both TICA (triiodoisocyanuric acid) in acidic medium,¹⁰ and Pb₃O₄-iodine-CF₃COOH¹¹ were capable of performing the desired transformation (**Figure 2-3**).



NIS

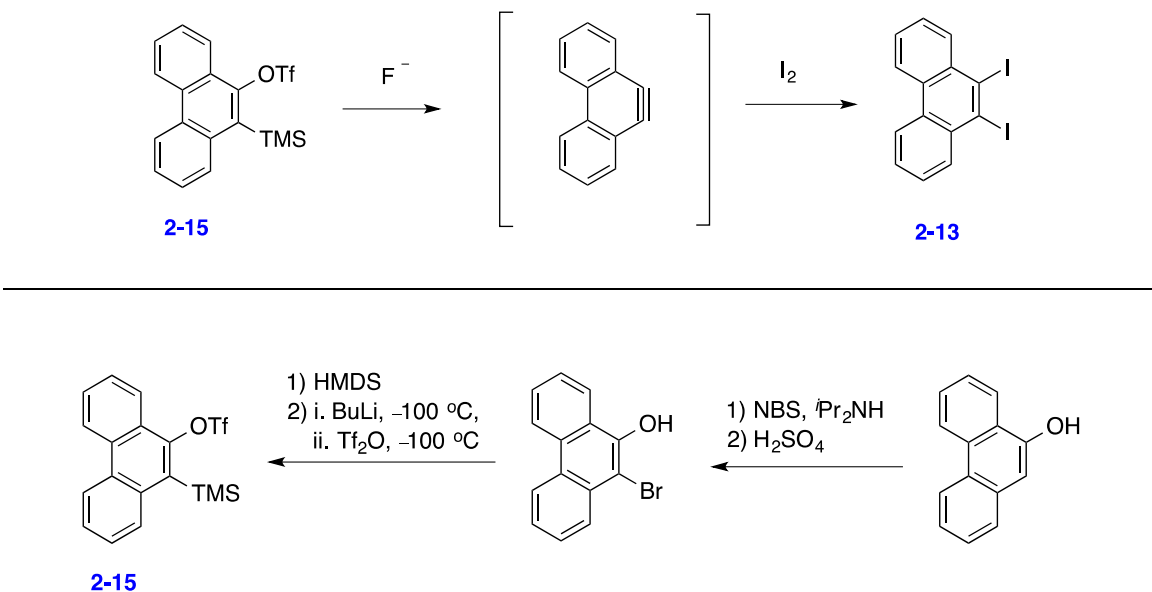


TICA

Figure 2-3: Electrophilic iodinating reagents.

These methods, however, led a mixture of di- and mono-iodophenanthrene (1:4), which was determined from gas chromatography (GC-MS). The desired di-iodophenanthrene was not separated since the product and starting material have the same R_f values based on thin layer chromatography (TLC).

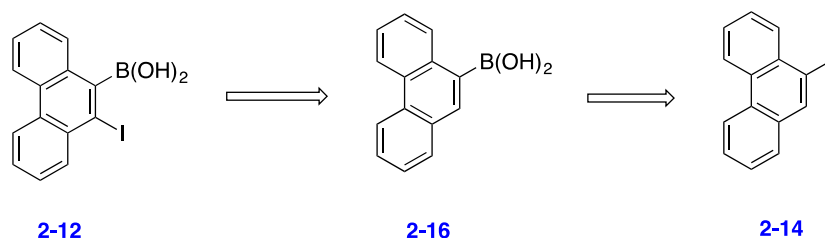
Another alternative approach that may be considered for future studies is shown in **Scheme 2-6**. In 2012, the insertion of arynes into the I-I σ -bond was developed to synthesize **2-13**.¹² In order to achieve this plan, *ortho*-trialkylsilylaryl triflate (**2-15**) first needs to be synthesized in two steps based on previously reported procedures.¹³



Scheme 2-6: A possible alternate route for synthesizing *ortho*-iodophenanthreneboronic acids (2-6).

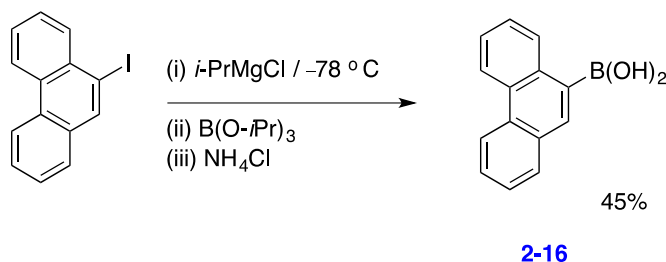
2.2.1.3.2.2 Directed *Ortho*-Iodination of Boronic Acids or Esters

Another retrosynthetic pathway is shown in **Scheme 2-7**, which involves the synthesis of the boronic acid or ester followed by halogenation. Unfortunately, the undesired *ipso*-displacement of boron was observed in the second step.



Scheme 2-7: Another retrosynthetic pathway for catalyst 2-12.

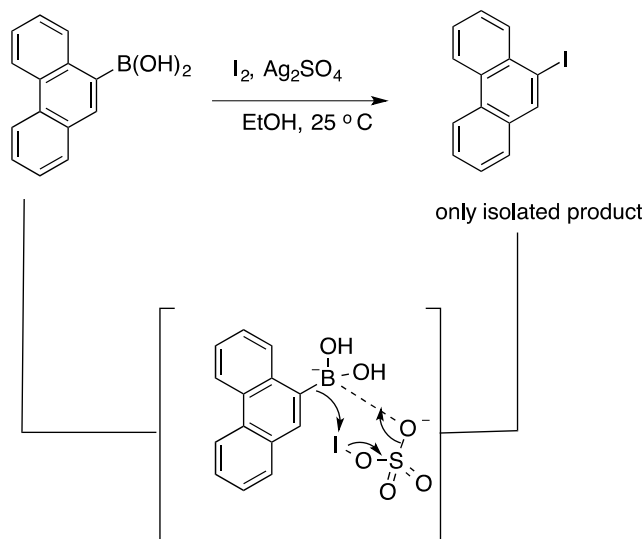
The first step was straightforward, selective metalation followed by borate trapping was successful (45% yield of the product) (**Scheme 2-8**).¹⁴



Scheme 2-8: Preparation of phenanthrene 9-boronic acid (2-16).

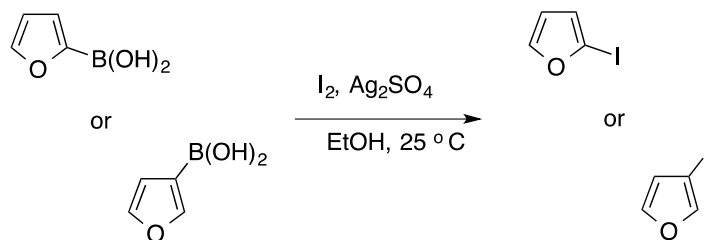
The next step did not give the desired *ortho*-iodoarylboronic acid (**2-12**). The conversion of boron to a borate species via the addition of an external nucleophile may lead to an intermolecular transfer of the alkenyl moiety to the electrophilic halogen (**Scheme 2-9**).¹⁵ The Lewis acidic nature of boronic acids makes them prone to react with commonly used organic reagents, such as strong acids, bases, oxidants, and metal salts. This reactivity typically causes a simple protodeboronation or a substitution of the boronic acid group to

form other products, such as haloarenes.¹⁶⁻²⁰



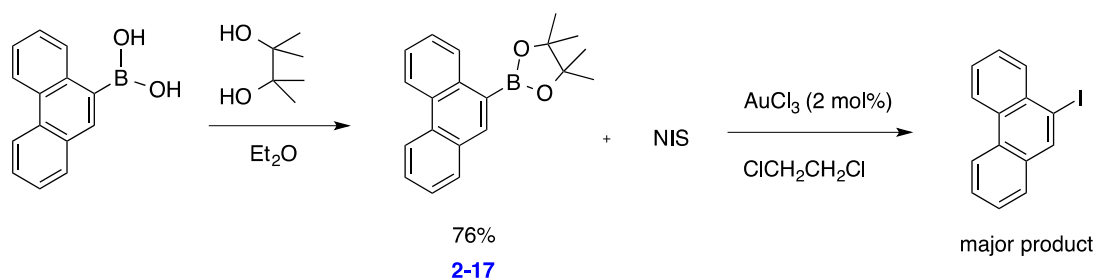
Scheme 2-9: Proposed mechanism for *ipso* displacement of boron.

The same phenomenon was observed in furan boronic acids **2-1** and **2-2**, the desired *ortho*-iodoarylboronic acid was not obtained (**Scheme 2-10**).



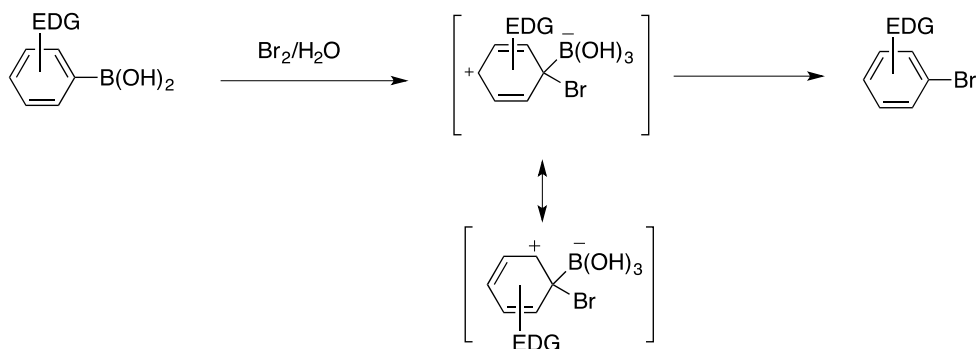
Scheme 2-10: *Ipsso*-displacement of boron.

Since boronic esters are known to be more persistent in *ipso*-displacement of boron with electrophile, a method developed by Jianbo Wang using AuCl_3 -catalyzed iodination of aromatic boronates with *N*-iodosuccinimides was chosen to synthesize the desired catalyst **2-12**.²¹ However, 9-iodophenanthrene was again obtained instead of the desired *ortho*-iodoarylboronic acid (**Scheme 2-11**).



Scheme 2-11: Preparation of pinacolboronate and regioselective iodination.

All the transformations shown above are believed to proceed via boron activation followed by an *ipso* displacement mechanism. The general *ipso* displacement mechanism follows the S_E2 pathway as shown in **Scheme 2-12**. This reaction is accelerated with the use of electron rich heterocycles.^{22, 23}

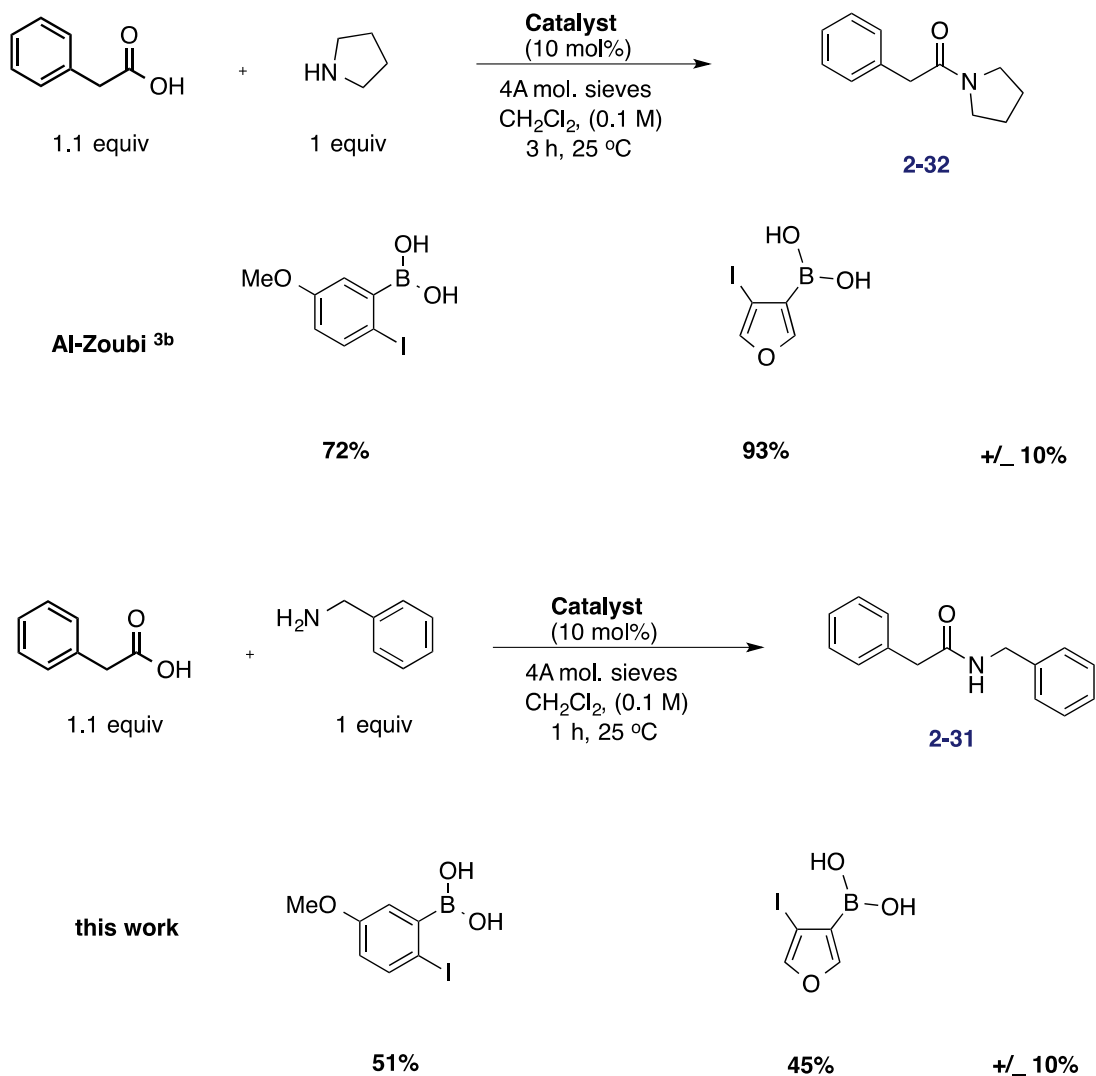


Scheme 2-12: General mechanism of boron ipso displacement.

2.2.1.4 Screening of the Heteroareneboronic Acids

It was shown before that the presence of FIBA catalyst **2-3** led to a relatively faster catalyzed amidation reaction providing a higher product yield in the more challenging model amidation reactions.³ In my own hands, however, a side-by-side evaluation of MIBA (**1-31**) and FIBA (**2-3**) using the other model amidation reaction did not show significant superior activity of FIBA when compared to MIBA (**Scheme 2-13**).

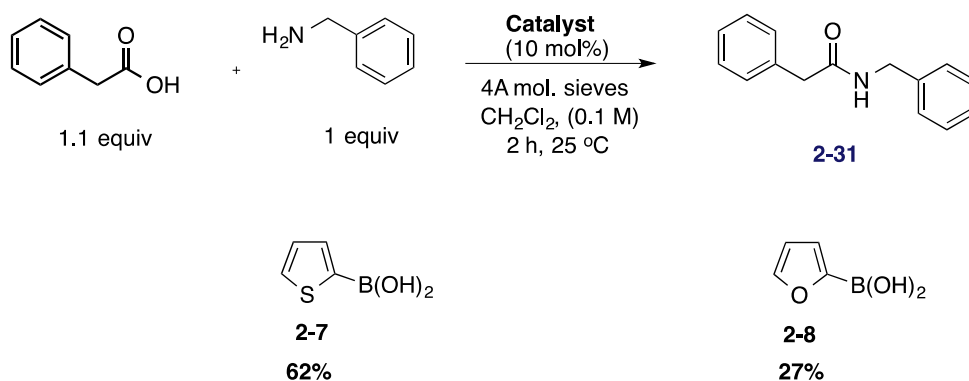
In order to evaluate the catalyst's performance, we usually employ two model amidation reactions, one between phenylacetic acid and pyrrolidine (the less reactive amine, slower reaction so required more time, 3 h) and one with benzylamine (the more reactive amine, faster reaction so required less time, 1 h) (**Scheme 2-13**).



Scheme 2-13: Examining the catalytic reactivity of MIBA (1-31) and FIBA (2-3) on direct amide bond formation.

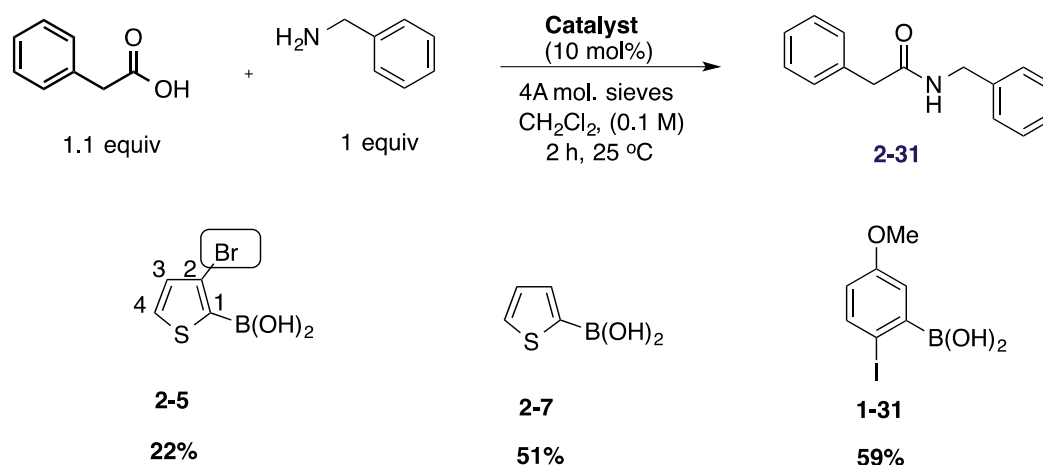
Next, the effect of other heterocycles (more electron-rich heteroareneboronic acids) was examined. In particular, the reactivity of a thiophene ring was investigated and compared with the furan ring (**Scheme 2-14**). Based on the obtained yields, 2-thiopheneboronic acid

provided a 51% yield of amide product while the boronic acid having the furan ring gave a 45% yield. These results demonstrated a little improved activity for 2-thiopheneboronic acid.



Scheme 2-14: Comparison of product yields of catalysts MIBA (1-31) and electron-rich heteroareneboronic acids in a direct amidation reaction.

In order to determine the effect of halogen, catalyst **2-5** containing a bromide group at position two (next to boronic acid) was synthesized. The relative activities of 2-bromothiopheneboronic acid (**2-5**), unsubstituted thiopheneboronic acid (**2-7**), and 2-iodoarylboronic acid (**1-31**, **MIBA**) were evaluated using the model amidation reaction between phenylacetic acid and benzylamine with 10 mol% catalyst loading. The set of reaction mixtures was monitored after one hour and it was found out that *ortho*-bromothiopheneboronic acid (**2-5**) did not display a superior activity (**Scheme 2-15**). Thus, bromide substitution at position two next to the boronic acid group provided no improvement of the catalytic activity (**Scheme 2-15**, **2-5**). It is noticeable that boron Lewis acidity is less in position two than three. A plausible explanation for this result is the occurrence protodeboronation of catalyst **2-5** as observed based on ^1H NMR analysis. The coupling of H_1 (as a result of protodeboronation) with the other thiophene hydrogens (H_{2-3}) appeared on ^1H NMR.



Scheme 2-15: Screening of *ortho*-bromoheteroarylboronic acids as catalysts in direct amide bond formation.

Two other possible positions on the aromatic ring scaffold, positions 2 and 3, are available for further manipulation. Provided that the catalyst is stable enough, small electronic changes of the boronic acid particularly at carbon three of the heteroarene ring in catalyst **2-5** might enhance the catalyst reactivity towards direct amide bond formation (**Figure 2-4**).

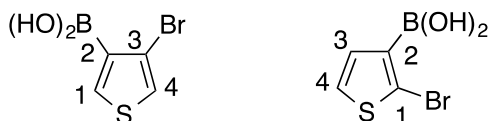


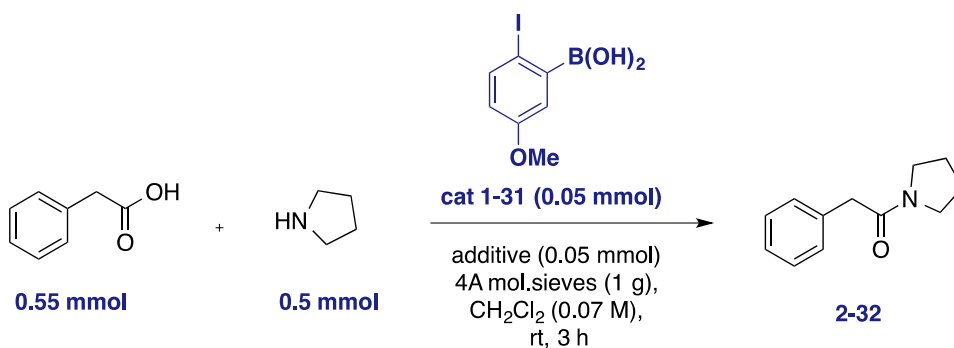
Figure 2-4: Other proposed thiophene boronic acids.

2.2.2 Effect of Additives

To further improve direct amide bond formation, we anticipated that the addition of catalytic amounts of activators as additives might lead to higher reaction efficiency. We tested different Lewis acids for their ability to further activate the carbonyl group of the carboxylic acid moiety or to make the acylborate a better leaving group.

2.2.2.1 Lewis Acids

Group (IV) metal complexes are generally used as catalysts in esterification of carboxylic acids with alcohols.²⁴⁻³⁰ The combination of $\text{Zr}(\text{O}t\text{-Bu})_4$ and HOAt facilitates a smooth conversion of carboxylic acids and amines into amide products.³¹ In 2011, Williams and coworkers found that zirconium complexes such as ZrCl_4 were efficient catalysts for direct amidation of carboxylic acids with primary and secondary amines.^{34,35} Furthermore, Lewis acidic metal triflates/halides and bifunctional metal alkoxides were found to be superior catalysts for the process of preparation of amides from unactivated esters and amines.³⁴ Based on these previous reports, early transition-metal complexes were then utilized as additives in the model amidation reaction and the results are presented in **Table 2-1** (the ratio of the additive and the catalyst **1-31** is 1:1). The reaction time was kept short (3 h) in order to be able to note a significantly improved yield over the control run without additive (**entry 1**).



Entry	Additive	Yield (%) ^a
1	none	25
2	$\text{Ti}(\text{O}i\text{-Pr})_4$ ^{31, 34}	30
3	$\text{Sc}(\text{OTf})_3$ ³³	35
4	ZrCl_4 ^{34, 35}	18
5	$\text{Zr}(\text{O}t\text{-Bu})_4$ ³⁴	35

6	Yb(OTf) ₃	22
7	ZnCl ₂ ³²	15
8	Zn(OTf) ₂ ³²	15
9	Zn(OAc) ₂	10
10	Cu(OTf) ₂ ³⁶	35
11	CuI	25
12	In(OTf) ₃ ³²	20
13	In(OH) ₃	18

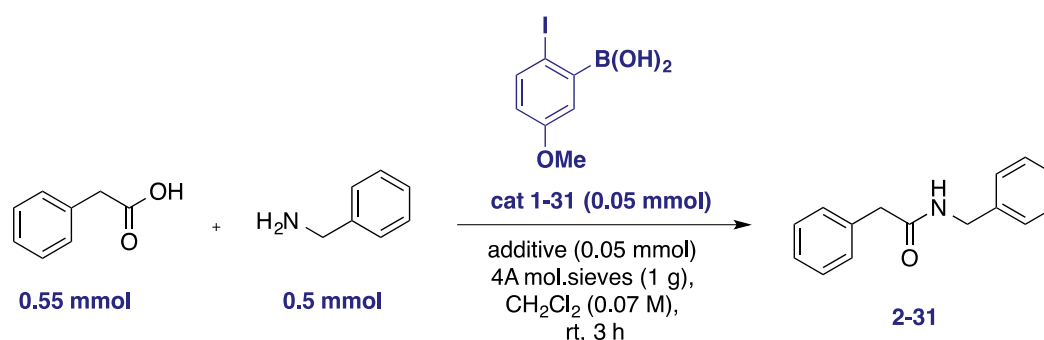
^a All yields refer to the isolated product.

Table 2-1: Effect of Lewis acids as additives on catalytic direct amide bond formation.

As it is shown in **Table 2-1**, Sc(OTf)₃, Cu(OTf)₂ and Zr(*Ot*-Bu)₄ have a slight positive effect on catalyst reactivity. In case of heavier metal salts, solubility may be an issue.

2.2.2.2 Protic Acid Additives

The preliminary screening of protic acid additives are shown in **Table 2-2**. Since, according to Marcelli's DFT studies,⁴ proton transfer may play a key role in the reaction mechanism of amide bond formation, some protic acids were used as additives in the model amidation reaction (**Table 2-2**). As the amine is prone to protonate first, its nucleophilicity may be affected by the acidic proton, which was observed with the use of TFA (**entry 4**). On the other hand, weaker protic acids such as *p*TsOH and MsOH gave slightly better results (**entries 2 and 3**) versus a control reaction (**entry 1**).



Entry	Additive	Yield (%) ^a
1	none	45
2	<i>p</i> -TsOH	70
3	MsOH	55
4	2-propanol	18
5	TFA	22

^a All yields refer to the isolated product

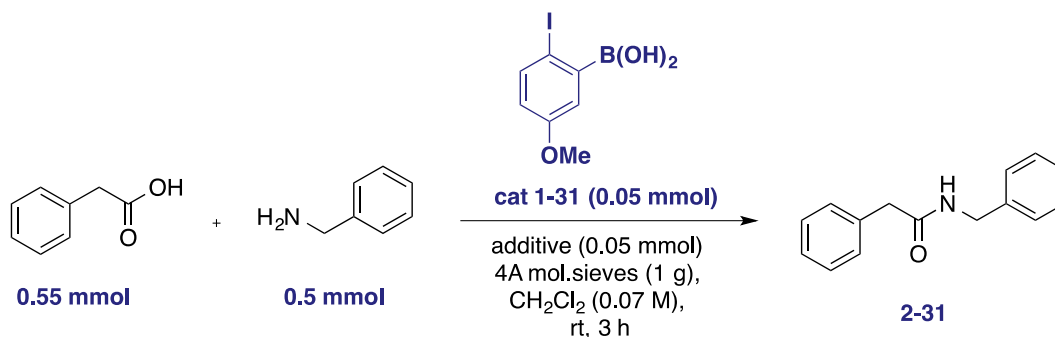
Table 2-2: Effect of protic acids as additives on direct amide bond formation.

Weaker acids provided better results, thus other similar or weaker protic acids may be considered in future studies. Furthermore, it is worth to re-examine the above results (specially *p*TsOH and MsOH additive) with another model amidation reaction (i.e., with a more challenging amine, pyrrolidine).

2.2.2.3 Nucleophilic Additives

Neutral nucleophiles have demonstrated to be very effective in acyl transfer during transesterification. Significant catalysis was therefore anticipated with compounds that form weak bases in organic solvents but are potent nucleophiles, such as N-alkylimidazoles and imidazolylidene carbenes.^{37, 40} Moreover, reports regarding the use of NHCs as nucleophilic catalysts for polymerization of lactones and transesterification

reactions have appeared since 2002.^{38, 39, 41} In 2005, the catalytic amidation of unactivated esters with amino alcohols was reported.³⁹ A carbene-based nucleophilic activation mechanism was proposed for the subsequent transformation. However, the pK_a of the acid could interfere with the action of the carbene catalyst.



Entry	Additive	Yield (%) ^a
1	none	20
2	IMes ^{38, 39, 41}	41
3	PBu ₃ ³⁷	42
4	Imidazole ⁴⁰	34

^a All yields refer to the isolated product

Table 2-3: Effect of nucleophilic additives on catalytic direct amide bond formation.

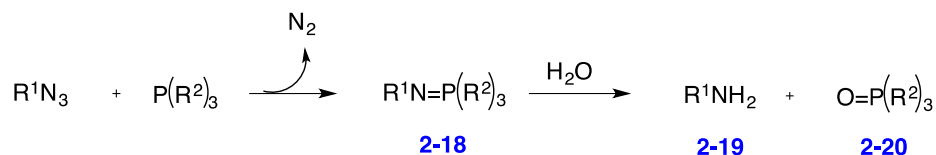
2.2.3 Plans To Replace the Molecular Sieves As a Drying Agents: Implication of Staudinger Reaction

Water is the only by-product in a catalytic direct amidation reaction, and to drive the amidation reaction toward the formation of product, it is necessary to eliminate this side-product. Our current procedure employs a large amount of highly activated molecular sieves. This technique, however, is not very attractive particularly in large-scale

syntheses. As an alternative, we came up with the idea to apply the Staudinger reaction to ambient amidation using a boronic acid catalyst to activate carboxylic acids, with nucleophilic attack of the nitrogen generated from the reaction between an azide and phosphine derivatives. The driving force for this transformation is formation of a thermodynamically stable phosphine oxide.

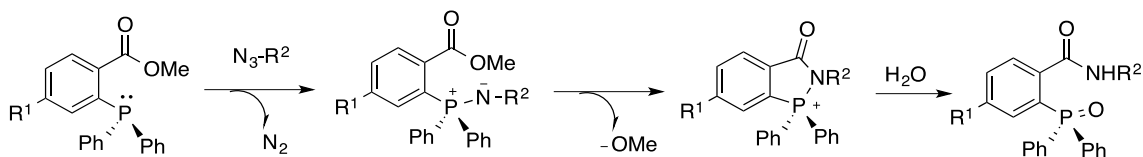
2.2.3.1 Introduction

The Staudinger reduction involves a nucleophilic attack of the phosphorus atom of a trialkyl or triaryl phosphine at the terminal nitrogen atom of the organoazide, which immediately loses nitrogen to form the iminophosphorane (**2-18**). In the presence of water, the iminophosphorane is spontaneously hydrolyzed to a primary amine (**2-19**) and to the corresponding phosphine oxide (**2-20**) as shown in **Scheme 2-16**.



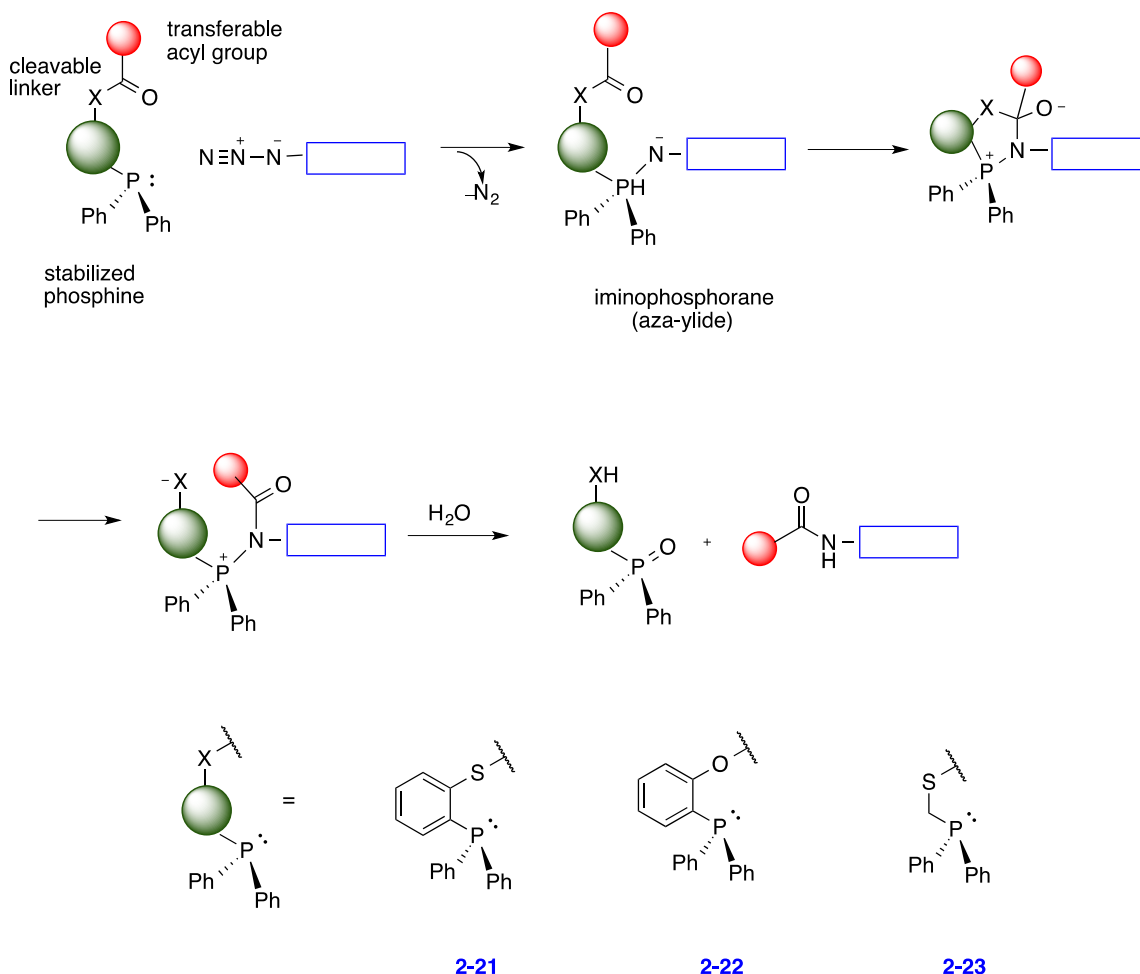
Scheme 2-16: The Staudinger reaction.

The Staudinger reaction between phosphines and organoazides has been useful in the synthesis of amides.^{42,43} In this process, the peptide having a C-terminal phosphinothioester is ligated to a peptide having an N-terminal azide through an iminophosphorane intermediate. Vilarrasa and co-workers showed that the nitrogen atom could attack an acyl donor in an intermolecular or intramolecular reaction.⁴⁴ Saxon and Bertozzi reported the intramolecular Staudinger ligation. They designed the ligand based on the rationale that an appropriately located electrophilic trap within the structure of the phosphane, such as an ester moiety, would capture the nucleophilic aza-ylide by intramolecular cyclization. This process generates an amide bond starting from organoazides and specifically functionalized phosphines (**Scheme 2-17**).⁴⁵



Scheme 2-17: Non-traceless Staudinger ligation according to Saxon and Bertozzi.

On the other hand, Bertozzi and coworkers developed the traceless Staudinger ligation. The phosphine oxide that remains in the non-traceless procedure is excised from the target molecule during amide bond formation (**Scheme 2-18**).⁴⁵ In general, the Staudinger ligation with alkyl azides is a second order reaction and proceeds more rapidly in polar, protic solvents indicating that the rate-limiting step involves a polar transition state that can be stabilized by polar solvents. Hammett analyses demonstrated that electron-donating substituents on the phosphine accelerate the overall reaction rate. The electronic and steric properties of the ester had no significant impact on the overall rate but did affect product ratios.⁴⁵ In other words, the size of the leaving group did not have a significant effect on the overall rate, indicating that ester cleavage is not involved in the rate-limiting step. Parameters such as electronic properties of both the phosphine and the azide, ester leaving groups and conformational rigidity of phosphine into the aza-ylide intermediate affect the rate and yield of the Staudinger ligation. The results demonstrate that the overall rate of the reaction is dependent on the electronic properties of both the phosphine and the azide, making it possible to tune the reactivity of the substrates for rate enhancement.

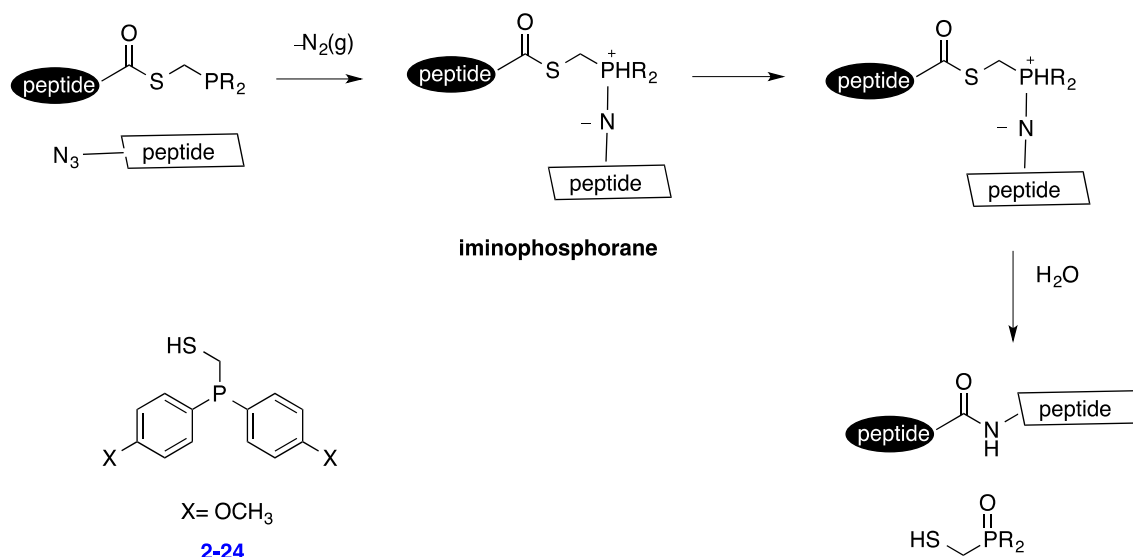


Scheme 2-18: The “traceless” Staudinger ligation according to Raines and Bertozzi.

Ligations mediated by reagents **2-21** or **2-23** display slow reaction kinetics and low product yields, which might be caused by an increase in the size of the ring formed during the nucleophilic attack of the iminophosphorane nitrogen on the thioester. With regards to electronic effects, substituents with greater electron-donating ability (**2-22**) provide higher rates of reaction.

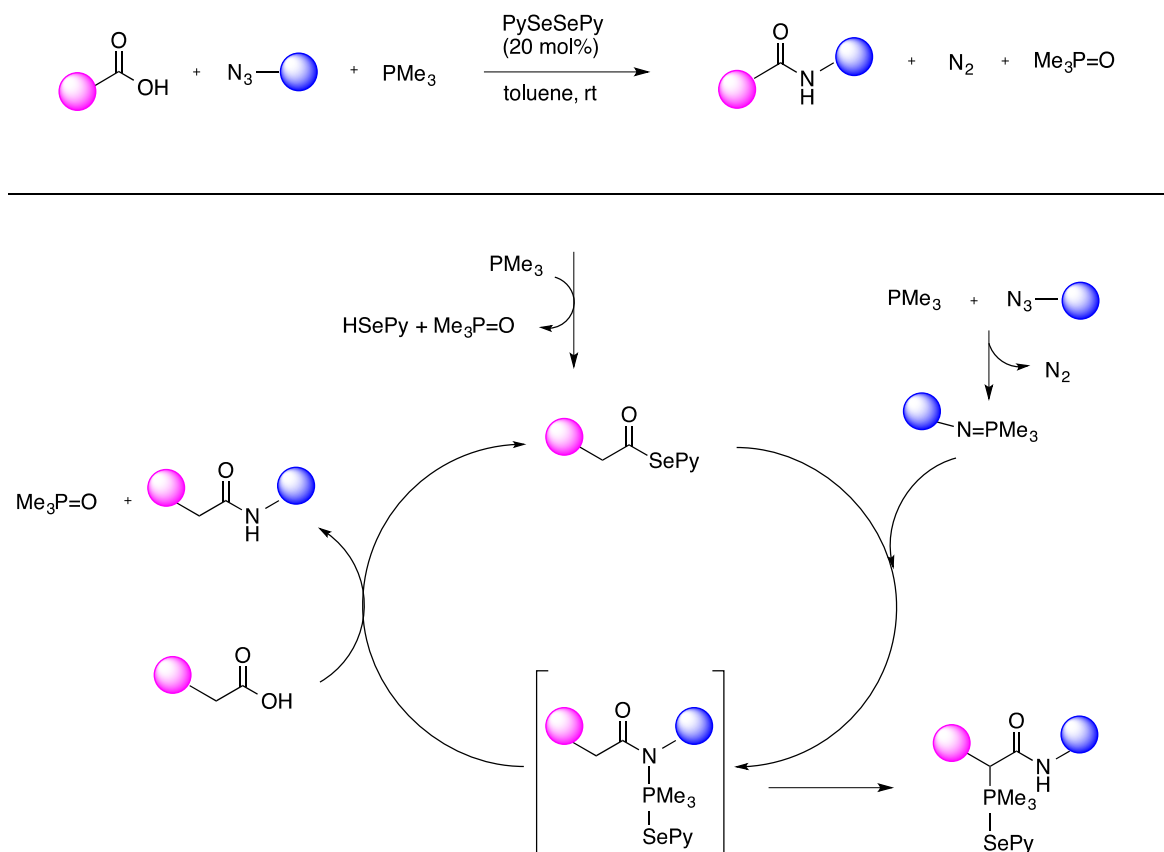
Initial mechanistic studies revealed that electron-donating phosphinothiol substituents as in **2-24** are advantageous in accelerating the intermolecular reaction, enhancing $\text{S} \rightarrow \text{N}$ acyl transfer in the iminophosphorane, and preventing undesirable $\text{P} - \text{O}$ bond formation in the ensuing tetrahedral intermediate. On the other hand, they promote the protonation of the iminophosphorane nitrogen, which impairs $\text{S} \rightarrow \text{N}$ acyl transfer in the iminophosphorane and leads to amine formation (**Scheme 2-19**).^{46, 47} Overall, this process

would ultimately produce a stable amide bond before the competing aza-ylide hydrolysis could take place.



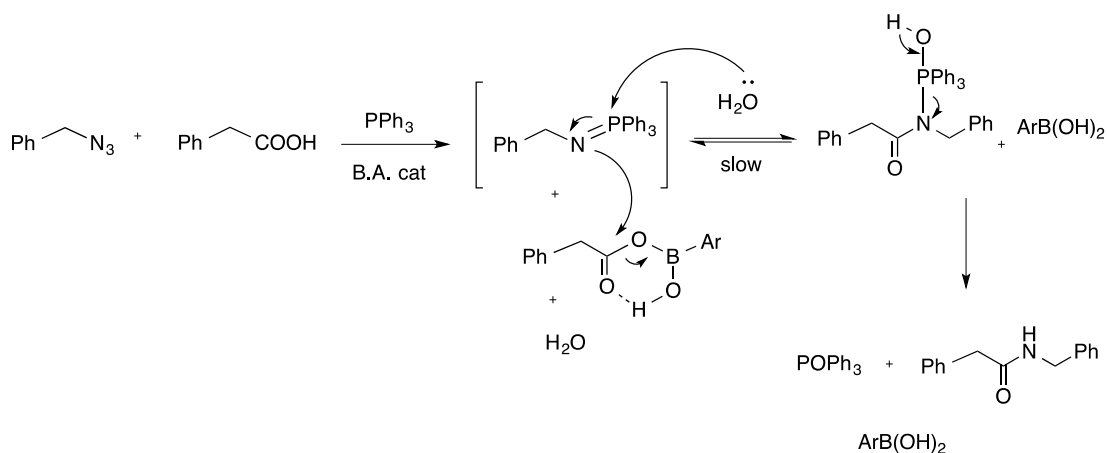
Scheme 2-19: Putative mechanism of the traceless Staudinger ligation.

In 2009, 2,2'-dipyridyl diselenide (PySeSePy) was found to be the catalyst or activator of choice for the direct reaction of carboxylic acids with azides and trimethylphosphine at room temperature (**Scheme 2-20**).⁴⁸



Scheme 2-20: Plausible mechanism and reaction scheme for Staudinger reaction and the effect of the activator.

According to the literature reports mentioned above, we designed a strategy shown in **Scheme 2-21** to remove water in the absence of molecular sieves by applying the Staudinger reaction in a model amidation reaction.

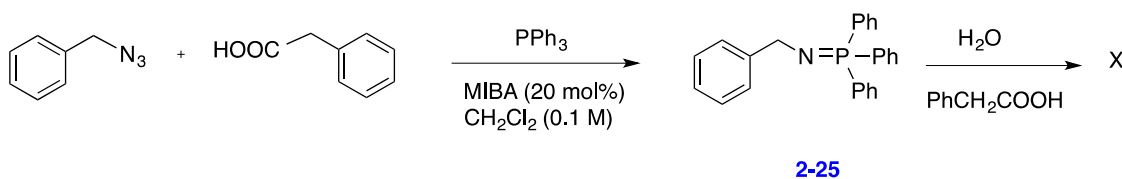


Scheme 2-21: The design of intermolecular direct amidation reaction combined with the Staudinger reaction.

The formation of phosphine oxide (**2-29**) in this reaction consumes the water by-product. Thus, it is unnecessary to add a drying agent such as molecular sieves in order to eliminate water. However, entropy is another factor that needs to be considered. For example, intramolecular reactions (considering the first step to form iminophosphine in intramolecular fashion) may proceed faster than intermolecular reactions.

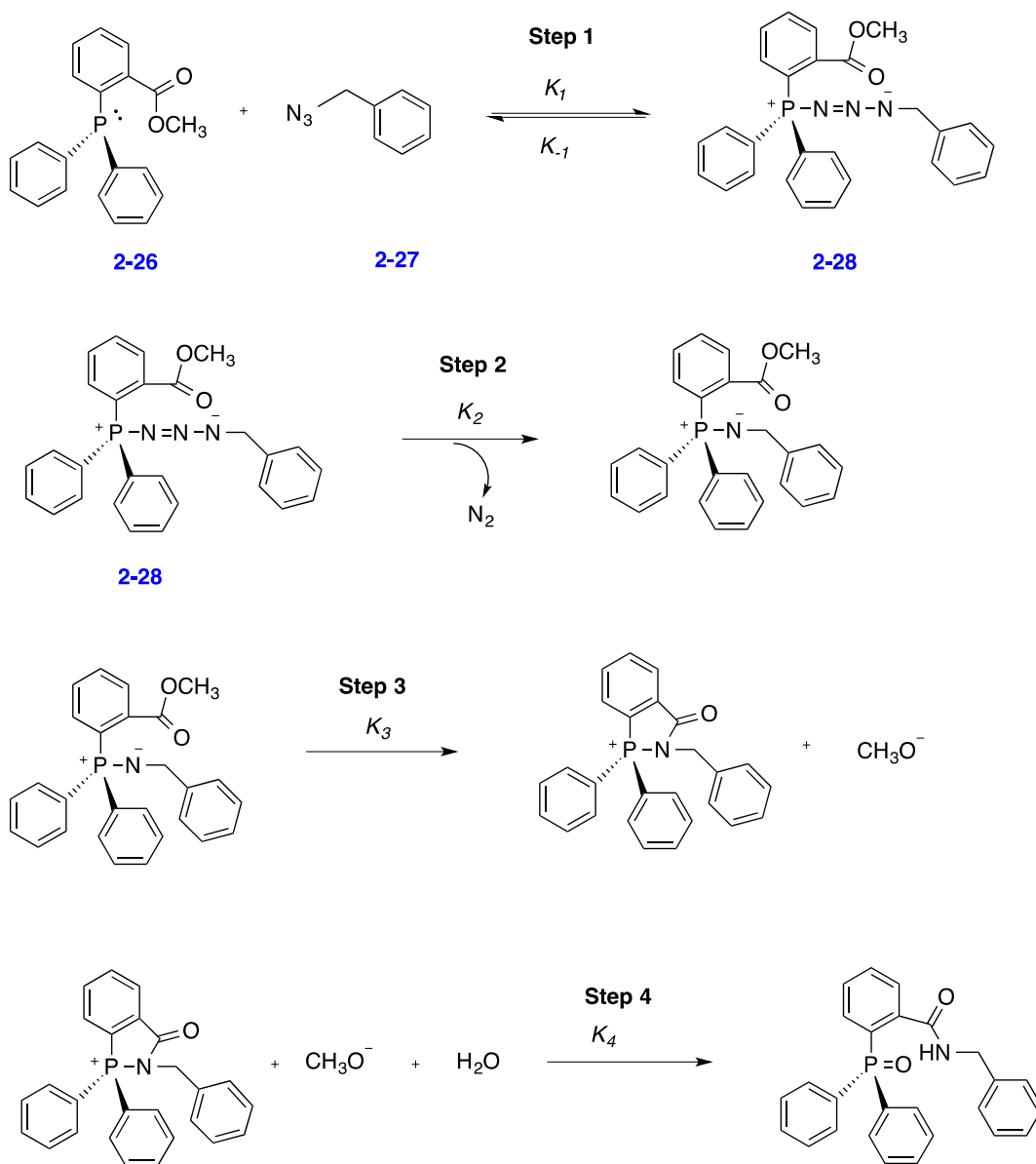
2.2.3.2 Results

Compound **2-25** (Scheme 2-22) was successfully formed with the use of triphenylphosphine as the Staudinger partner (characterization of the resulting product by ^1H NMR and ^{31}P NMR spectroscopy). The reaction shown in Scheme 2-22 did not go to completion and stopped at iminophosphine **2-25**, even after addition of five equivalents of water (water was added to break down the stable iminophosphine **2-25**). Next, we tried to increase the reactivity of phosphazide (**2-25**) by changing CH_2Cl_2 to more polar-aprotic solvent such as (THF). However, this condition did not affect the reactivity of stable phosphazide (**2-25**).



Scheme 2-22: Staudinger reaction.

As it is claimed in the reported mechanistic investigation of the Staudinger ligation,⁴⁹ the rate-limiting step is the reaction between **2-26** and **2-27** to yield phosphazide **2-28** (Scheme 2-23).



Scheme 2-23: Mechanistic steps in the Staudinger ligation.

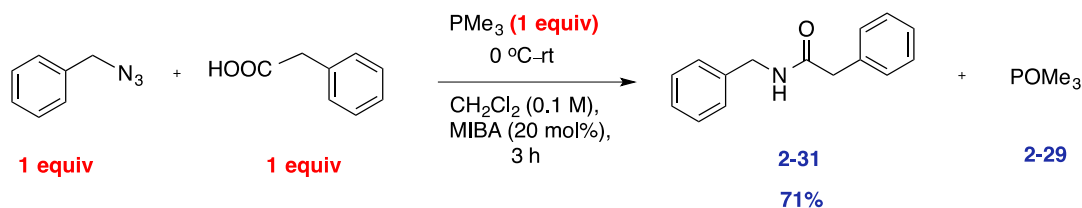
Three parameters were investigated in the Staudinger ligation:

1- Solvent effect: The rate-limiting step involves a polar transition state that can be stabilized by polar solvents.

2- Ester group: The size of the leaving group did not have a significant effect on the overall rate, indicating that ester cleavage is not involved in the rate-limiting step.

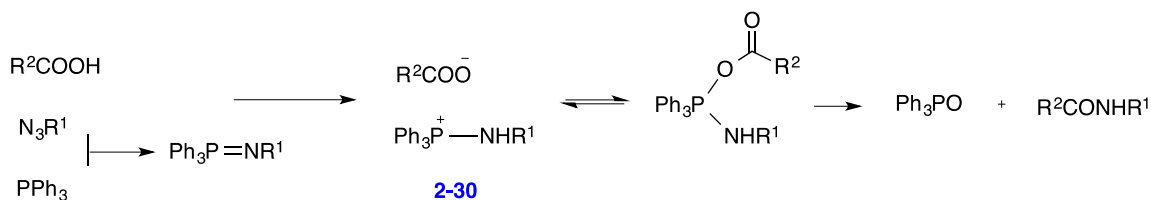
3- Effects of phosphine substituents: From a practical standpoint, the overall rate of the Staudinger ligation can be accelerated by electron-donating substituents on the phosphine.⁴⁹

Taking these parameters into account, the phosphine partner PPh₃ was changed to the more reactive PMe₃ to avoid a highly stabilized iminophosphorane intermediate (**2-25**) and to accelerate the rate of the first step. Gratifyingly, the desired amide product **2-31** was obtained this time (**Scheme 2-24**).⁴⁴



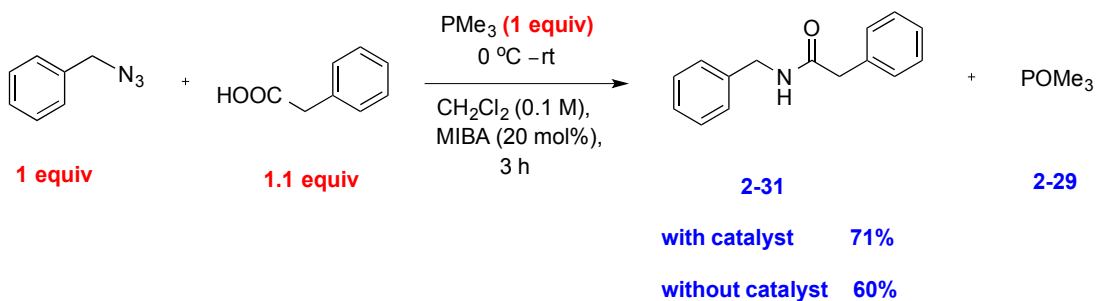
Scheme 2-24: Staudinger reaction in direct amidation.

To decrease the possibility of formation of the phosphonium salt (**2-30**) shown in **Scheme 2-25**,⁵⁰ low temperatures, addition of excess of acid and a dropwise addition of the phosphazene solution to the carboxyl derivative were considered in the model reaction.



Scheme 2-25: Proposed mechanism for the role of phosphine in Staudinger coupling.

In the control experiment, a slight beneficial effect (only 11% increase of product yield) of the catalyzed reaction using boronic acid was observed (**Scheme 2-26**).



Scheme 2-26: Control Staudinger experiment.

Based on the results obtained, further investigation and modification of the Staudinger reaction partner is required. For example, the rate-determining step may vary when the nature of the monoacylborate is changed, allowing this step to play a more important role in the reaction rate. Perhaps, an intramolecular reaction (either traceless or non-traceless) could be designed to overcome the entropy barrier of intermolecular reaction.

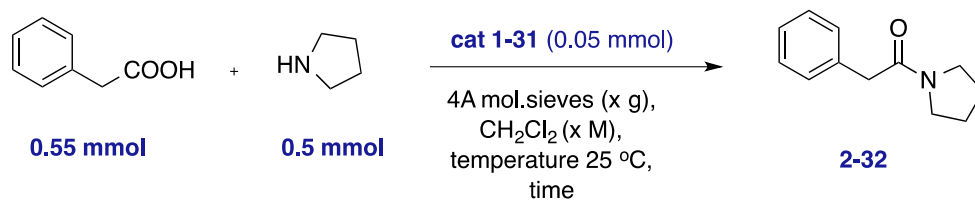
2.3 Scalability Study of the Direct Amidation of Carboxylic Acids Catalyzed by Arylboronic Acids

Increasing efforts have been devoted to developing amide bond syntheses with high consideration on atom- and step-economy, low cost and minimal environmental impact. The drawbacks of our current catalytic approach include low reactant concentration and the requirement of large quantity of molecular sieves to drive the reaction. Consequently, this limits the synthetic utility of the reaction in larger scale applications. To address these concerns, optimization of the reaction conditions such as solvent, reactant concentration, and the amount of molecular sieves was performed.

2.3.1 Optimization of Reaction Parameters

It was found that an increase in reaction concentration and addition of high excess of molecular sieves are required ($\sim 20 - 25$ equiv) in order to promote faster reactions.⁵¹ Previous optimization work indicated that 1.0 g of molecular sieves was the minimum required in a 0.5 mmol scale reaction to obtain a near-quantitative yield of product within a short reaction time.

To achieve greener reaction conditions, the model amidation reaction was conducted in a more concentrated solution with a lesser amount of molecular sieves at room temperature. The amount of molecular sieve was varied and the optimal quantity in order to achieve the highest yield at a particular reactant concentration and temperature was determined (**Table 2-4**).



Entry	Conc. (M)	Mol. sieves (g)	Time (h)	Temperature (°C)	Yield (%) ^a
1	0.2	1.0	18	rt	68
2	0.2	1.0	24	rt	81
3	0.5	1.0	18	rt	52
4	0.5	1.0	24	rt	60
5	0.2	0.6	18	rt	58
6	0.5	0.6	18	rt	49
7	1.0	0.6	18	rt	29
8	0.2	0.5	18	rt	58
9	0.5	0.5	18	rt	48
10	1.0	0.5	18	rt	34
11	1.0	0.5	18	rt	39
12	1.0	0.5	18	rt	33
13	0.2	0.5	48	rt	65
14	0.5	0.5	48	rt	52
15	1.0	0.5	48	rt	42
16	1.0	0.25	18	rt	10

^aIsolated yields

Yield (%)

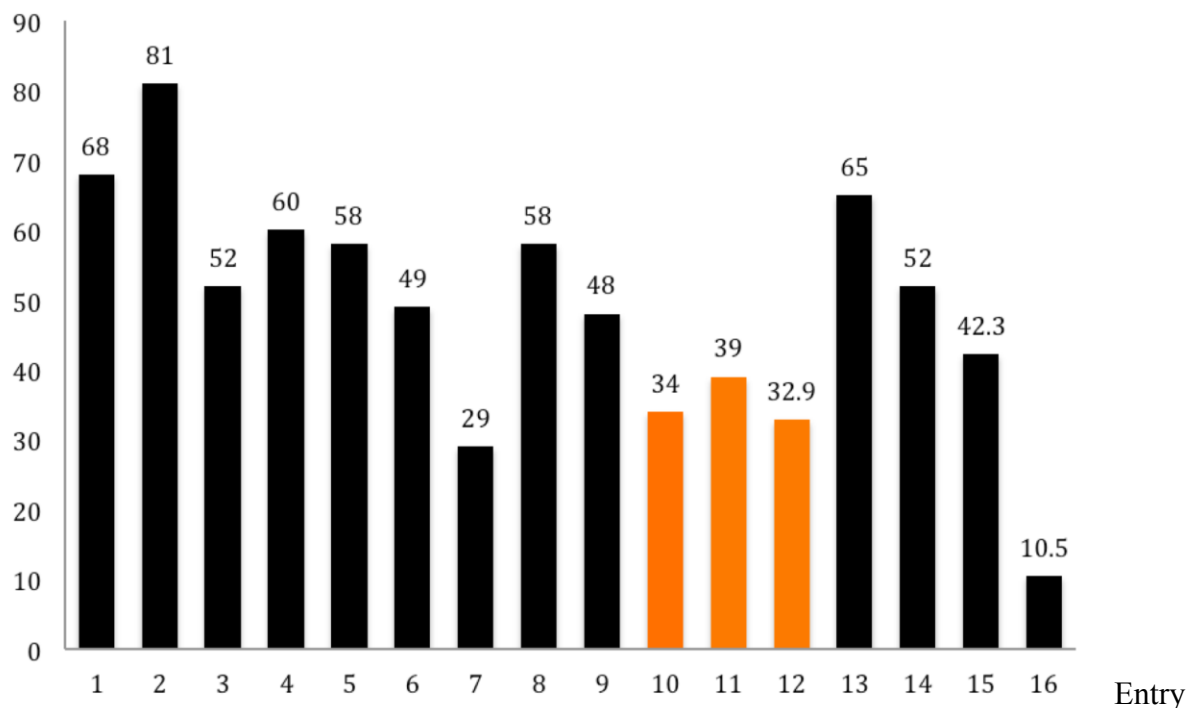


Table 2-4: Optimization of reactant concentration and amount of molecular sieves in the amidation reaction.

As shown above, the reaction yield was lower at higher concentrations. This may result from the possibility of other side reactions. Above 0.1 M, the proportion of salt increases and the amount of free acid and free amine may diminish to a detrimental level.

Based on the results listed in **Table 2-4**, it is apparent that lower dilution provided greener condition, with 1.0 M as the optimum concentration of substrates in dichloromethane. There is a minimization of the solvent being used; and hence, lesser waste is generated. It was also found that the two-fold reduction of the amount of molecular sieves (0.5 g molecular sieves per mmol of the limiting reagent instead of one gram per mmol) can still provide the model amide product in reasonable yield.

2.3.2 Optimization of Reaction Solvent and Temperature

Amidation reactions catalyzed by arylboronic acids were found to perform best when performed in CH_2Cl_2 and toluene as solvents. However, only a small difference in the product yields was observed when CH_2Cl_2 was used. Thus, because it is considered to be a greener solvent, toluene was tested in subsequent reactions.

Temperature was also a contributing factor in the overall product yield. When the reaction was performed at room temperature in toluene, a product yield of 38% was achieved, which is significantly higher than the 25% yield in CH_2Cl_2 . It was found that the organocatalyzed amidation reaction occurred the most effectively in toluene when heated to 50 °C, providing 45% of the product after a set time of 18 h (**Table 2-5**).

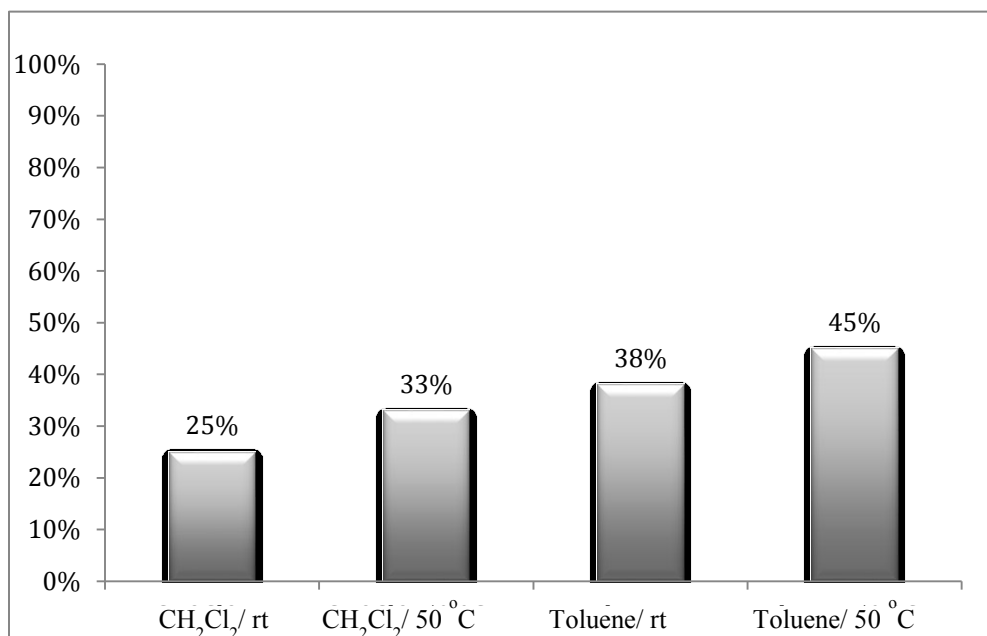
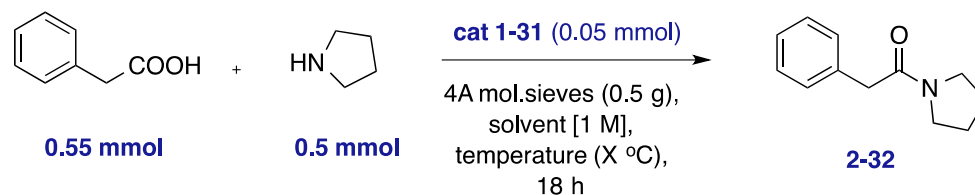
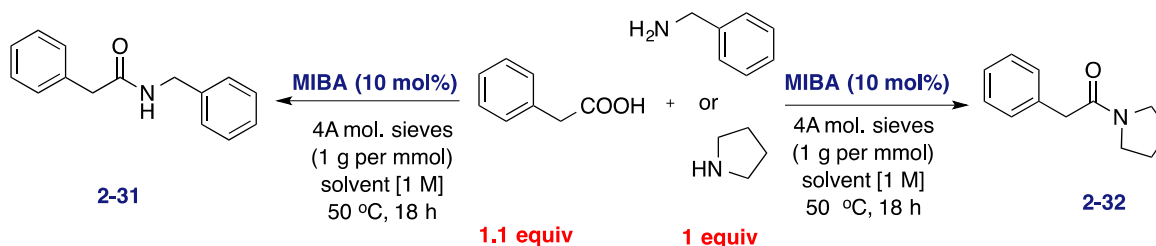


Table 2-5: Optimization of amidation reaction solvent.

2.3.3 Multigram-Scale Results

So far, we have demonstrated that amide synthesis when catalyzed by an arylboronic acid can be scaled up quite successfully using a reduced amount of molecular sieves. Additionally, toluene as a non-halogenated solvent and a reaction temperature of 50 °C were identified as the optimum conditions for achieving a reasonable yield of amide product. With these optimized conditions at hand, the reaction was then performed in a large scale (5 g) (**Table 2-6**). As presented in **Table 2-6**, the amidation reaction of phenylacetic acid proceeded successfully giving 89% and 46% product yields with benzylamine and pyrrolidine respectively. These observations could have significance in industrial applications.

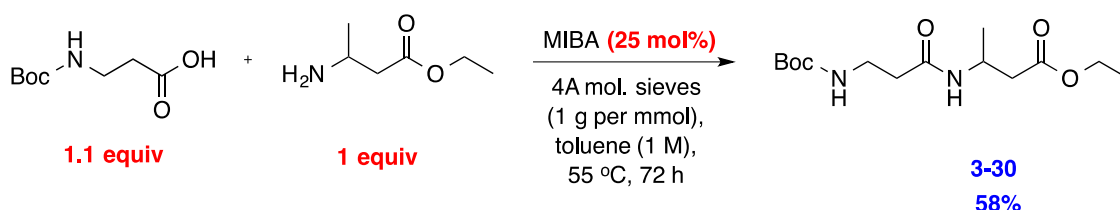


Solvent	Yield (%) ^a (2-31)	Yield (%) ^a (2-32)
CH ₂ Cl ₂	72	29
toluene	89	46

Reaction conditions: carboxylic acid (36.7 mmol, 1.10 equiv), boronic acid (3.34 mmol, 10 mol%), and the amine (33.4 mmol, 1.00 equiv) were stirred at 50 °C for 18 h in dry toluene containing the drying agent (33.0 g). ^aIsolated yields.

Table 2-6: Scale up result for the direct amidation reaction using 5 g of carboxylic acid.

Furthermore, the scope of scalability was expanded to di-peptide synthesis using the MIBA catalyst, *N*-Boc β -alanine and β -amino ethyl ester. Obviously, more catalyst loading and longer reaction time was required for less reactive β -amino acids substrates, in comparison to previous amines (benzylamine and pyrrolidine) (**Scheme 2-27**).



Scheme 2-27: Scale up result for the direct amidation reaction in dipeptide synthesis using 5 g of of Boc- β -Ala-OH.

2.4 Conclusion

Following Al-Zoubi's discovery of the superior activity of a third-generation boronic acid FIBA (**2-3**), this catalyst was synthesized and subjected to a model amidation reaction. Result revealed that FIBA did not outperform the second generation catalyst in providing the amide products in higher yields with shorter reaction times. In an effort to improve the catalyst activity, more electron rich heterocyclic boronic acids having a thiophene core were synthesized; however, the obtained product yields were low. We further attempted to tune the Lewis acidity of boron and reactivity of the catalyst while preserving catalyst stability towards protodeboronation (because electron rich heteroareneboronic acids have a tendency to undergo such an undesirable reaction).

To expand the scope and overcome on some limitations of the catalytic amidation method, we examined the effect of additives such as imidazole. However, the use of additives did not provide better results.

Next, a modified Staudinger reaction was performed to trap the water generated in the amidation reaction instead of using molecular sieves as dehydrating agent. When compared to the control experiment (uncatalyzed reaction), the amide product yield

improved only by 11% for the catalyzed reaction, a difference that is probably not significant.

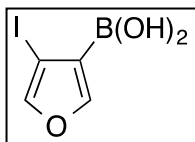
Finally, optimal amidation conditions were identified using arylboronic acid catalyst **1-31**. These include reactant concentration (0.5-1.0 M) and molecular sieves (0.5 g per mmol reactants), both of which are also considered to be “greener” conditions. Furthermore, changing the solvent to toluene, and heating the reaction mixture to 50 °C provided the best yields. The synthetic usefulness of the reaction was demonstrated in a large-scale reaction (up to 5 g), in which a reasonable yield of amide product was obtained for two model amines as well as a β -amino ester.

2.5 Experimental

2.5.1 General Information

Unless otherwise stated, all reactions were performed under a nitrogen atmosphere using flame-dried glassware. THF, toluene and dichloromethane were dried from a double cartridge solvent purification system. Analytical thin layer chromatography was performed on Merck Silica Gel 60 F254 plates. NMR spectra were recorded on Varian INOVA-300, INOVA-400 or INOVA-500 MHz instruments. *J* accuracy: (+/-) 0.5 Hz. The residual solvent protons (^1H) or the solvent carbon (^{13}C) were used as internal standards. Carbon attached to the $\text{B}(\text{OH})_2$ group was generally not detected by ^{13}C -NMR (exhaustive peak broadening due to quadrupolar relaxation of ^{11}B). ^1H -NMR data are presented as follows: chemical shift in ppm (δ) downfield from tetramethylsilane (multiplicity, coupling constant, integration). The following abbreviations are used in reporting NMR data: s, singlet; br s, broad singlet; d, doublet; t, triplet; q, quartet; dd, doublet of doublets; m, multiplet; sept, septet. High-resolution mass spectra were recorded by the University of Alberta mass spectrometry service laboratory using either electron impact (EI) or electrospray ionization (ESI) techniques. Infrared spectra were obtained on a Nicolet Magna-IR 750 with frequencies expressed in cm^{-1} . Powdered 4A molecular sieves (< 5 micron, Aldrich) were dried overnight in an oven (300 °C) prior to use.

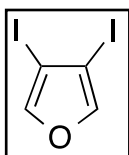
2.5.1.1 Preparation and Analytical Data of 4-Iodofuran-3-yl-3-Boronic Acid (2-3)



To a solution of 3,4-diiodofuran (**2-3**) (1.27 g, 3.98 mmol) in 60 mL of a mixture of THF and Et₂O (1:1) was added dropwise at -78 °C *isopropylmagnesium chloride* (2 M in THF, 4.37 mmol). After the mixture was stirred for 2 h at that temperature, B(O*i*-Pr)₃ (6.91 mL, 11.9 mmol) was added. The solution was allowed to warm to room temperature overnight; then a saturated solution of NH₄Cl was added, and the resulting mixture was stirred for 30 min at room temperature. The aqueous layer was extracted with Et₂O (40 mL, 3 times) and the ether extracts were dried over Na₂SO₄, filtered and concentrated in vacuo. The crude mixture was purified by column chromatography (hexanes/ethyl acetate 3/1) to give the desired product in 54% yield (0.51 g).

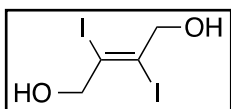
¹H-NMR (400 MHz, DMSO-*d*₆) δ 7.93 (s, 2H), 7.77 (d, 1H, *J* = 2.0 Hz), 7.75 (d, 1H, *J* = 2.0 Hz). **HRMS** (ESI) for C₄H₃¹¹BIO₃ (M-H)⁻: calcd. 236.9226; found, 236.9222.

2.5.1.2 Preparation and Analytical Data of 3,4-Diiodofuran (Scheme 2-6 step 2)



To a 2 L three-necked flask equipped with a stirrer, fitted with a water cooled condenser, and a 100 mL dropping funnel was added 2,3-diiodo-2-butene-1,4-diol (25.0 g, 73.5 mmol), NMP (300 mL), and hexanes (500 mL). The mixture was stirred vigorously at 85 °C. To this solution was added a preheated (85 °C) solution of K₂Cr₂O₇ (21.6 g, 73.5 mmol) in H₂SO₄ (3 M, 90 mL), dropwise in portions (30 mL) over a period of one hour. The biphasic mixture was stirred at 85 °C for five hours and then allowed to cool to room temperature. The hexane layer was decanted, and the remaining solvent was extracted once with hexanes (250 mL). The hexane layers were combined, washed successively with water (2 × 120 mL), a saturated Na₂S₂O₃ solution (120 mL), and brine (120 mL), dried over Na₂SO₄, passed over a short plug of silica gel, and concentrated to give the desired product in 10% yield (1.60 g) as a pale yellow liquid.⁵²

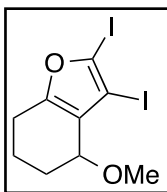
2.5.1.3 Preparation and Analytical Data of (E)-2,3-Diiodobut-2-ene-1,4-Diol (Scheme 2-6 step 1)



2-Butyne-1,4-diol (2.00 g, 23.2 mmol), iodine (6.00 g, 23.6 mmol), potassium iodide (8.00 g, 48.2 mmol) and water (70 mL)

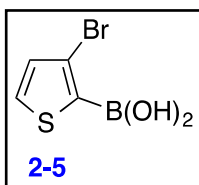
were heated to 70 °C on a steambath for an hour. The precipitate was separated, washed and crystallized from water to provide the desired iodinated product in 81% yield (6.40 g). Characterization of the product matched that of a previous report.⁵²

2.5.1.4 Preparation and Analytical Data of 2,3-Diiodo-4-methoxy-4,5,6,7-tetrahydrobenzofuran (2-11)



To a solution of 2-(1-alkynyl)-2-alken-1-ones (0.08 g, 0.20 mmol) in 2 mL CH₂Cl₂ was added MeOH (0.30 mmol), K₃PO₄ (0.13 g, 0.60 mmol) and I₂ (0.15 g, 0.60 mmol) at 0 °C. After 5 minutes, the above suspension was warmed to room temperature and stirred for an appropriate time. The reaction mixture was then diluted with ethyl acetate, washed with saturated Na₂S₂O₃ solution, dried over Na₂SO₄, and filtered. The solvent was evaporated under reduced pressure, and the product was isolated by chromatography on an Al₂O₃ column in 55% yield (0.05g). Characterization of the product matched that of a previous report.⁵³

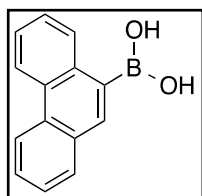
2.5.1.5 Preparation and Analytical Data of 3-Bromo-2-Thienylboronic Acid (2-5)



A solution of anhydrous diisopropylamine (1 mL, d = 0.72 g mL⁻¹ at 25 °C, 7.14 mmol) in anhydrous THF (20 mL) was stirred and cooled using a dry ice/acetone bath under argon. Next *n*-butyllithium (2.05

M in cyclohexane, 2.80 mL, 5.74 mmol) was added dropwise by syringe with the reaction temperature maintained at $-70\text{ }^{\circ}\text{C}$ to $-65\text{ }^{\circ}\text{C}$. After 30 minutes of stirring at this temperature range, the reaction mixture was transferred to an ice/salt bath and warmed to $0\text{ }^{\circ}\text{C}$ over 15 minutes. A solution of 3-bromothiophene (0.98 g, 6.02 mmol) in anhydrous THF (10 mL) was added dropwise by syringe pump over one h with the reaction temperature maintained at $-3\text{ }^{\circ}\text{C}$ to $1\text{ }^{\circ}\text{C}$. Stirring at this range continued for one more hour before trimethyl borate (1 mL, $d = 0.93\text{ g mL}^{-1}$ at $25\text{ }^{\circ}\text{C}$, 8.97 mmol) was added dropwise by syringe over 15 minutes with the reaction temperature maintained at $-1\text{ }^{\circ}\text{C}$ to $1\text{ }^{\circ}\text{C}$. The reaction mixture was allowed to warm to room temperature overnight. Aq HCl (1 M, 25 mL) was added and the resulting biphasic mixture was stirred vigorously. The layers were then separated and the organic layer was washed with saturated aq NH_4Cl ($\sim 25\text{ mL}$). The combined aqueous washings were extracted with diethyl ether ($\sim 25\text{ mL}$). The combined organic extracts were washed with brine (40 mL), dried (MgSO_4), filtered and concentrated by rotary evaporation to afford the desired product as a brown solid in 74% yield (0.92 g). Characterization of the product matched that of a previous report.⁵⁴

2.5.1.6 Preparation and Analytical Data of Phenanthreneboronic Acid (2-16)

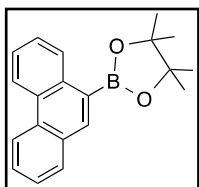


To a solution of 9-iodo-phenanthrene (**2-14**) (1.21 g, 3.98 mmol) in 60 mL of a mixture of THF and Et_2O (1:1) was added dropwise at $-78\text{ }^{\circ}\text{C}$ *isopropylmagnesium chloride* (2 M in THF, 4.37 mmol).

After the mixture was stirred for 2 h at that temperature, $\text{B}(\text{O}i\text{-Pr})_3$ (6.91 mL, 11.90 mmol) was added. The solution was warmed to room temperature overnight; then a saturated solution of NH_4Cl was added, and the resulting mixture was stirred for 30 min at room temperature. The aqueous layer was extracted with Et_2O (40 mL, 3 times) and the ether extracts were dried over Na_2SO_4 , filtered, concentrated and the crude product was purified by column chromatography (hexanes/ethyl acetate 3/1) to give the desired product in 45% yield (0.40 g).

$^1\text{H NMR}$ (400 MHz, CDCl_3): δ 8.78 (dd, $J = 7.0\text{ Hz}$, 3.5 Hz , 2H), 7.87 (d, 2H, $J = 7.0\text{ Hz}$), 7.80 (s, 1H), 7.58-7.62 (m, 5H), $^{11}\text{B NMR}$ (129 MHz, CDCl_3): δ 28 (1B).

2.5.1.7 Preparation and Analytical Data of Phenanthreneboronic Ester (**2-17**)



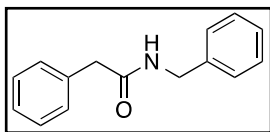
Boronic acid (0.22 g, 1 mmol) and pinacol (0.12 g, 1 mmol) were stirred in anhydrous Et₂O (1 mL) at ambient temperature under a nitrogen atmosphere for 15 h. Flame dried MgSO₄ (5 mmol) was added to the reaction mixture and stirring continued for 12 h. The reaction mixture was filtered and the solvent carefully removed in vacuo. The crude material was purified by flash column chromatography to yield the pure boronic ester in 76% yield (0.23 g).

¹H NMR (400 MHz, CDCl₃): δ 8.78 (dd, *J* = 7.0 Hz, 3.4 Hz, 2H), 8.41 (s, 1H), 7.91 (d, 1H, *J* = 7.0 Hz), 7.58-7.62 (m, 5H), 1.45 (s, 9H). ¹¹B NMR (129 MHz, CDCl₃): δ 28 (1B). HRMS (ESI) for C₂₀H₂₁¹¹BO₂ (M-H)⁻: calcd. 304.1635; found, 304.1635

2.5.2 General Procedure for Multigram Organocatalytic Direct Amidation.

Into a 250 mL round bottom flask equipped with a stir bar was added phenylacetic acid (**7**) (36 mmol, 1.1 equiv), 5-methoxy-2-iodophenylboronic acid (**1-31**) (3.3 mmol, 10 mol%) and 33 g (1 g per mmol of amine substrate) of activated 4A molecular sieves. Toluene was added to maintain a concentration at 1 M and the mixture was stirred. After 10 minutes, the amine (33 mmol, 1.0 equiv) was added. The resulting mixture was stirred for 18 h at 50 °C. The reaction mixture was filtered through a pad of Celite 545 with 50 mL of CH₂Cl₂, and the filtrate was washed with aqueous acidic solution (50 mL × 4, 1 M), aqueous basic solution (50 mL × 4, 1 M) and brine (50 mL). The organic layer was collected, dried over anhydrous Na₂SO₄, filtered and evaporated to dryness to yield the title amide product.

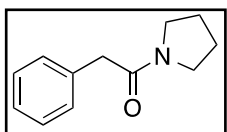
2.5.2.1 Preparation and Characterization Data of N-Benzyl-2-Phenyl-Acetamide (**2-31**)



The title compound was prepared using the general procedure for the multigram organocatalytic amidations, affording 6.693 g of **2-31** and 89% yield, 5.415 g of **2-31** and 72%

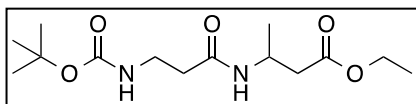
yield, in toluene (50 °C) and CH₂Cl₂; respectively. Characterization of the product matched that of a previous report.⁵⁵

2.5.2.2 Preparation and Characterization Data of Phenyl-1-Pyrrolidin-1-yl-Ethanone (**2-32**)



The title compound was prepared using the general procedure for the multigram organocatalytic amidations, affording 2.893 g of **2-32** and 46% yield, 1.83 g and 29% yield, in toluene (50 °C) and CH₂Cl₂ respectively. Characterization of the product matched that of a previous report.⁵⁶

2.5.2.3 Preparation and Characterization Data of **3-30**



The title compound was prepared using the general procedure for the multigram organocatalytic amidations catalyst **1-31** (25 mol%), 5 g (26.4 mmol) of Boc-β-Ala-OH and 3.25 mL (24 mmol) of 3-aminobutanoic acid ethyl ester, affording 4.629 g of **3-30** and 58% yield, in toluene (55 °C). M.p. 64-66 °C. ¹H NMR (CDCl₃, 400 MHz): δ = 6.20 (br. s, 1 H), 5.20 (br. s, 1 H), 4.38 (m, 1 H), 4.22 (q, *J* = 6.1 Hz, 2 H), 3.38 (dt, *J* = 6.2, 6.2 Hz 2 H), 2.44 (d, *J* = 5.4 Hz, 2 H), 2.31 (t, *J* = 6.2 Hz, 2 H), 1.40 (s, 9 H), 1.25 (t, *J* = 6.6 Hz, 3 H), 1.20 (d, *J* = 6.7 Hz, 3 H); ¹³C NMR (100.6 MHz, CDCl₃): δ = 171.5, 170.4, 155.6, 78.7, 60.1, 41.5, 40.0, 36.1, 35.8, 27.9 (3 C), 19.5, 13.6; IR (Microscope, cm⁻¹) 3311, 3078, 2935, 1736, 1716, 1648, 1529, 1454; HRMS (ESI) for C₁₄H₂₇N₂O₅ (M+H)⁺: calcd. 303.1914; found, 303.1915.

2.6 References

-
- (1) Gernigon, N.; Al-Zoubi, R. M.; Hall, D. G. *J. Org. Chem.* **2012**, 77, 8386.
 - (2) Al-Zoubi, R. M.; Marion, O.; Hall, D. G. *Angew. Chem. Int. Ed.* **2008**, 47, 2876.

- (3) (a) Al-Zoubi, R. M. PhD thesis **2011**, *Section 3.3.1*, p. 139. (b) Al-Zoubi, R. M. PhD thesis **2011**, *Section 3.3.1*, p. 142.
- (4) Marcelli, T. *Angew. Chem. Int. Ed.* **2010**, *49*, 6840.
- (5) Krus, G. A.; Wang X. *Synth. Commun.* **1998**, *28*, 1093.
- (6) Tietz, J. I.; Seed A. J.; Sampson P. *Org. Lett.* **2012**, *14*, 5058.
- (7) Fuller, L. S.; Iddon B.; Smith K. A. *J. Chem. Soc., Perkin Trans.1* **1997**, 3465.
- (8) Liu, Y.; Zhou, S. *Org. Lett.* **2005**, *7*, 4609.
- (9) Prakash, G. K.; Mathew, T.; Hoole, D.; Esteves, P. M.; Wang, Q.; Rasul, G.; Olah, G. A. *J. Am. Chem. Soc.* **2004**, *126*, 15770.
- (10) Ribeiro, R. S.; Esteves, P. M.; Mattos, C. S. *Synthesis* **2011**, *5*, 0739.
- (11) Makhon'kov, D. I.; Cheprakov, A. V.; Rodkin, M. A.; Serguchev, Yu. A.; Davydova, V. G.; Beletskaya, I. P. From *Izvestiya Akademii Nauk SSSR, Seriya Khimicheskaya* **1987**, *11*, 2609.
- (12) Laouiti, A.; Rammah, M. M.; Rammah, M. B.; Marrot, J.; Couty, F.; Evano, G. *Org. Lett.* **2012**, *14*, 6.
- (13) Peña, D.; Cobas, A.; Pérez, D.; Guitián, E. *Synthesis* **2002**, *10*, 1454.
- (14) Gandeepan P.; Cheng C.H. *Org. Lett.* **2013**, *15*, 2084.
- (15) Petasis, N. A.; Zavialov, I. A. *Tetrahedron Lett.* **1996**, *37*, 567.

- (16) Furuya, T.; Ritter, T. *Org. Lett.* **2009**, *11*, 2860.
- (17) Furuya, T.; Kaiser, H. M.; Ritter, T. *Angew. Chem.* **2008**, *47*, 5993.
- (18) Cazorla, C.; Métay, E.; Andrioletti, B.; Lemaire, M. *Tetrahedron Lett.* **2009**, *50*, 3936.
- (19) Sniady, A. *Synlett* **2006**, *6*, 960.
- (20) Thiebes, C.; Prakash, G. K. S.; Petasis, N. A.; Olah, G. A. *Synlett* **1998**, 141.
- (21) Qiu, D.; Mo, F.; Zheng, Z.; Zhang, Y.; Wang, J. *Org. Lett.* **2010**, *12*, 5474.
- (22) Kuivila, H. G.; Nahabedian, K. V. *J. Am. Chem. Soc.* **1961**, *83*, 2164.
- (23) Fukuto, J.; Jens, F. R. *Acc. Chem. Res.* **1983**, *16*, 177.
- (24) Ishihara, K. *Tetrahedron* **2009**, *65*, 1085.
- (25) Ishihara, K.; Ohara, S.; Yamamoto, H. *Science* **2000**, *290*, 1140.
- (26) Ishihara, K.; Nakayama, M.; Ohara, S.; Yamamoto, H. *Synlett* **2001**, 1117.
- (27) Ishihara, K.; Nakayama, M.; Ohara, S.; Yamamoto, H. *Tetrahedron* **2002**, *58*, 8179.
- (28) Nakayama, M.; Sato, A.; Ishihara, K.; Yamamoto, H. *Adv. Synth. Catal.* **2004**, *346*, 1275.
- (29) Sato, A.; Nakamura, Y.; Maki, T.; Ishihara, K.; Yamamoto, H. *Adv. Synth. Catal.*

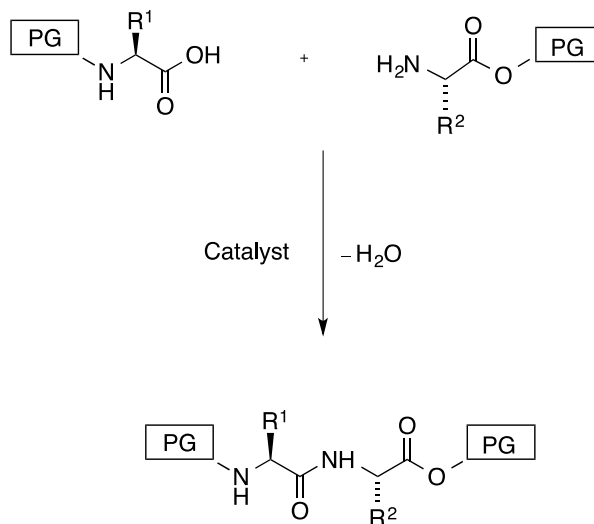
2005, 347, 1337.

- (30) Nakamura, Y.; Maki, T.; Wang, X.; Ishihara, K.; Yamamoto, H. *Adv. Synth. Catal.* **2006**, 348, 1505.
- (31) Han, C.; Lee J. P.; Lobkovsky, E.; Porco, J. A. Jr. *J. Am. Chem. Soc.* **2005**, 127, 10039.
- (32) Allen, C. L.; Burel, C.; Williams, J.M. J. *Tetrahedron Lett.* **2010**, 51, 2724.
- (33) Allen, C. L.; Chhatwal, A. R.; Williams, J.M. J. *Chem. Commun.* **2012**, 48, 666.
- (34) Lundberg, H.; Tinnis, F.; Adolfsson H. *Synlett* **2012**, 2201.
- (35) Lundberg, H.; Tinnis, F.; Adolfsson, H. *Chem. Eur. J.* **2012**, 18, 3822.
- (36) Allen, C. L.; Lawrence, R.; Emmett, L.; Williams, J. M. J. *Adv. Synth. Catal.* **2011**, 353, 3262.
- (37) Yang, X.; Birman, V. B. *Org. Lett.* **2009**, 11, 1499.
- (38) Nyce, G. W.; Lamboy, J. A.; Connor, E. F.; Waymouth, R. M.; Hedrick, J. L. *Org. Lett.* **2002**, 4, 3587.
- (39) Movassaghi, M.; Schmidt, M. A. *Org. Lett.* **2005**, 7, 2453.
- (40) Birman, V. B.; Li, X.; Han, Z. *Org. Lett.* **2007**, 9, 37.
- (41) Grasa, G. A.; veli, T. G.; Singh, R.; Nolan, S. P. *J. Org. Chem.* **2003**, 68, 2812.
- (42) Fuchs, J. R.; Fuchs, R.L. *J. Am. Chem. Soc.* **2004**, 126, 5068.

- (43) Palacios, F.; Retana, A. M. O.; Pagalday, J. *Eur. J. Org. Chem.* **2003**, 913.
- (44) Bosch, I.; Gonzalez, A.; Urpi', F.; Vilarrasa, J. *J. Org. Chem.* **1996**, 61, 5638.
- (45) Saxon, E.; Armstrong, J. I.; Bertozzi, C. R. *Org. Lett.* **2000**, 2, 2141.
- (46) Tam, A.; Soellner, M. B.; Raines, R.T. *Org. Biomol. Chem.* **2008**, 6, 1173.
- (47) Soellner, M. B.; Nilsson, B. L.; Raines, R. T. *J. Am. Chem. Soc.* **2006**, 128, 8820.
- (48) Bure's, J.; Marti'n, M.; Urpi', F.; Vilarrasa, J. *J. Org. Chem.* **2009**, 74, 2203.
- (49) Lin, F. L.; Hoyt, H. M.; Halbeek, H.; Bergman, R. G.; Bertozzi, C. R. *J. Am. Chem. Soc.* **2005**, 127, 2686.
- (50) Molina, P.; Alajarin, M.; Leonardo, C. L. *Tetrahedron Lett.* **1991**, 32, 4041.
- (51) Considering the 20% weight absorption capacity of 4 A molecular sieves, 1 g can absorb up to ca. 200 mg water.
- (52) C. C. Hughes, J. J. Kennedy-Smith, D. Trauner, *Org. Lett.* **2003**, 5, 4113.
- (53) Liu, Y.; Zhou, S. *Org. Lett.* **2005**, 7, 4609.
- (54) Tietz, J. I.; Seed A. J.; Sampson P. *Org. Lett.* **2012**, 14, 5058.
- (55) W. K. Chan, C. M. Ho, M. K. Wong, C. M. Che, *J. Am. Chem. Soc.* **2006**, 128, 14796.
- (56) J. H. Smitrovich, L. DiMichele, C. Qu, G. N. Boice, T. D. Nelson, M. A. Huffman, J. Murry, *J. Org. Chem.* **2004**, 69, 1903.

Application of Catalytic System for the Direct Amide-Bond Formation in Dipeptide Synthesis

This chapter focuses on the formation of dipeptides via direct amidation of amino acid derivatives using boronic acids as catalysts. The first section describes catalyst screening and optimization. The optimized reaction parameters that were applied in the substrate scope investigation are also presented. It ensues that a particular design of the substrate is necessary in order to couple *N*-terminal to *C*-terminal protected α -amino acids catalytically. The last section outlines the reaction methodology that was employed in the substrate scope.



3.1 Introduction

There are numerous biologically active peptides that provide interesting synthetic targets. By the end of 2010, there were about 60 approved peptide drugs that generated annual sales of approximately US\$ 13 billion.^{1a} Most of these peptides are prepared by chemical synthesis, with solid-phase peptide synthesis as the predominant method for the preparation of peptides on a laboratory scale and increasingly so on an industrial scale. Twenty different natural amino acids can be joined together by amide bonds to form peptides, and are the basic building blocks for proteins. Peptides are rather small molecules compared to proteins. They usually contain less than 50 amino acid residues and do not possess a well-defined three-dimensional structure. Synthetic peptides have

emerged as highly versatile tools, useful in a broad range of research and commercial applications. For example, they are often considered as active pharmaceutical components.^{1b,c} A series of new technologies have been developed that allow peptides to be viable drug candidates in areas usually restricted to protein therapeutics, such as monoclonal antibodies. Having demonstrated their potential as protein mimics, synthetic polypeptides have found applications in biotechnology such as tissue engineering and drug delivery.^{1d}

A key step in peptide production is the formation of the peptide bond, which involves amide bond formation. Chemical synthesis of large peptides is achieved by intermolecular coupling of smaller peptides using conventional peptide bond-forming techniques. Peptides are difficult to synthesize because amidation reactions are plagued by the occurrence of side reactions. For example, acyl chlorides have limited value in peptide coupling because of the danger of hydrolysis, racemisation, cleavage of protecting groups and other side reactions.

The amino acids that constitute the desired chain sequence must be added in the correct order. Complementary to this are the protection and activation of the functional groups to increase chemoselectivity of the reaction. Appropriate activation of *N*-protected amino acids is required to perform amide bond formation with amino esters.

3.1.1 Properties of Amino Acids

The amino group is mainly protonated to an ammonium ion to form a dipolar ion or a zwitterion (**Figure 3-1**).

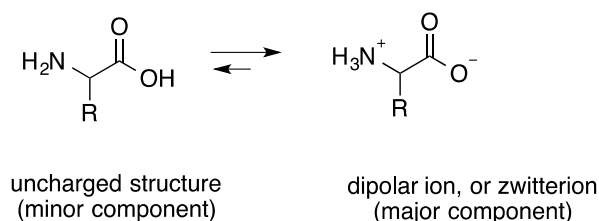


Figure 3-1: Neutral and zwitterion structures of amino acids.

Some unique properties stemming from the zwitterionic nature of amino acids include the following:

1. They have high melting points, generally over 200 °C.
2. Amino acids are more soluble in water than they are in ether, dichloromethane, and other common organic solvents.
3. Amino acids have much larger dipole moments than simple amines or simple acids.
4. Amino acids are less acidic than most carboxylic acids and less basic than most amines. The predominant form of the amino acid depends on the pH of the solution (**Figure 3-2**).

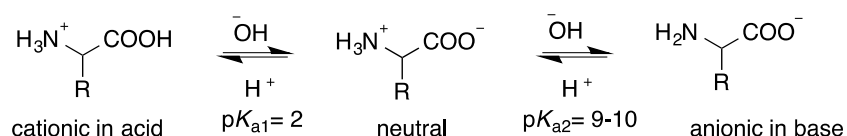


Figure 3-2: The effect of pH on the equilibrium of amino acids.

Amines and acids can condense with the loss of water to form amides. Industrial processes often produce amides simply by mixing the acid and the amine, then heating the mixture to drive off water. Amides are the most stable acid derivatives. This stability is partly due to the strong resonance interaction between the nonbonding electrons on nitrogen and the carbonyl group (**Figure 3-3**). Compared to amines the amide nitrogen is no longer a base, and the bond has restricted rotation because of its partial double-bond character.

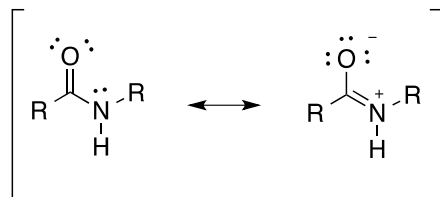
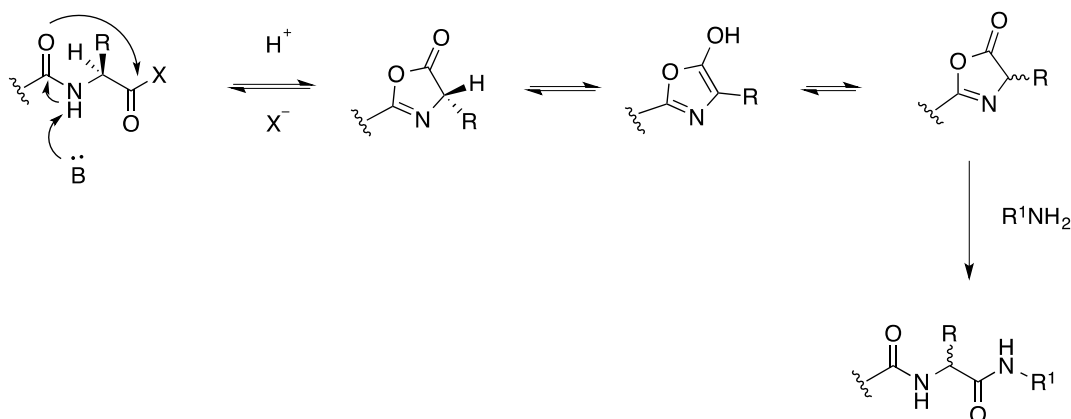


Figure 3-3: Resonance structures in amides.

Laboratory peptide synthesis is an important area of chemistry. Chemists have developed

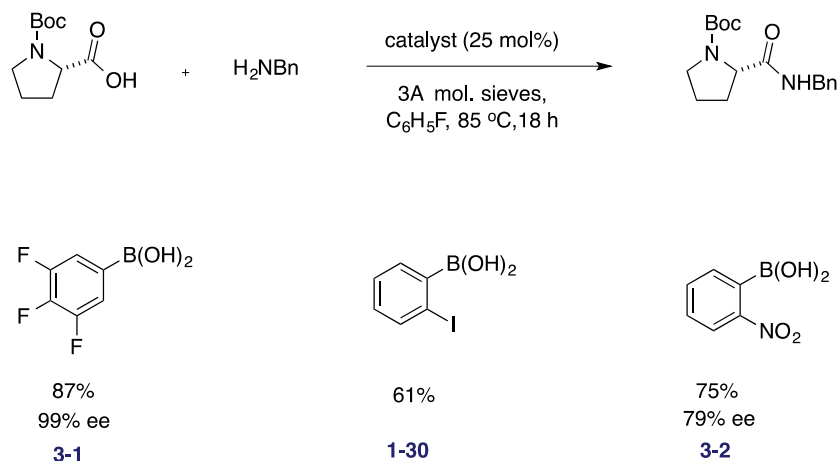
many ways of synthesizing peptides that are classified into two major groups. One of which is the solution-phase (homogeneous) method, which involves adding reagents to solutions of growing peptide chains and purifying the products as needed. On the other hand, the solid-phase (heterogeneous) method involves adding reagents to growing peptide chains bound to solid polymer particles. Another way of classifying the different methodological approaches include fragment and stepwise condensations.² The former strategy is based on the synthesis of several fragments of the polypeptide to be synthesized, followed by coupling of the segments to form the final desired product.^{3,4,5} The stepwise condensation strategy is based on the repetitive addition of single *N*-protected amino acids, usually in molar excess, to a growing amino component, starting generally from the *C*-terminal amino acid of the chain to be synthesized. Synthetic techniques, such as the solid-phase synthesis,⁶ polymeric reagents,^{7,8} stepwise synthesis using active esters^{9,10,11,12} and symmetrical^{13,14} and mixed anhydrides^{15,16} fall into this category. For larger peptides and proteins, solid-phase peptide synthesis is usually preferred since the large amounts of time required and the low overall yields using solution-phase methods are due largely to the purification steps.

Racemization-free peptide synthesis is of key importance to acquire the required peptide chains in diastereomerically pure form. In general, the way to synthesize peptides with full stereochemical integrity is by elongation at the N terminus to avoid oxazolone formation. Racemization may occur because activation of the terminal carboxyl moiety of a peptide is followed by nucleophilic attack of the flanking amide bond leading to oxazolone mediated racemization (**Scheme 3-1**).^{17a,b,c}



Scheme 3-1: Oxazolone-mediated racemization occurring during peptide coupling.

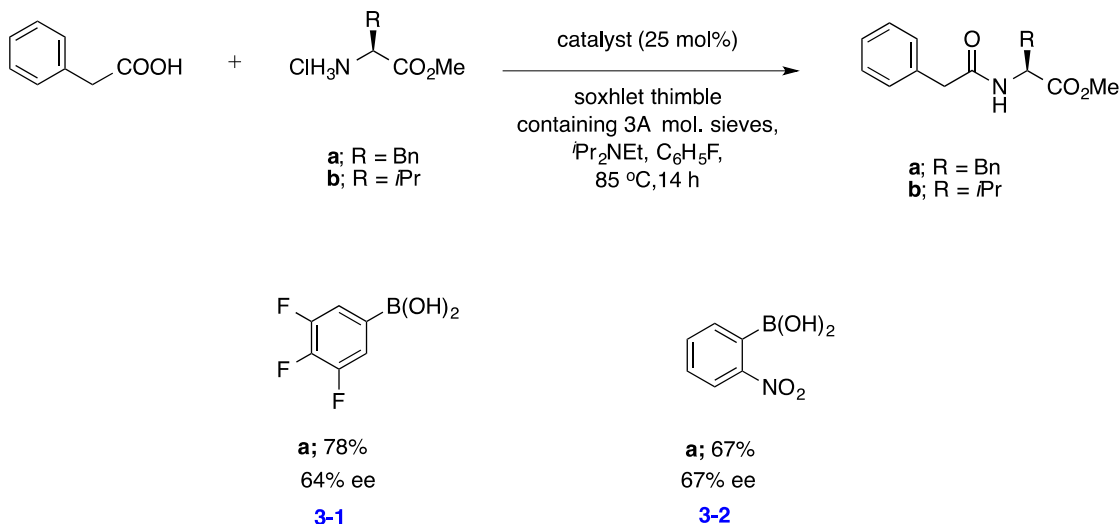
Recently, Whiting and coworkers reported the direct amidation of amino acid derivatives using a catalytic amount of 3,4,5-trifluorophenylboronic (TFPBA, **3-1**) and *o*-nitrophenylboronic acids (*o*-NPBA, **3-2**) in the model reaction of *N*-tert-butyloxycarbonyl(Boc)-proline with benzylamine (**Scheme 3-2**).¹⁸ It was demonstrated that different arylboronic acids exhibit considerably different activities.^{19a,b} For example, catalyst **3-1** was efficient for the coupling of *N*-Boc-proline with benzylamine, while the most efficient catalyst for *N*-Boc-phenylalanine was catalyst **3-2**.



Scheme 3-2: Comparison of different catalysts in the amidation of Boc-proline by Whiting and co-workers.

Three factors were optimized in the reaction of **Scheme 3-2**, such as catalyst, temperature and solvent. Catalysts TFPBA (**3-1**) and *o*-NPBA (**3-2**) showed the highest catalytic reactivity under the same reaction conditions (i.e., in fluorobenzene heated to reflux at 85 °C). The solvent employed was also an important factor as expected from previous work.²⁰ For this reason, fluorobenzene was chosen as the best solvent at 85 °C. The desired product was obtained without any racemization when catalyst TFPBA (**3-1**) was used. On the other hand, the enantiomeric purity was diminished to 79% ee when catalyst *o*-NPBA (**3-2**) was used under the same reaction conditions (**Scheme 3-2**).

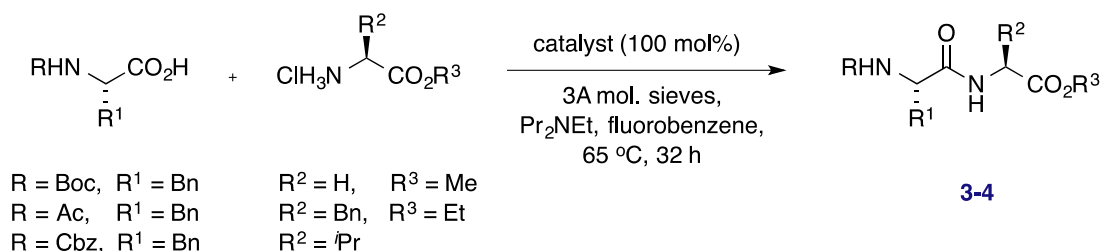
In the same report,¹⁸ C-protected amino acids were evaluated with different catalysts and temperature. The best results are summarized in **Scheme 3-3**.



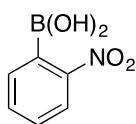
Scheme 3-3: Comparison of different catalysts in the amidation of C-protected amino acids by Whiting and co-workers.

Using catalyst TFPBA (**3-1**) and *o*-NPBA (**3-2**), some racemization was observed especially when a benzyl side-chain was present, giving 64% ee and 67% ee respectively (**Scheme 3-3, a**).

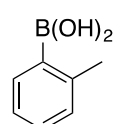
To produce dipeptide derivatives, a stoichiometric amount of the optimal boronic acid was necessary in order to couple C-protected amino and N-protected amino acids (**Table 3-1**). Using electron deficient aryl boronic acids as catalyst **3-2** and **3-3**, it was shown that C-protected amino and N-protected amino acids react quite efficiently to form the corresponding dipeptide **3-4**.



catalysts



3-2



3-3

Catalyst/s	R	R ¹	R ²	R ³	Yield (%) ^b
					3-4
3-2	Boc	Bn	Bn	Me	58
3-2, 3-3 (1:1)^a	Boc	Bn	<i>i</i> -Pr	Me	55
3-2	Ac	Bn	H	Et	47
3-2	Ac	Bn	Bn	Me	48
3-2, 3-3 (1:1)^a	Ac	Bn	<i>i</i> -Pr	Me	51
3-2, 3-3 (1:1)^a	Cbz	Bn	Bn	Me	62

^a 1:1 mixture of both **3-2** and **3-3**, ^b isolated yield.

Table 3-1: Direct dipeptide synthesis using boronic acids 3-2 or a mixed catalyst system 3-2 and 3-3 (1:1).

There was little effect upon changing an *N*-Boc group to the less hindered *N*-Ac in the yield of resulting dipeptide **3-4**. The major impact appears to be the hindrance effect of the amino donor partner (*C*-protected amino acid). Furthermore, a 1:1 mixture of both *o*-tolyl- and *o*-nitrophenyl-boronic acids system (**3-2** and **3-3**) is preferable in some cases.

For example, the synthesis of dipeptide Boc-Phe-Val methyl ester improved from < 2% to 55% yield when a 1:1 mixture of both **3-2** and **3-3** was used instead of catalyst **3-2** alone. As shown with these results, catalyst optimization was not consistent with the substrate structure. Moreover, a high catalyst loading was required (i.e., 100 mol%, stoichiometric amount).

Ideally, peptide bond formation should be fast, quantitative and achieved under mild conditions without affecting adjacent stereogenic centers, without side reactions and with easily removable side products. Currently, there is no general catalytic approach to perform direct amidation of amino acid derivatives. Thus, the research presented in this chapter aims to address the application of arylboronic acids in the synthesis of dipeptides directly from protected amino acids. Specifically, atom economy and reduction of waste are addressed by using a boronic acid catalyst. Efforts directed to the identification of effective catalyst for this purpose and the development of optimum reaction conditions are described.

Considering the results of Whiting and co-workers, and the previous results obtained in our group, we decided to reevaluate reaction conditions as well as a re-optimization of potential catalysts to achieve optimal conditions for a catalytic dipeptide synthesis methodology.

3.2 Results

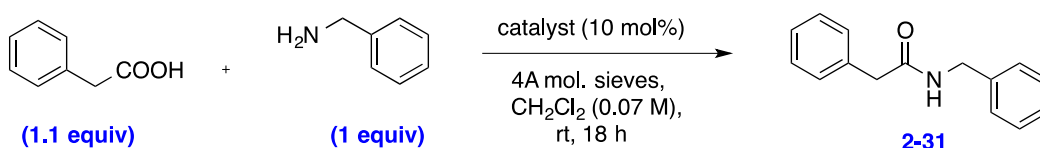
3.2.1 Initial Screening of *Ortho*-Functionalized Arylboronic Acids

In order to identify the best catalysts for peptide synthesis, we decided to initiate this study by screening different potential *ortho*-substituted arylboronic acids in a simple model amidation reaction. The selection featured previously reported catalysts by our group²¹ or the recent ones reported by Whiting and co-workers in 2013 (**Table 3-1**).¹⁸

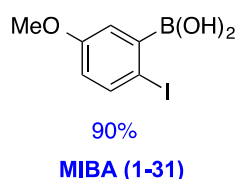
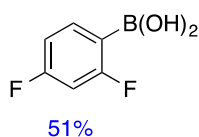
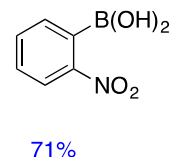
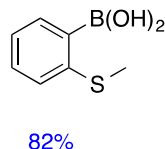
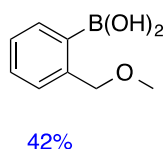
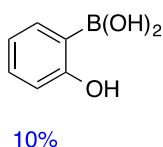
Previous catalyst screening studies revealed a few active *ortho*-functionalized arylboronic acids in the model amidation reaction between benzylamine and phenylacetic acid. The most promising candidate was *ortho*-iodophenylboronic acid (**IBA**, **1-30**).²¹ The reverse

trend of efficacy was observed in the ortho-halide series (I > Br > Cl > F). Owing to the size and electron density of the iodo substituent subtle electronic or structural effects may be at play. Next, the arene core of *ortho*-iodoarylboronic acid catalysts (**IBA**, **1-30**) has been optimized with regards to the electronic effects of ring substitution.²² Examination of substituent electronic effects on the catalytic activity of *ortho*-iodoarylboronic acids revealed that the antagonistic effect of electron-withdrawing groups on the catalyst reactivity. It was then found that electron-donating substituents, positioned para to the iodide, showed a superior reactivity compared to *ortho*-iodoarylboronic acid. The perturbation of the boron center by the electronic density of the large iodide substituent might be responsible for the surprising catalytic activity of **MIBA (1-31)**. Elimination of water from the orthoaminal intermediate as depicted in the DFT-calculated transition state (TS) becomes the rate-determining step.²² The optimal ring substitution pattern of catalyst **MIBA (1-31)**, with an electron-donating 5-methoxy group, supports a role for the ortho-iodo substituent as hydrogen-bond acceptor in the orthoaminal transition structure.

The results shown in **Scheme 3-4** encouraged us to apply catalyst **1-31** as the catalyst of choice in peptide synthesis. As can be seen this catalyst provided the best yield in the model amidation reaction in comparison with *o*-NPBA (Whiting's catalyst for peptide synthesis) and *ortho*-methylthioboronic acid. The latter can be considered for future modification of the catalyst reactivity in direct amidation reactions.



catalysts:



Scheme 3-4: Effect of different catalysts on the model amidation reaction.

3.2.2 Direct Amide Formation of Amino Acid Derivatives

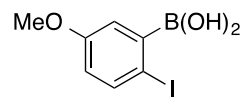
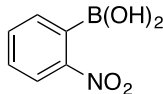
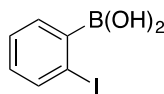
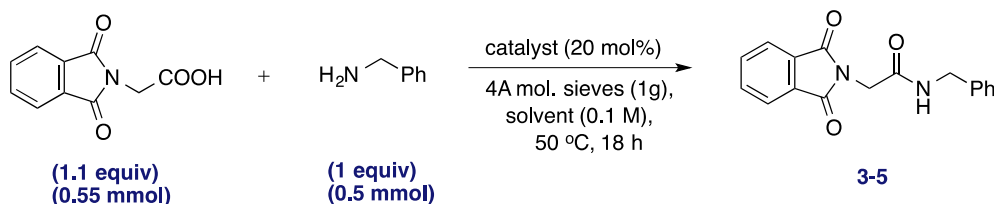
Described in this section are studies on the development of a catalytic direct amidation of amino acids derivatives with arylboronic acid catalysts, particularly under conditions that cause no racemization. The effect of the solvent and molecular sieves on catalyst reactivity was scrutinized.

3.2.2.1 The Effect of Drying Agents on Catalyst Reactivity

One of the important aspects of the boronic acid catalyzed amidation reaction is the use of activated molecular sieves as a dehydrating agent. In order to determine the effect of this drying agent, reactions were initially performed in dichloromethane, which is considered to be the ideal solvent for these types of reactions according to the previous reports from our group.²¹ Furthermore, 4A molecular sieves (activated powder, \approx 325 mesh particle size) are the most efficient dehydrating agent over 3A molecular sieves for

catalyst reactivity.²²

Initially, double *N*-protected α -amino acids and benzylamine were subjected to the amidation reaction in CH₂Cl₂ and activated molecular sieves. The reason for choosing these particular *N*-protected α -amino acids is discussed in Section 3-4.



Entry	Catalyst	Solvent	T °C	Mol. sieves	Yield (%) ^a
1	1-30	CH ₂ Cl ₂	50	3A	42
2	1-30	CH ₂ Cl ₂	50	4A	58
3	3-2	CH ₂ Cl ₂	50	3A	30
4	3-2	CH ₂ Cl ₂	50	4A	20
5	1-31	CH ₂ Cl ₂	50	4A	74
6	1-31	CH ₂ Cl ₂	50	3A	62

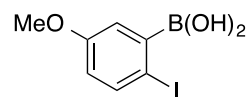
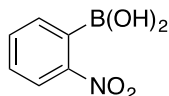
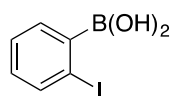
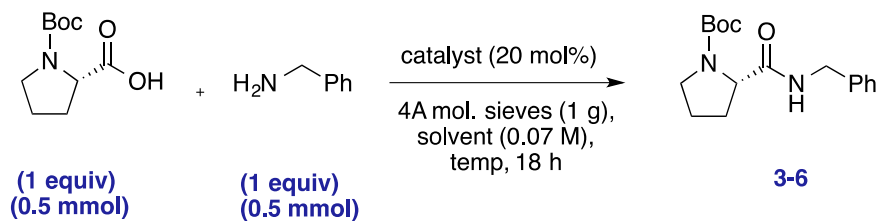
^a Isolated yields.

Table 3-2: Comparison in product yields for different dehydrating agents and catalysts 1-30 and 1-31 in a direct amidation reaction between double *N*-protected amino acids and benzylamine.

Based on **Table 3-2**, it is apparent that 4A molecular sieves are a better dehydrating agent over 3A molecular sieves when using catalyst **1-31**. These results show the role of water provided by molecular sieves in the reactivity of catalyst **1-31** in direct amidation reactions. However, the reactivity of electron deficient catalyst **3-2** is reverse and provided a better yield with 3A molecular sieves. Furthermore, the reaction catalyzed by arylboronic acid **1-31** provided the highest yield compared to catalyst **1-30** or **3-2** (**Table 3-2, entry 5-6**).

3.2.2.2 Evaluation of Whiting's Catalyst Versus *Ortho*-Iodoarylboronic Acid Catalysts in Direct Amide Formation of Amino Acid Derivatives

Whiting's model amidation reaction between *N*-*tert*-butoxycarbonyl (Boc)-proline and benzylamine was repeated under the indicated reaction conditions using CH₂Cl₂ or fluorobenzene as solvent and molecular sieves as dehydrating agent to compare the reactivity of three catalysts (**Table 3-3**).



Entry	Catalyst	Mol. sieves	T °C	Solvent	Yield (%) ^a
1	1-30	3A	85	C ₆ H ₅ F	48
2	1-30	4A	85	C ₆ H ₅ F	54
3	3-2	3A	85	C ₆ H ₅ F	74
4	3-2	4A	85	C ₆ H ₅ F	67
5	1-31	3A	85	C ₆ H ₅ F	64
6	1-31	4A	85	C ₆ H ₅ F	74
7	1-30	3A	50	CH ₂ Cl ₂	60
8	1-30	4A	50	CH ₂ Cl ₂	69
9	3-2	3A	50	CH ₂ Cl ₂	51
10	3-2	4A	50	CH ₂ Cl ₂	42
11	1-31	3A	50	CH ₂ Cl ₂	82
12	1-31	4A	50	CH ₂ Cl ₂	91

^a Isolated yields.

Table 3-2: Comparison in product yields for different dehydrating agents and catalysts 1-30, 1-31, 3-2 and solvents in a direct amidation reaction between (Boc)-proline and benzylamine.^{21, 22}

The reactivity of the electron rich *ortho*-iodoarylboronic acid catalyst **1-31** was enhanced in CH₂Cl₂ with 4A molecular sieves as the dehydrating agent (**Table 3-3, entry 12**). However, its reactivity was reduced in fluorobenzene (**entry 6**, 74%) or with 3A molecular sieve (**entry 5**, 64%). On the contrary, the reactivity of *o*-nitrophenyl-boronic acid (**3-2**) is inferior in CH₂Cl₂ with 4A molecular sieves (**entry 10**, 42%) and comparatively higher when using fluorobenzene and 3A molecular sieves (**entry 3**, 74%) at reflux. Although temperature played a role, these results support the idea that the choice of solvent and molecular sieves is crucial in optimizing the catalyst's reactivity and every catalyst requires different conditions. Furthermore, the choice of molecular sieves type affects the reactivity of catalysts **1-30** and **1-31**, which is consistent with Marcelli's DFT studies that water plays a role in the reaction mechanism.

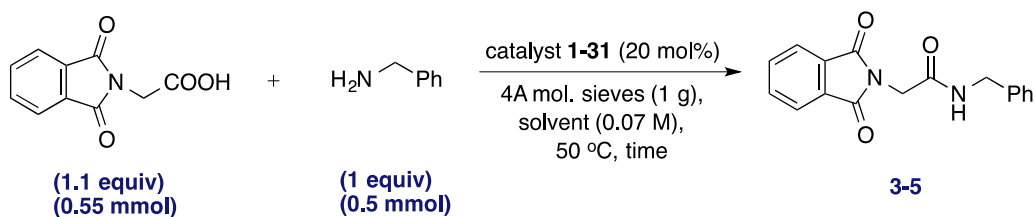
It can be concluded that catalyst **1-31** was the optimal catalyst with CH₂Cl₂ as the solvent and 4A molecular sieves as the dehydrating agent (**Table 3-3, entry 12**). *Thus, from our results, it appears that Whiting and coworkers neglected the effect of the type of molecular sieves and solvent in their comparison of different catalysts.*¹⁸

3.3 Optimization of Reaction Parameters

After finding the best-performing catalyst, we then turned our attention to optimize other reaction parameters, including the solvent, the stoichiometry of substrates, and the concentration of the reaction.

3.3.1 Optimization of Reaction Solvent

We observed before that the optimal reaction solvent varied depending on the particular combination of substrates employed.²² Therefore, we decided to optimize any new combination of substrates with at least a few different solvents (typically, CH₂Cl₂ and toluene). We also reexamined these solvents for each particular substrates such as the doubly protected α -amino acids (**Table 3-4**) and mono protected β -amino acids (**Table 3-5**).

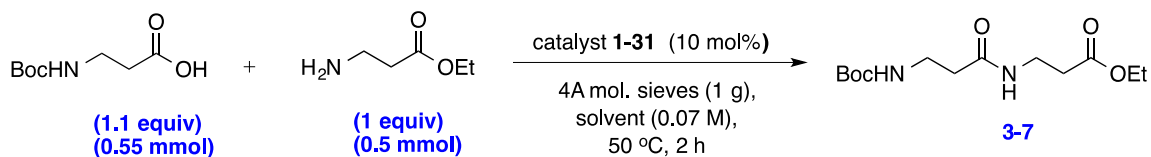


Entry	Solvent	Yield (%) ^a
1	CH ₂ Cl ₂	71
2	toluene	22

^a Isolated yields

Table 3-4: Optimization of solvent for amidation of doubly protected α -amino acids.

Dichloromethane was found to be the solvent of choice for α -amino acids (**Table 3-4, entry 1**), however, in the case of a β -alanine both solvents are comparable (**Table 3-5, entry 2**).



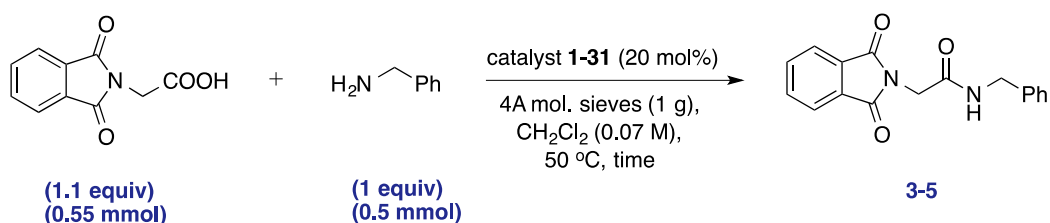
Entry	Solvent	Yield (%) ^a
1	CH ₂ Cl ₂	39
2	toluene	45

^a Isolated yields

Table 3-5: Optimization of solvent for amidation of a monoprotected β -amino acid.

3.3.2 Optimization of Reaction Concentration and Time

In our previous study with catalyst **1-31**, a concentration of 0.07 M for the carboxylic acid was found to be optimal when using CH₂Cl₂ as the solvent.²¹ A slight increase in the reaction concentration led to a higher yield of amide product.²² Hoping to take advantage of increased reaction rates at higher concentrations (0.1 M), I checked whether a higher concentration would benefit the reaction yield using 20 mol% of the catalyst **1-31** in direct amide formation of amino acid derivatives (**Table 3-6, entry 2**).



Entry	Conc (M)	Time	Yield (%) ^a
1	0.07	24 h	64
2	0.14	24 h	62
3	0.07	48 h	66

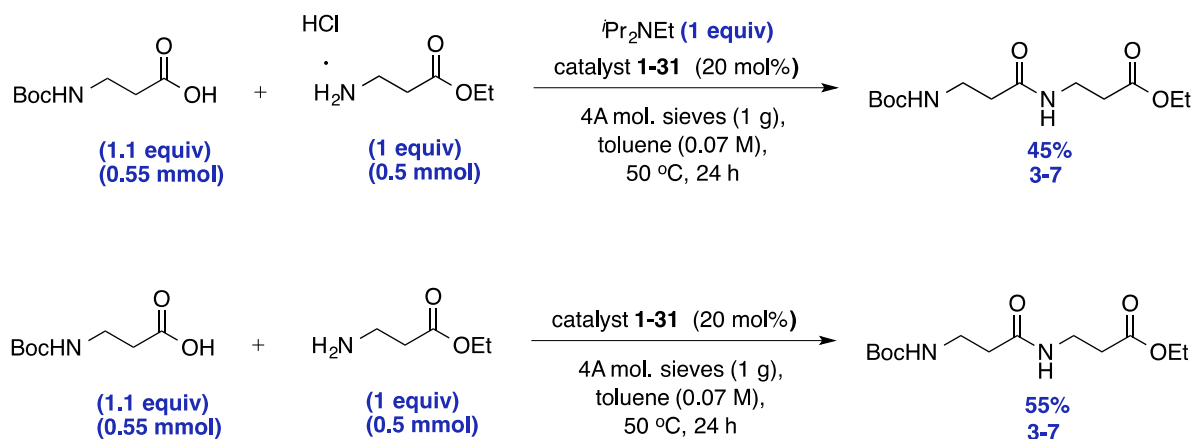
^a Isolated yields.

Table 3-6: Optimization of reactant concentration with catalyst 1-31.

3.3.3 Optimization of Amine Stoichiometry

Analogous to previous work in the Hall Group,²¹ a slight excess of carboxylic acid was used to prepare dipeptides (1.1 equivalent of *N*-protected amino acids and 1 equivalent of *C*-protected amino ester). Then, the corresponding *C*-protected β -amino acids, in the form of ethyl ester HCl salts, were conveniently neutralized by Hünig's base (**Scheme 3-5**).¹⁸ A comparison of the results shows that using Hünig's base for *in situ* neutralization

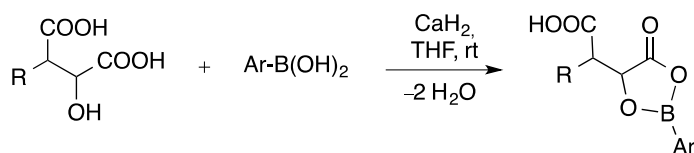
slightly decreases the yield of the reaction (by 10%).



Scheme 3-5: In situ neutralization using Hünig's base.

3.4 Design of New Substrates to Optimize the Catalytic Direct Dipeptide Synthesis

It is well documented that boronic acids are able to form complexes with the bidentate substrates such as α -hydroxy carboxylic acids (**Scheme 3-6**).²⁵

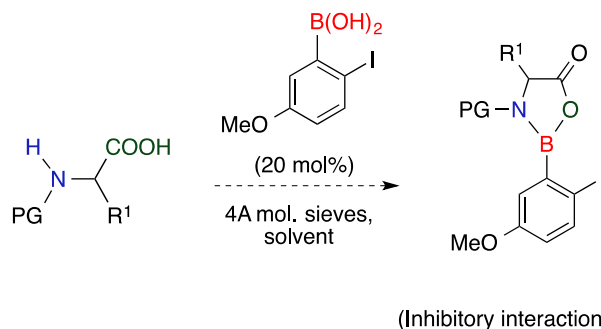


Scheme 3-6: General reaction scheme for the reaction of arylboronic acids with malic acid.

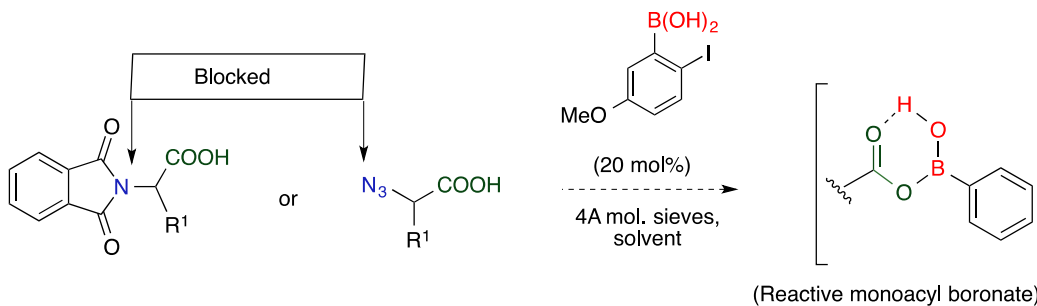
A similar complex may inhibit catalyst recycling in the amidation process when using bidentate, monoprotected α -amino acids. Therefore, it became necessary to design protected or masked amino acids to avoid catalyst inhibition and provide a suitable substrate to perform the amidation reaction in catalytic fashion. Thus, modifying the substrate as a phthaloyl or using an azidoamino acid as a masked amino acid (**Scheme 3-**

7) enabled us to develop a novel catalytic approach in dipeptide synthesis.

Possible inhibitory interaction between the catalyst and substrate:



Substrate design:



Scheme 3-7: Substrate modification to avoid irreversible complexation with a boronic acid catalyst.

It was shown in our previous study that monoprotected α -amino acids are inefficient substrates for catalytic amidation.²⁶ For instance, the reaction of *N*-Boc- α -glycine with hexylamine did not lead to any amide product at 25 °C after two hours using catalyst **1-31**, which could be explained by inhibitory interaction of boron with the bidentate substrates (**Scheme 3-7**).²⁶ Furthermore, this inhibitory phenomenon may explain the stoichiometric use of a boronic acid in the dipeptide synthesis of Whiting and coworkers.¹⁸

3.5 Substrate Scope for Catalytic Direct Amide Bond Formation Between Amino Acids Derivatives

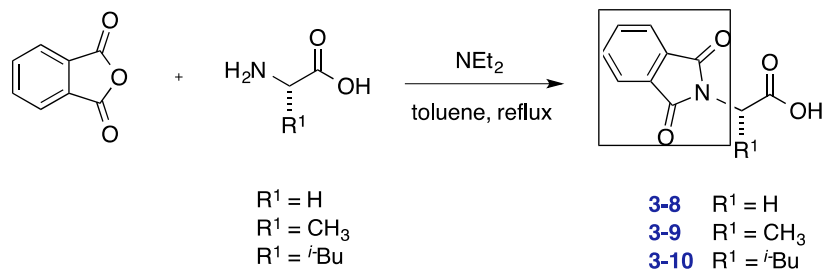
With optimal conditions in hand using the *ortho*-iodophenylboronic acid catalyst **1-31** for catalyzing direct amide bond formation between *N*- and *C*-protected α - and β -amino acids, the versatility and scope of this method was investigated next. According to the rationale described in Section 3.4,²⁵ the preferred substrates for direct amidation using catalyst **1-31** turned out to be the doubly protected *N*-phthaloyl α -amino acids (**Figure 3-4**). To ensure reaction completion in the case of less active amino acid substrates, a reaction time of 48 h was chosen (**Table 3-6**). Satisfactorily, it is possible to couple *N*-terminal to *C*-terminal protected amino acids in CH₂Cl₂ or toluene (depending on the substrate) at 50 °C under conditions that would hopefully avoid racemization in the formation of the dipeptide products. It was found that a change in substituent from hydrogen to *isobutyl* in the amino donor also depresses the reactivity of the substrate led to lower yield, even with a higher catalyst loading (**Figure 3-4, entry 3-16, 3-19, 3-21**).

A panel of modified α -amino acids, including phthaloyl and azido derivatives was studied in catalytic direct dipeptide synthesis with *C*-protected amino esters (**Figure 3-4, Figure 3-5**). *N*-Boc- β -amino acids are suitable substrates providing good yields in peptide syntheses using optimal conditions and catalyst (**Figure 3-6**).

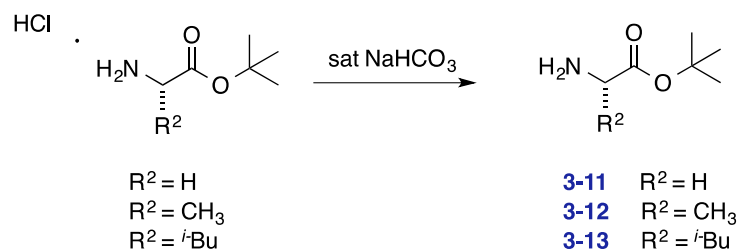
3.5.1 Peptide Synthesis from Protected α -Amino Acid

The doubly *N*-protected phthaloyl amino acids (as free carboxylic acids) and the neutralized amino esters (as a free amines) were prepared as shown in **Scheme 3-8**. Then, the two fragments were subjected to the optimized catalytic amidation conditions to make the corresponding dipeptides. The results are summarized in **Figure 3-4**.

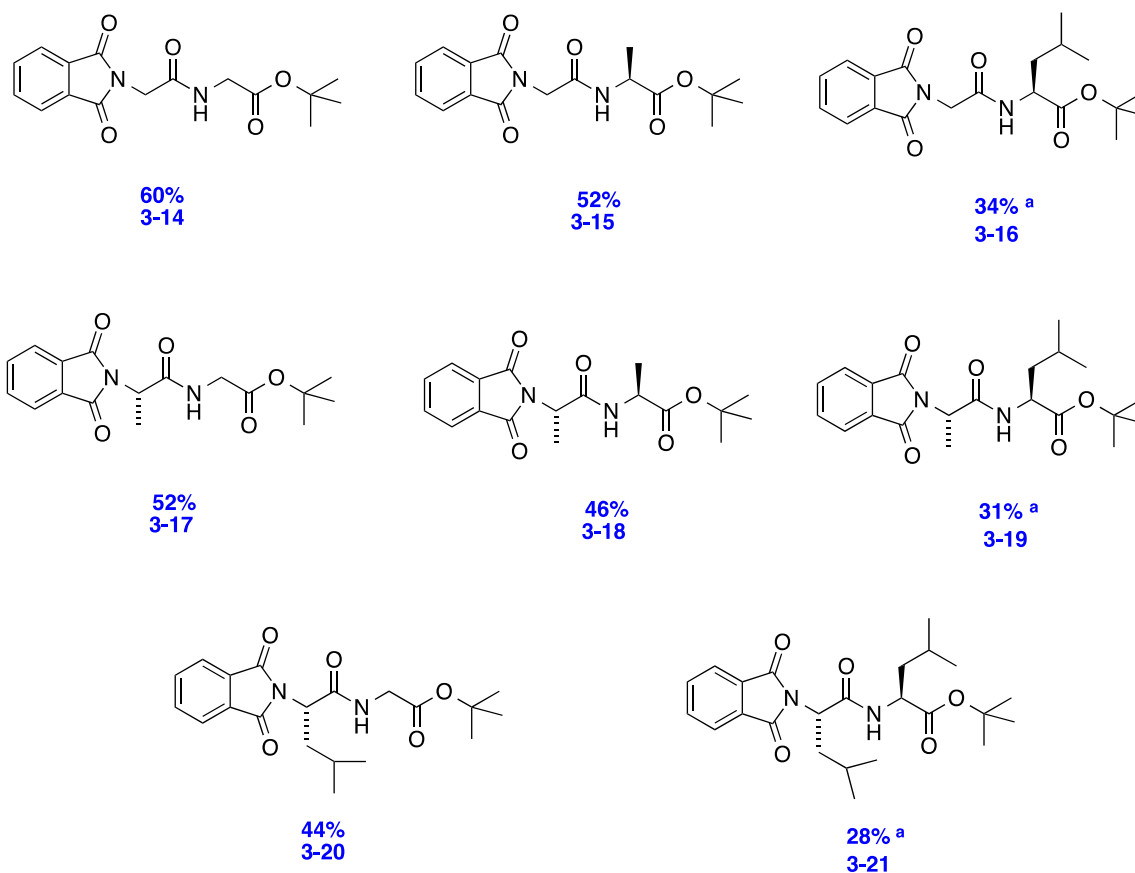
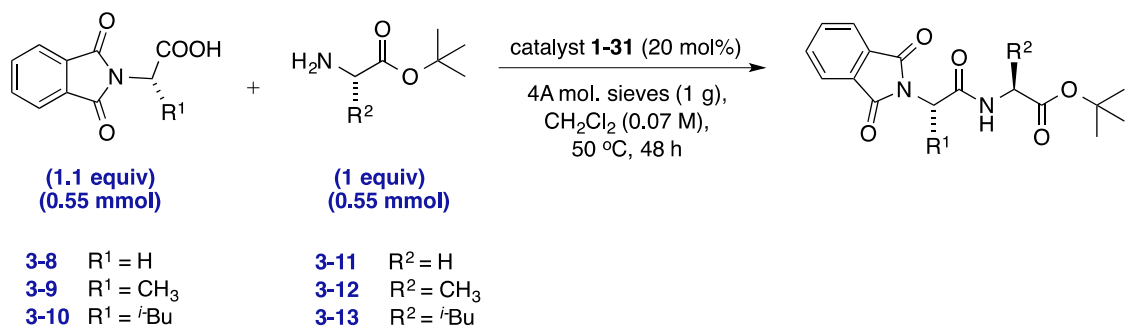
A- *N*-protected amino acid



B- *C*-protected amino acid (neutralization)



Scheme 3-8: Synthesis of double *N*-phthaloyl α -amino acid (A) and neutralization of α -amino ester salt (B).



^a catalyst loading (25 mol%).

Figure 3-4: Direct amidations between fully *N*-phthaloyl α -amino acids and *C*-protected α -amino esters catalyzed by boronic acids 1-31 at 50 °C.

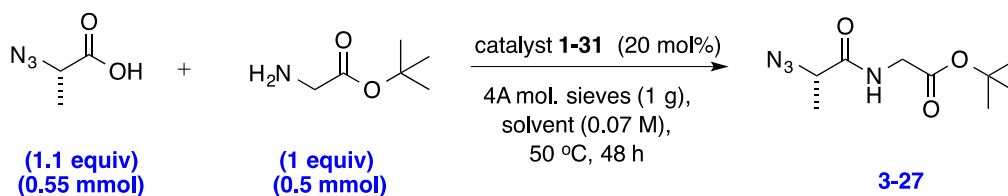
From the results in **Figure 3-4**, employing doubly *N*-protected phthaloyl amino acids successfully avoided inhibition of catalyst **1-31** by the substrate and the desired dipeptides were obtained in moderate to low yields. More hindered, branched amino ester derivatives reacted poorly with *N*-protected amino acids (**3-16**, **3-19** and **3-21**), demonstrating that sterics in the amino donor is a major negative factor in the reaction rate, which is consistent with Whiting's observation.¹⁸ In order to further enhance the rate of the reaction, raising the temperature to 60 °C or increasing the catalyst loading (30 mol%) may afford better yields in the case of more sterically demanding amino acids (**3-16**, **3-19** and **3-21**). Despite the moderate yields, highly hindered substrates were effectively employed to make amide products using this simple and highly atom-economical process (**3-21**).

3.5.2 Peptide Synthesis Using α -Azido Carboxylic Acids

In this study, α -azido carboxylic acids were used as the masked *C*-terminal α -amino acid. The α -azido carboxylic acids (as free carboxylic acids) and the neutralized amino esters were prepared as shown in **Scheme 3-9**. The two fragments were prepared and subjected to the optimized catalytic amidation conditions to obtain the corresponding dipeptides (**Figure 3-5**).

3.5.2.1 Optimization of the Reaction Solvent

According to previous observations,^{21,24} the use of different carboxylic acid-amine combinations often required different solvent systems. An examination of different solvents was performed for the particular substrates shown in **Table 3-7**.



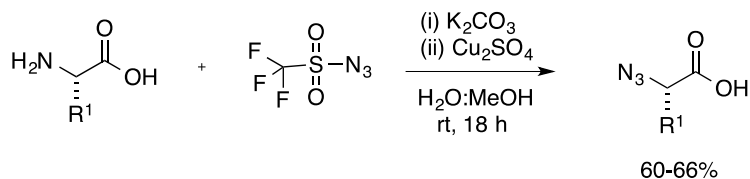
Solvent	Temperature	Yield (%) ^a
THF	60	10
CH ₂ Cl ₂	50	58
CH ₂ Cl ₂	25	38
toluene	50	70

^a Isolated yields.

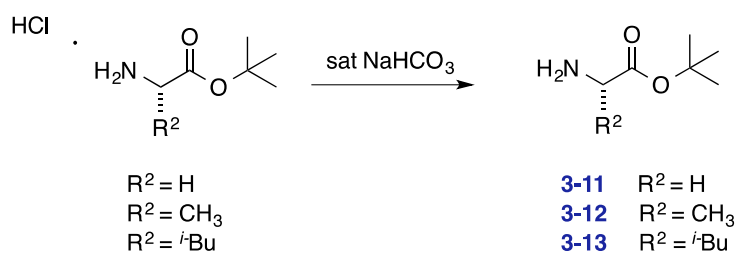
Table 3-7: Solvent optimization in dipeptide synthesis.

Having established that using toluene as a non-polar solvent leads to an improvement in the amidation of α -azido carboxylic acids and amino esters, the scope of substrates was then examined (**Figure 3-5**). The optimal reaction conditions were determined to be 50 °C with a reactant concentration of 0.07 M.

A- *N*-protected azido carboxylic acid



B- C-protected azido carboxylic acid



Scheme 3-9: Synthesis of α -azido acid (A) and neutralization of α -amino ester salt (B).

The examples compiled in **Figure 3-5** demonstrate the scope of direct amidations of these α -azido carboxylic acid substrates and provide the expected dipeptide products in good to moderate yields (**Figure 3-5**, 41 to 70 % yield).

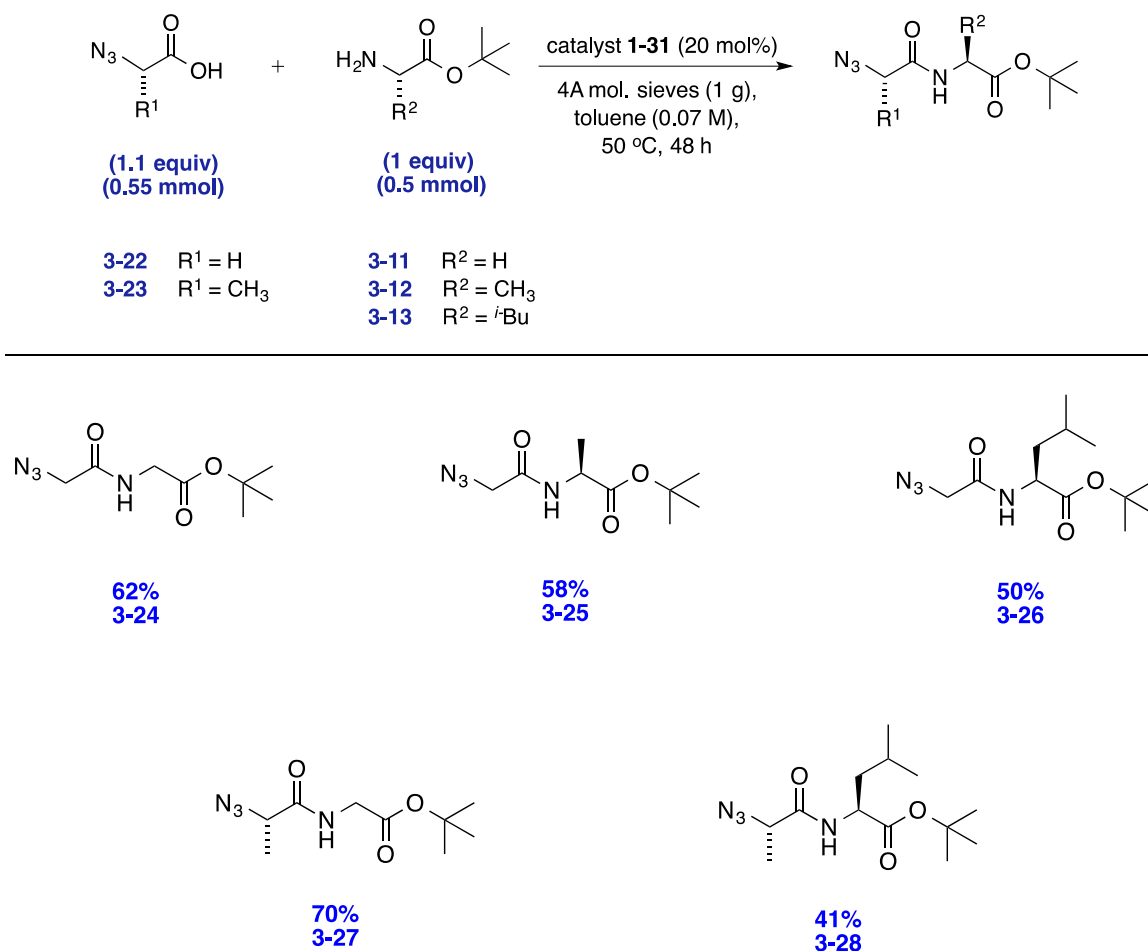


Figure 3-5: Direct amidations between protected α -azido carboxylic acids and C-protected α -amino acids catalyzed by boronic acid 1-31 at 50 °C.

Changing the masking group from a phthalimide to an azide enhanced the reaction efficiency. Both branched and unbranched amino acids are effective substrates using the optimized reaction conditions. Branched amino ester derivatives, however, still have slower conversion than less sterically demanding amino donor (**3-28** vs **3-24** and **2-27**; 41 vs 62 and 70 % yield respectively).

3.5.3 Dipeptide Synthesis Using *N*-Boc Protected β -amino acids

In order to conduct a thorough examination of substrate scope, catalytic direct dipeptide synthesis of *N*-Boc protected β -amino acids (mono protected β -amino acids) was investigated as well. Results are summarized in **Figure 3-6**.

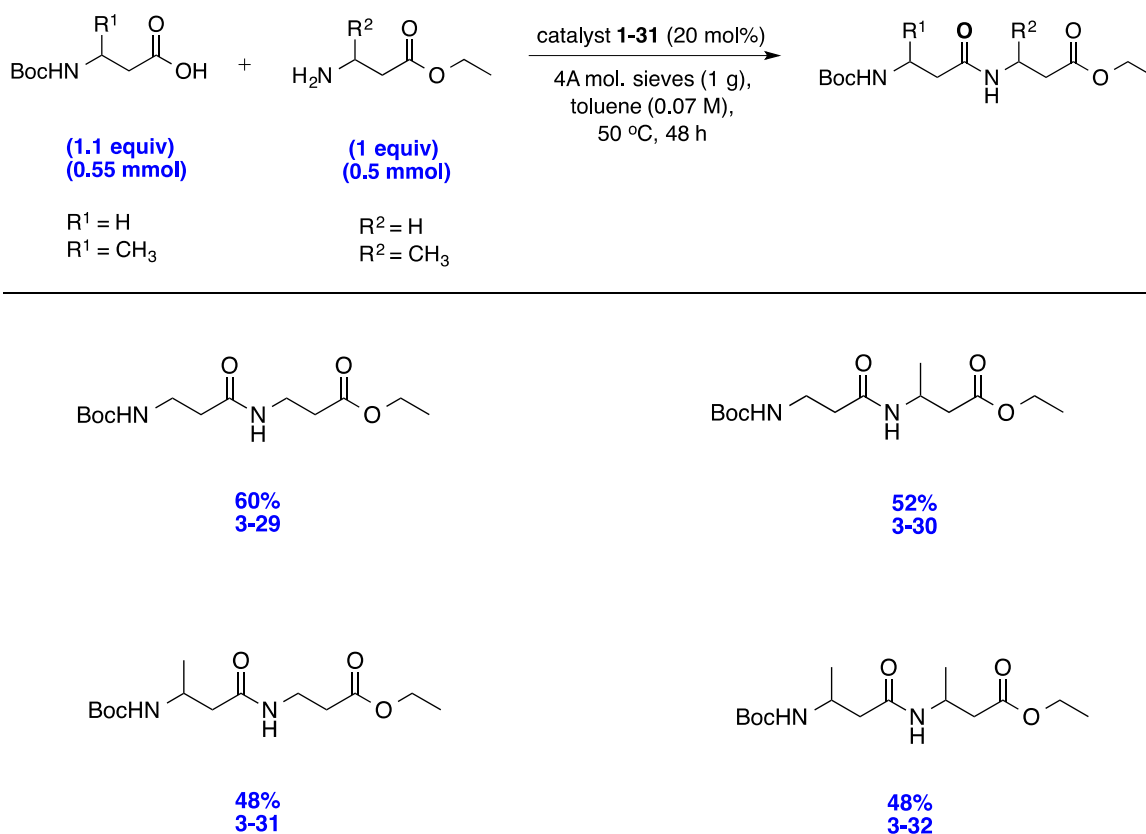


Figure 3-6: Direct amidations between *N*-protected β -amino acids and *C*-protected β -amino acids (as free amines) catalyzed by boronic acids **1-31 at 50 °C.**

Monoprotected β -amino acids (branched and unbranched) were successfully employed using optimal catalyst **1-31** (20 mol%) at 50 °C and toluene as the optimal solvent for 48 h, affording products in good to moderate yield. The inhibitory interaction between the catalyst and substrate (Section 3.4) was not an issue in these catalytic β -peptide syntheses. Then, the method was applied in scale up studies (Chapter Two, Section 2.3.2). Using 5 g of *N*-Boc β -alanine, conversion into the peptide **3-30** was achieved

under the reoptimized “greener” reaction conditions and the isolated yield was found to be 58% (4.208 g) at 55 °C after 72 h using 4A molecular sieves (1 g per mmol of substrate). This gram-scale application highlights the versatility of this catalytic, direct dipeptide synthesis methodology.

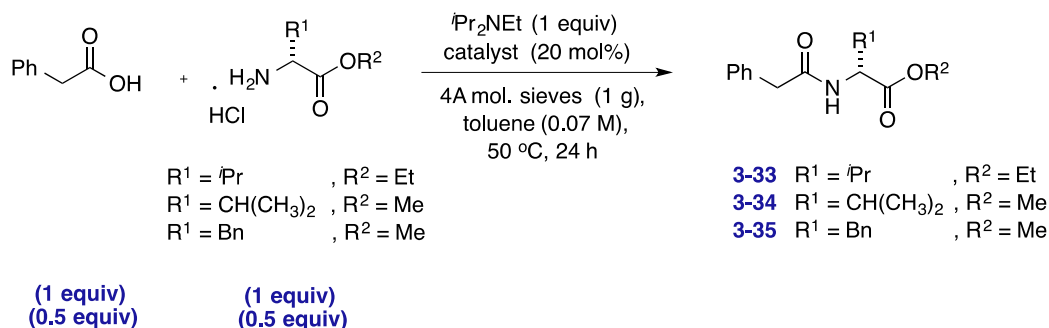
The results shown in **Figure 3-4, 3-5** and **3-6** obtained under low temperature conditions provide a clear testimony to the mildness of arylboronic acid catalyzed amidations. These direct catalytic amidations are operationally very simple. They employ equimolar amounts of *C*-terminal amino acids and *N*-terminal amino acids substrates, require low heating (50 °C). The pure dipeptide products can be isolated after a simple filtration and acid-base extractions to remove any unreacted substrates and the catalyst. Moreover, the boronic acid catalyst can be recovered in high yield from the basic aqueous phase (Chapter Two, Section 2.3.2).

3.6 Investigation of Possible Racemization in Catalytic Direct Dipeptide Synthesis

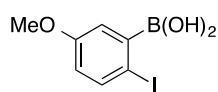
A comparison of the results for catalysts **3-1** and **3-2** (under Whiting’s conditions)¹⁸ and for **1-31**, showed no observable racemization with catalyst **1-31** at 50 °C (**Scheme 3-10**). On the contrary, with catalysts **3-1** and **3-2**, Whiting observed partial racemization at 85 °C, particularly when a benzyl side-chain is present on the amino acid structure (**3-35**). According to their observation, the enantiomeric purity was diminished particularly when catalyst **3-2** was used under the reaction conditions, causing some racemization in products **3-34** and **3-35**. When using our optimal catalyst **1-31**, however, no racemization was observed on the three model amides (**Scheme 3-10, entry 3-33, 3-35** and **3-36**). The enantiomeric excesses for chiral compounds were determined by Mr. Ed Fu using a chiral HPLC analysis.

The advantage of using catalyst **1-31** over the other two Whiting’s preferred catalysts **3-2** and **3-1** is highlighted in the enantiomeric purity of resulting product **3-35**, in which no racemization occurred through the catalytic direct dipeptide synthesis. In contrast,

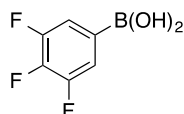
Whiting and coworkers observed partial racemization with both catalysts **3-2** and **3-1** (67 and 64% ee respectively) for this particular product (**3-35**).



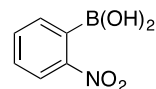
Catalysts:



1-31

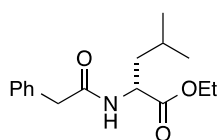


3-1 (Whiting's catalyst)

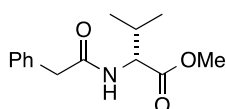


3-2 (Whiting's catalyst)

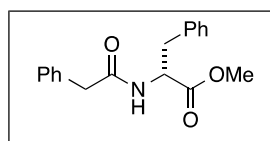
Amide product:



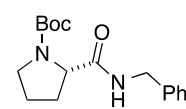
3-33



3-34



3-35

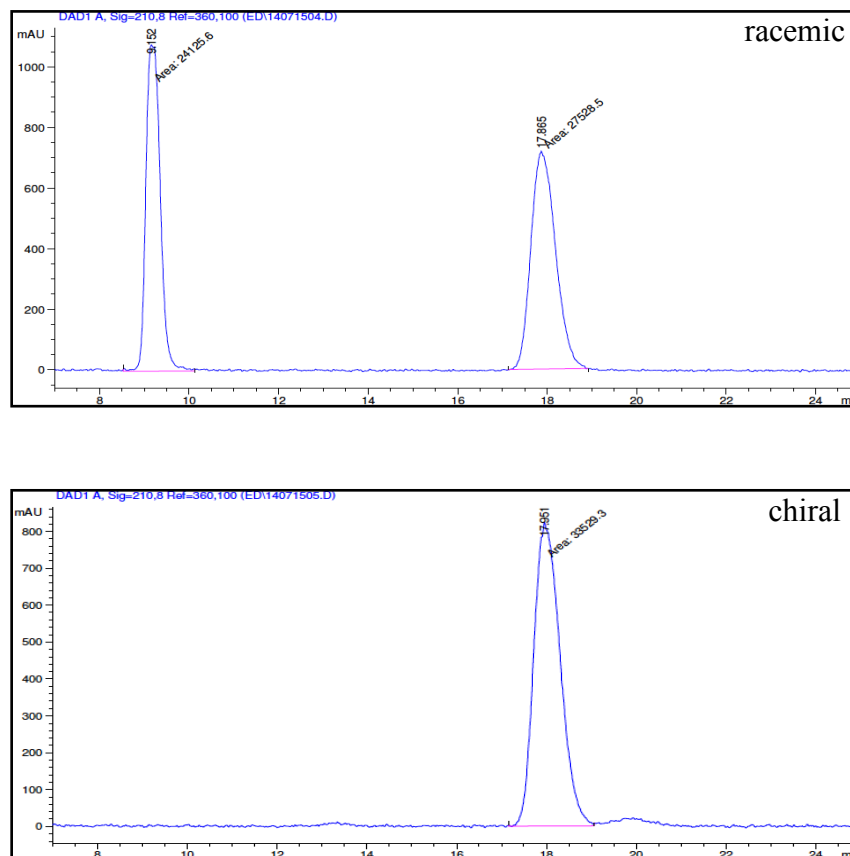


3-36

Summary of Whiting epimerization study versus our results under milder condition

Entry	Amide product	Temp. (°C)	Catalyst	ee (%)
1	3-36	85	3-1	99 ¹⁸
2	3-36	85	3-2	79 ¹⁸
3	3-36	50	1-31	99
4	3-35	85	3-1	64 ¹⁸
5	3-35	85	3-2	67 ¹⁸
6	3-35	50	1-31	99
7	3-34	85	3-1	99 ¹⁸
8	3-34	85	3-2	71 ¹⁸
9	3-33	50	1-31	99

Chiral HPLC chromatogram for 3-35 using catalyst 1-31:



Scheme 3-10: Study of stereochemical integrity in direct peptide synthesis methodology.

Whiting and coworkers rationalized that neither the temperature nor the catalyst played the major role in the observed erosion of enantiomeric purity, rather the amino acid structure itself, such as the presence of a benzyl side-chain in **3-35**, which results in a greater propensity for racemization under the reaction conditions. In contrast, based on the results obtained from **Scheme 3-10**, the nature of the catalyst itself and the temperature play a major role in avoiding a loss of enantiomeric purity.

3.7 Conclusion

The development of a catalytic process in which the peptide bond can be formed directly from *N*-terminal and *C*-terminal amino acids under mild reaction conditions would be the optimum solution to overcome the limitations of racemization, decomposition, unwanted side reactions and poor atom economy. Recently, boron reagents have provided a prospect for much “greener” alternatives and an attractive approach for the long-standing problem of catalytic peptide synthesis.¹⁸ The use of a catalytic amount of arylboronic acids for direct peptide formation offers environmentally friendlier conditions compared to coupling reagents.

The exceptional and remarkable ability of 5-methoxy-2-iodophenylboronic acid **1-31** to serve as a catalyst to couple *N*-terminal to *C*-terminal amino acids in proper solvents (depending on the substrate) under conditions that avoid racemization in the formation of dipeptide derivatives has been demonstrated. This simple process represents a significant step towards the goal of atom economical and cost efficient syntheses of peptide.

These results also demonstrate that catalytic direct dipeptide synthesis using *N*-terminal to *C*-terminal protected amino acids can be conducted under mild reaction conditions at low temperature (50 °C). The versatility and scope of this methodology was demonstrated using different substrates such α -phthaloyl amino acids or α -azido carboxylic acids and mono protected β -amino acids. It is noteworthy that special protection of the substrate is necessary when α -amino acids are subjected to the reaction conditions. The reason is probably to avoid boron complexation with the bidentate monoprotected α -amino acids (Section 3-4). It is assumed that inhibitory complexation of the boronic acid catalyst with the substrate was not significant in the case of monoprotected β -amino acids (Section 3-4).

Slower conversion was observed when more hindered, branched amino ester derivatives (as amine donor) were used. However, changing from phthaloyl to azide as the masking group in the substrate resulted in a higher yield. This result indicates that further modification of the substrate may enhance its reactivity profile. The reaction worked well

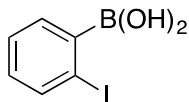
on a multigram scale (5 g) to obtain β -peptide **3-30** in 58% yield (Section 2.3.2). Finally, the present procedure with catalyst **1-31** offers another advantage in suppressing racemization in peptide synthesis.

3.8 Experimental

3.8.1 General Information

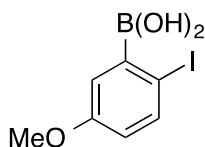
Unless otherwise stated, all reactions were performed under a nitrogen atmosphere using flame-dried glassware. Toluene, THF and dichloromethane were dried from a double cartridge solvent purification system. Analytical thin layer chromatography was performed on Merck Silica Gel 60 F254 plates and was visualized with UV light and KMnO₄ stain. NMR spectra were recorded on 400, or 500 MHz instruments. The residual solvent protons (¹H) or the solvent carbon (¹³C) were used as internal standards. ¹H-NMR data are presented as follows: chemical shift in ppm (δ) downfield from tetramethylsilane (multiplicity, coupling constant, integration). The following abbreviations are used in reporting NMR data: s = singlet, d = doublet, dd = doublet of doublets, ddd = doublet of doublet of doublets, dt = doublet of triplets, t = triplet, td = triplet of doublets, m = multiplet, q = quartet, qd = quartet of doublets, qt = quartet of triplets, app = apparent, br. s = broad singlet. *J* accuracy: (+/-) 0.5 Hz. ¹³C signals arising from the quaternary carbon bearing the boronic acid group were not always observed and therefore were not always listed (exhaustive peak broadening due to quadrupolar relaxation of ¹¹B). High-resolution mass spectra (TOF analyzer) were recorded using either electron impact (EI) or electrospray ionization (ESI) techniques. Infrared spectra were obtained with frequencies expressed in cm⁻¹. Infrared spectra were obtained on a Nicolet Magna-IR 750 with frequencies expressed in cm⁻¹. The enantiomeric excesses for chiral compounds were determined using a HPLC Agilent instrument with Chiralcel-OD or Chiralpak-AS columns with UV detection (in comparison to racemic products). Powdered 4A molecular sieves (< 5 micron, Aldrich) were dried overnight in an oven (300 °C) prior to use. All the different catalysts were stored in a fridge, under inert atmosphere.

3.8.2 Preparation and Characterization Data for *Ortho*-Iodophenylboronic Acid (**1-30**):



To a solution of 1,2-diiodobenzene (10.2 g, 30.8 mmol, 1.0 equiv) in 300 mL of a mixture of THF and Et₂O (1:1) at -78 °C was added dropwise *isopropyl* magnesium chloride (2 M in THF, 15.4 mL, 30.8 mmol). The mixture was stirred at that temperature for 2 h and then, triisopropyl borate (17.4 g, 92.4 mmol) was added. The solution was slowly allowed to warm up to room temperature and stirred overnight. HCl (10% aq., 400 mL) was added and the resulting mixture was stirred 30 min at room temperature. The aqueous layer was extracted with Et₂O (3×500 mL). Drying of the organic phase (Na₂SO₄), filtration and evaporation gave the crude that was purified by flash chromatography (100% hexanes, then hexane/EtOAc; 4:1) to yield the desired product (0.62 g, 82% yield) as a white solid. Characterization of the compound matched that of a previous report.²¹

3.8.3 Preparation and Characterization Data of 5-Methoxy-2-Iodophenylboronic Acid (**1-31**):



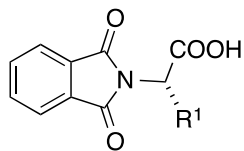
A solution of iodine in EtOH (1.20 g, 4.72 mmol, 1.0 equiv, 0.3 M) was added dropwise to a mixture of 4-methoxyphenylboronic acid (717 mg, 4.72 mmol, 1.0 equiv) and silver (I) sulfate (811 mg, 2.60 mmol, 0.55 equiv) in EtOH (15 mL) at room temperature. After complete addition of iodine the reaction was stirred at room temperature until the iodine color completely disappeared. The reaction mixture was filtered through a pad of Celite 545 using ethyl acetate, water (50 mL) was added to the filtrate and the mixture was extracted with ethyl acetate (2×30 mL). The combined organic layers were washed with aqueous sodium sulfite, brine, dried over Na₂SO₄, filtered and concentrated. The residue was chromatographed on silica gel (hexane/ethyl acetate 3:1) to yield the pure desired product (0.92 g, 70% yield). Characterization of the compound matched that of a previous report.²²

3.8.4 General Procedure for Table 3-2: Comparison in product yields for different dehydrating agents and catalysts **1-30**, **1-31**, **3-2** and solvents in a direct amidation reaction between (Boc)-proline and benzylamine.

Into a 25 ml round bottom flask equipped with a stir bar was added *N*-tert-butyloxycarbonyl(Boc)-proline (108 mg, 0.50 mmol, 1.0 equiv), catalysts **1-30**, **1-31**, **3-2** (0.1 mmol, 20 mol%) and 1 g of activated 4A or 3A molecular sieves. Solvent [0.07 M] was added to the mixture and was stirred for 10 min. Then, benzylamine (55 μ L, 0.5 mmol, 1.0 equiv) was added. The resulting mixture was stirred for 18 h at 50 or 85 $^{\circ}$ C. The reaction mixture was filtered through a pad of Celite $\text{\textcircled{R}}$ 545 with 15 mL of CH_2Cl_2 , the filtrate was washed with aqueous acidic solution (15 mL, 1 M), aqueous basic solution (15 mL, 1 M) and brine (15 mL). The organic layer collected, dried over anhydrous Na_2SO_4 , filtered and evaporated to yield the title compound **3-6** as a pure product. Characterization data of the product matched that found in the literature.¹⁸

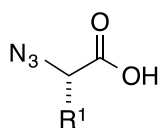
3.8.5 General Procedure for Preparation of *N*-Protected Amino Acids

3.8.5.1 General Procedure for Preparation of L-*N*-Phthaloyl Amino Acids



In fitted three-neck round-bottom flask with Dean-stark apparatus and a reflux condenser, phthalic acid anhydride (1.48 g, 10 mmol) and appropriate L-amino acids (10 mmol) were refluxed in toluene in the presence of 0.1 mL triethylamine for 10 h. After the completion of reaction the organic solvent was removed in a rotary evaporator to get a sticky oily mass. Water was added to this oily mass and the mixture was acidified with hydrochloric acid and stirred for 30 min to get a solid product. This solid was filtered off, washed with water, and dried to get a target compound in 98% yield of phthaloyl α -amino acid as a white powder. Characterization of the compound matched that of a previous report.²⁷

3.8.5.2 General Procedure for Preparation of Azide Derivatives of L-Amino Acid



Preparation of triflyl azide: Sodium azide (2.00 g, 30.8 mmol, 5.16 equiv) was dissolved in distilled water (5 mL) and then dichloromethane (CH_2Cl_2 , 8 mL) was added. This mixture was cooled on an ice bath for 20 min. Triflyl anhydride (1 mL, 5.97 mmol, 1.00 equiv) was added slowly over 5 min and the mixture was stirred for 2 h. The mixture was transferred to a separatory funnel and then CH_2Cl_2 phase removed. The aqueous phase was extracted with CH_2Cl_2 (2×4 mL). The organic portions, containing the triflyl azide, were pooled and washed once with saturated Na_2CO_3 and used without further purification.

Preparation of azido acid: Preparation of azido acid: Amino acid (3.00 mmol) was combined with K_2CO_3 (595 mg, 4.50 mmol) and $\text{Cu}^{\text{II}}\text{SO}_4 \cdot 5\text{H}_2\text{O}$ (7.53 mg, 30.0 μmol , 1 mol%) in a distilled water (10 mL) and methanol (MeOH , 20 mL). The triflyl azide in CH_2Cl_2 (16 mL) was added and the mixture was stirred at ambient temperature and pressure overnight. Subsequently, the organic solvents were removed under reduced pressure and the aqueous slurry was diluted with water (50 mL). This was acidified to pH 6 with conc. HCl and diluted with phosphate buffer (250 mM, pH 6.20, 50.0 mL) and extracted with ethyl acetate (EA , 4×20 mL) to remove sulfonamide by-product. The aqueous phase was then acidified to pH 2 with conc. HCl . The product was obtained from another round of EA extractions (3×20 mL). These EA extracts were combined, dried with MgSO_4 , filtered and evaporated to dryness giving pale yellow oil in 60-66% yield with no need for further purification. Characterization of the compounds matched that of a previous report.²⁸

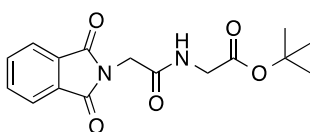
Safety notes for preparation of triflyl azide: It is prepared before use by reacting trifluoromethanesulfonic anhydride with sodium azide, traditionally in dichloromethane.^{29a} However, use of dichloromethane should be avoided because sodium azide is known to generate highly explosive azido-chloromethane and diazidomethane in situ by nucleophilic substitution on dichloromethane. Moreover, the volatility of dichloromethane is a liability, as unsolvated triflyl azide is a detonation hazard. The reaction may also be carried out in toluene, acetonitrile, or pyridine. The

trifluoromethanesulfonic anhydride starting material is rather expensive, and the product is explosive, and does not store well. As a result, imidazole-1-sulfonyl azide has been developed as an alternative.^{29b} It is commercially available, and shelf-stable. Neat TfN₃ is explosive. Small amounts of a solution of TfN₃ in hexane can be made repeatedly for small scale. There is a procedure to make it in hexane/water biphasic, which is fairly safe on small scale.

3.8.6 General Procedure for Dipeptide Synthesis Using Optimal Catalyst **1-31**

Into a 25 mL round-bottom flask equipped with a magnetic stir bar was added α or β *N*-Protected (L-azido/phthaloyl or Boc) amino acid (0.55 mmol, 1.1 equiv), 2-iodo-5-methoxyphenylboronic acid **1-31** (0.10 mmol, 20 mol%) and 1 g of activated 4A molecular sieves. Dichloromethane or toluene (7 mL) was added, and the mixture was stirred vigorously for 10 min. The choice of solvent depends on the substrates. Then, L- α or β -amino alkyl ester (0.50 mmol, 1.0 equiv) was added to the reaction mixture with gastight 100 μ L syringe. The resulting mixture in a sealed flask was stirred for 48 h under vigorous stirring at 50 °C temperature. The reaction mixture was filtered through a pad of Celite 545 with 15 mL of CH₂Cl₂; the filtrate was washed with aqueous acidic solution (15 mL \times 2, 1 M), aqueous basic solution (15 mL \times 2, 1 M) and brine (15 mL \times 2). The organic layer was collected, dried over anhydrous Na₂SO₄, filtered and evaporated to yield pure dipeptide product.

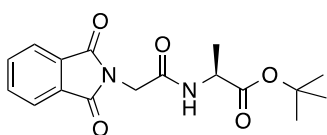
3.8.6.1 Preparation and Characterization Data of *t*-Butyl (2-(1,3-Dioxoisindolin-2-yl)acetyl)glycinate (**3-14**)



The title compound was prepared using the general procedure for dipeptide synthesis and CH₂Cl₂ as a solvent yielded **3-14** (60%). ¹H NMR (CDCl₃, 400 MHz): δ = 7.89 (m, 2 H), 7.78 (m, 2 H), 6.40 (br. s, 1 H), 4.40 (s, 2 H), 3.98 (d, *J* = 4.8 Hz, 2 H), 1.42 (s, 9 H); ¹³C NMR (100.6 MHz, CDCl₃): δ = 168.6, 167.8, 165.9, 134.2, 132.0, 123.6, 82.6, 42.4, 40.6, 28.0 (3 C); IR (Microscope, cm⁻¹) 3306, 3087, 2976, 2931, 1776,

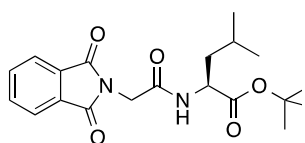
1728, 1660, 1561; **HRMS** (ESI) for C₁₆H₁₉N₂O₅ (M+H)⁺: calcd. 319.1288; found, 319.1290.

3.8.6.2 Preparation and Characterization Data of *t*-Butyl (2-(1,3-Dioxoisindolin-2-yl)acetyl)-*L*-alaninate (**3-15**)



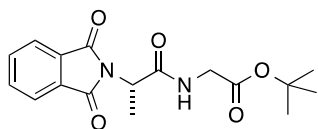
The title compound was prepared using the general procedure for dipeptide synthesis and CH₂Cl₂ as a solvent yielded **3-15** (52%). ¹H NMR (CDCl₃, 400 MHz): δ = 7.89 (m, 2 H), 7.78 (m, 2 H), 6.60 (br. d, *J* = 6.9 Hz, 1 H), 4.48 (app pent, *J* = 7.0 Hz, 1 H), 4.38 (m, 2 H), 1.76 (s, 9 H), 1.42 (d, *J* = 7.0 Hz, 3H); ¹³C NMR (100.6 MHz, CDCl₃): δ = 169.0, 168.9, 167.8, 134.3, 131.9, 123.6, 82.5, 49.3, 42.4, 28.0 (3 C), 15.3; **IR** (Microscope, cm⁻¹) 3306, 3067, 2980, 2936, 1776, 1725, 1650, 1540; **HRMS** (ESI) for C₁₇H₂₁N₂O₅ (M+H)⁺: calcd. 333.1445; found, 333.1445.

3.8.6.3 Preparation and Characterization Data of *t*-Butyl (2-(1,3-Dioxoisindolin-2-yl)acetyl)-*L*-leucinate (**3-16**)



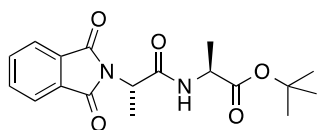
The title compound was prepared using the general procedure for dipeptide synthesis, 5-methoxy-2-iodoarylboronic acids **1-31** as a catalyst (25 mol%) and CH₂Cl₂ as a solvent yielded **3-16** (34%). ¹H NMR (CDCl₃, 400 MHz): δ = 7.89 (m, 2 H), 7.78 (m, 2 H), 6.20 (br. d, *J* = 8.2 Hz, 1 H), 4.54 (ddd, *J* = 8.2, 8.1, 5.7 Hz, 1 H), 4.40 (m, 2 H), 1.50-1.70 (m, 3 H), 1.42 (s, 9 H), 0.96 (d, *J* = 6.5 Hz, 6 H); ¹³C NMR (100.6 MHz, CDCl₃): δ = 171.9, 167.7, 165.4, 134.2, 132.1, 123.6, 82.3, 51.7, 42.2, 40.7, 28.0 (3 C), 24.9, 22.7, 22.3; **IR** (Microscope, cm⁻¹) 3333, 3067, 2959, 2871, 1776, 1725, 1543, 1468; **HRMS** (ESI) for C₂₀H₂₇N₂O₅ (M+H)⁺: calcd. 375.1914; found, 375.1914.

3.8.6.4 Preparation and Characterization Data of *t*-Butyl (*S*)-(2-(1,3-Dioxoisindolin-2-yl)propanoyl)glycinate (**3-17**)



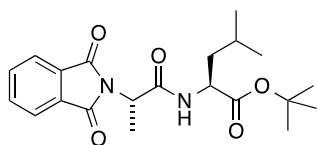
The title compound was prepared using the general procedure for dipeptide synthesis and CH_2Cl_2 as a solvent yielded **3-17** (52%). ^1H NMR (CDCl_3 , 400 MHz): δ = 7.89 (m, 2 H), 7.78 (m, 2 H), 6.58 (br. s, 1 H), 5.00 (q, J = 7.2 Hz, 1 H), 3.90 (d, J = 4.8 Hz, 2 H), 1.80 (d, J = 7.3 Hz, 3 H), 1.42 (s, 9 H); ^{13}C NMR (100.6 MHz, CDCl_3): δ = 169.0, 168.7, 167.8, 134.3, 131.9, 123.6, 82.6, 49.3, 42.4, 28.0 (3 C), 15.3; IR (Microscope, cm^{-1}) 2967, 1596, 1458, 1377, 1265, 1232, 998; HRMS (ESI) for $\text{C}_{17}\text{H}_{21}\text{N}_2\text{O}_5$ ($\text{M}+\text{H}$) $^+$: calcd. 333.1445; found, 333.1445.

3.8.6.5 Preparation and Characterization Data of *t*-Butyl ((*S*)-2-(1,3-Dioxoisindolin-2-yl)propanoyl)-*L*-alaninate (**3-18**)



The title compound was prepared using the general procedure for dipeptide synthesis and CH_2Cl_2 as a solvent yielded **3-18** (46%). ^1H NMR (CDCl_3 , 400 MHz): δ = 7.89 (m, 2 H), 7.78 (m, 2 H), 6.62 (br. s, 1 H), 4.90 (q, J = 7.3 Hz, 1 H), 4.40 (m, 1 H), 1.78 (d, J = 7.3 Hz, 3 H), 1.42 (s, 9 H), 1.40 (d, J = 7.0 Hz, 3 H); ^{13}C NMR (100.6 MHz, CDCl_3): δ = 172.0, 168.3, 167.8, 134.2, 131.9, 123.6, 82.2, 49.3, 49.0, 28.5 (3 C), 18.6, 15.3; IR (Microscope, cm^{-1}) 3347, 3063, 2980, 2936, 1715, 1682, 1531, 1457. HRMS (ESI) for $\text{C}_{18}\text{H}_{23}\text{N}_2\text{O}_5$ ($\text{M}+\text{H}$) $^+$: calcd. 347.1601; found, 347.1602.

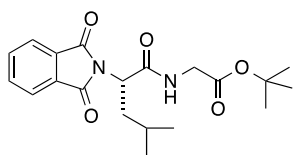
3.8.6.6 Preparation and Characterization Data of *t*-Butyl ((*S*)-2-(1,3-Dioxoisindolin-2-yl)propanoyl)-*L*-leucinate (**3-19**)



The title compound was prepared using the general procedure for dipeptide synthesis, 5-methoxy-2-iodoarylboronic acids **1-31** catalyst (25 mol%) and CH_2Cl_2 as a solvent yielded **3-19** (31%). ^1H NMR (CDCl_3 , 400 MHz): δ = 7.89 (m, 2 H), 7.78 (m, 2 H), 6.42 (br. S, 1 H), 4.96 (q, J = 7.5 Hz, 1 H), 4.45 (m, 1 H), 1.75 (d, J = 7.3 Hz, 3 H), 1.43-1.68 (m, 3 H), 1.42 (s, 9 H), 0.94 (d, J = 6.3 Hz, 6 H); ^{13}C NMR (100.6 MHz, CDCl_3): δ = 171.8, 168.6, 167.7, 134.2, 131.9, 123.5, 82.0,

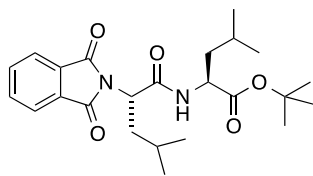
53.8, 51.7, 42.0, 28.0 (3 C), 24.9, 22.7, 22.3, 15.3; **IR** (Microscope, cm^{-1}) 3356, 3066, 2960, 2872, 1780, 1718, 1684, 1531, 1469. **HRMS** (ESI) for $\text{C}_{21}\text{H}_{29}\text{N}_2\text{O}_5$ ($\text{M}+\text{H}^+$): calcd. 389.2071; found, 389.2064.

3.8.6.7 Preparation and Characterization Data of *t*-Butyl (*S*)-(2-(1,3-Dioxoisindolin-2-yl)-4-methylpentanoyl)glycinate (**3-20**)



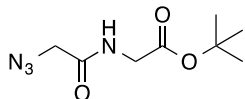
The title compound was prepared using the general procedure for dipeptide synthesis and CH_2Cl_2 as a solvent yielded **3-20** (44%). **^1H NMR** (CDCl_3 , 400 MHz): δ = 7.89 (m, 2 H), 7.78 (m, 2 H), 6.65 (br. s, 1 H), 4.49 (dd, J = 11.4, 4.8 Hz, 1 H), 3.90 (d, J = 4.8 Hz, 2 H), 2.42 (ddd, J = 13.9, 11.4, 4.4 Hz, 1 H), 1.83 (ddd, J = 14.0, 9.6, 4.8 Hz, 1 H), 1.44-1.49 (m, 1 H), 1.42 (s, 9 H), 0.95 (d, J = 6.6 Hz, 3 H), 0.94 (d, J = 6.6 Hz, 3 H); **^{13}C NMR** (100.6 MHz, CDCl_3): δ = 169.2, 168.7, 168.2, 134.2, 131.7, 123.6, 82.4, 53.0, 42.3, 37.4, 28.0 (3 C), 25.3, 23.1, 21.2; **IR** (Microscope, cm^{-1}) 3342, 3067, 2962, 2873, 1716, 1681, 1537, 1469; **HRMS** (ESI) for $\text{C}_{20}\text{H}_{27}\text{N}_2\text{O}_5$ ($\text{M}+\text{H}^+$): calcd. 375.1914; found, 375.1916.

3.8.6.8 Preparation and Characterization Data of *t*-Butyl ((*S*)-2-(1,3-Dioxoisindolin-2-yl)-4-methylpentanoyl)-*L*-leucinate (**3-21**)



The title compound was prepared using the general procedure for dipeptide synthesis, 5-methoxy-2-iodoarylboronic acids **1-31** as a catalyst (25 mol%) and CH_2Cl_2 as a solvent yielded **3-21** (28%). **^1H NMR** (CDCl_3 , 400 MHz): δ = 7.89 (m, 2 H), 7.78 (m, 2 H), 6.60 (br. d, 8.0 Hz, 1 H), 4.94 (dd, 11.3, 5.0 Hz, 1 H), 4.50 (ddd, 13.5, 7.5, 5.3 Hz, 1 H), 1.43-1.70 (m, 6 H), 1.42 (s, 9 H), 0.94 (m, 12 H); **^{13}C NMR** (100.6 MHz, CDCl_3): δ = 171.3, 168.3, 167.7, 133.8, 131.2, 123.1, 81.5, 52.7, 51.2, 41.5, 37.0, 27.5 (3 C), 24.8, 24.5, 22.6, 22.4, 21.7, 20.8; **IR** (Microscope, cm^{-1}) 3348, 3062, 2959, 2872, 1717, 1683, 1529, 1469; **HRMS** (ESI) for $\text{C}_{24}\text{H}_{35}\text{N}_2\text{O}_5$ ($\text{M}+\text{H}^+$): calcd. 431.2540; found, 431.2539.

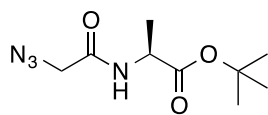
3.8.6.9 Preparation and Characterization Data of *t*-Butyl (2-Azidoacetyl)glycinate (3-24)



The title compound was prepared using the general procedure for dipeptide synthesis and toluene as a solvent yielded **3-24** (62%).

¹H NMR (CDCl₃, 400 MHz): δ = 6.80 (br. s, 1 H), 4.00 (s, 2 H), 3.98 (d, J = 5.3 Hz, 2 H), 1.51 (s, 9 H); **¹³C NMR** (100.6 MHz, CDCl₃): δ = 168.0, 166.2, 82.2, 52.1, 41.3, 27.6 (3 C); **IR** (Microscope, cm⁻¹) 3323, 3082, 2979, 2935, 1735, 1716, 1653, 1527, 1449; **HRMS** (ESI) for C₈H₁₄N₄NaO₃ (M+Na)⁺: calcd. 237.0958; found, 237.0956.

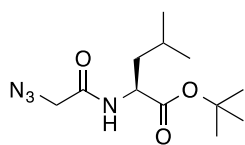
3.8.6.10 Preparation and Characterization Data of *t*-Butyl (2-Azidoacetyl)-*L*-alaninate (3-25)



The title compound was prepared using the general procedure for dipeptide synthesis and toluene as a solvent yielded **3-25** (58%). **¹H NMR** (CDCl₃, 400 MHz): δ = 6.90 (br. s, 1 H), 4.51

(app pent, J = 7.2 Hz, 1 H), 4.00 (s, 2 H), 1.51 (s, 9 H), 1.41 (d, J = 7.2 Hz, 3 H); **¹³C NMR** (100.6 MHz, CDCl₃): δ = 171.7, 166.0, 82.4, 52.6, 48.6, 28.0 (3 C), 18.6; **IR** (Microscope, cm⁻¹) 3311, 3072, 2981, 2934, 2108, 1735, 1664, 1535, 1479; **HRMS** (ESI) for C₉H₁₆N₄NaO₃ (M+Na)⁺: calcd. 251.1115; found, 251.1113.

3.8.6.11 Preparation and Characterization Data of *t*-Butyl (2-Azidoacetyl)-*L*-leucinate (3-26)

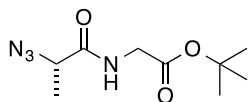


The title compound was prepared using the general procedure for dipeptide synthesis and toluene as a solvent yielded **3-26** (50%).

¹H NMR (CDCl₃, 400 MHz): δ = 6.70 (br. d, J = 8.4 Hz, 1 H), 4.50 (ddd, J = 8.5, 8.5, 5.2 Hz, 1H), 4.00 (s, 2 H), 1.51-1.72 (m, 3 H), 1.46 (s, 9 H), 0.95 (d, J = 6.0 Hz, 3 H), 0.94 (d, J = 6.2 Hz, 3 H); **¹³C NMR** (100.6 MHz, CDCl₃): δ = 171.7, 166.2, 82.2, 52.5, 52.1, 41.7, 27.6 (3 C), 24.9, 22.8, 22.0; **IR**

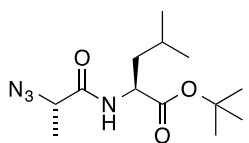
(Microscope, cm^{-1}) 3317, 3070, 2961, 2935, 2107, 1736, 1665, 1537, 1471; **HRMS** (ESI) for $\text{C}_{12}\text{H}_{22}\text{N}_4\text{NaO}_3$ ($\text{M}+\text{Na}$) $^{+}$: calcd. 293.1584; found, 293.1585.

3.8.6.12 Preparation and Characterization Data of *t*-Butyl (*S*)-(2-Azidopropanoyl)glycinate (**3-27**)



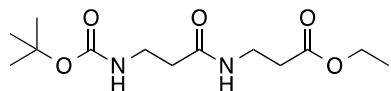
The title compound was prepared using the general procedure for dipeptide synthesis and toluene as a solvent yielded **3-27** (70%). **^1H NMR** (CDCl_3 , 400 MHz): δ = 6.80 (br. s, 1 H), 4.15 (q, J = 7.0 Hz, 1 H), 3.95 (d, J = 5.1 Hz, 1 H), 3.94 (d, J = 5.2 Hz, 1 H), 1.58 (d, J = 7.0 Hz, 3 H), 1.45 (s, 9 H); **^{13}C NMR** (100.6 MHz, CDCl_3): δ = 169.9, 168.5, 82.6, 59.0, 41.9, 28.0 (3 C), 17.0; **IR** (Microscope, cm^{-1}) 3306, 3094, 2981, 2935, 2110, 1743, 1665, 1540, 1478; **HRMS** (ESI) for $\text{C}_9\text{H}_{16}\text{N}_4\text{NaO}_3$ ($\text{M}+\text{Na}$) $^{+}$: calcd. 251.1115; found, 251.1117.

3.8.6.13 Preparation and Characterization Data of *t*-Butyl ((*S*)-2-Azidopropanoyl)-*L*-leucinate (**3-28**)



The title compound was prepared using the general procedure for dipeptide synthesis and toluene as a solvent yielded **3-28** (41%). **^1H NMR** (CDCl_3 , 400 MHz): δ = 6.70 (br. s, 1 H), 4.47 (ddd, J = 8.4, 8.4, 5.3 Hz, 1 H), 4.08 (q, J = 7.0 Hz, 1 H), 1.60-1.70 (m, 3 H), 1.60-1.70 (m, 3 H), 1.54 (d, J = 7.0 Hz, 3 H), 1.46 (s, 9 H), 0.95 (d, J = 6.5 Hz, 3 H), 0.94 (d, J = 6.0 Hz, 3 H); **^{13}C NMR** (100.6 MHz, CDCl_3): δ = 171.7, 169.4, 82.2, 59.2, 51.3, 41.7, 28.0 (3 C), 25.0, 22.7, 22.1, 17.1; **IR** (Microscope, cm^{-1}) 3311, 3082, 2960, 2873, 2115, 1737, 1660, 1536, 1470; **HRMS** (ESI) for $\text{C}_{13}\text{H}_{24}\text{N}_4\text{NaO}_3$ ($\text{M}+\text{Na}$) $^{+}$: calcd. 307.1741; found, 307.1741.

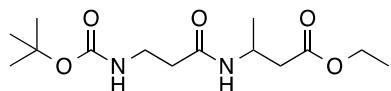
3.8.6.14 Preparation and Characterization Data of Ethyl 3-(3-((*t*-Butoxycarbonyl)amino)propanamido)propanoate (**3-29**)



The title compound was prepared using the general procedure for dipeptide synthesis and toluene as a solvent yielded **3-29** (60%). M.p. 59-61 °C; ¹H NMR

(CDCl₃, 400 MHz): δ = 6.40 (br. s, 1 H), 5.20 (br. s, 1 H), 4.14 (q, *J* = 7.2 Hz, 2 H), 3.50 (td, *J* = 6.2, 6.2 Hz, 2 H), 3.36 (td, *J* = 6.2, 6.2 Hz, 2 H), 2.52 (t, *J* = 6.2 Hz, 2 H), 2.36 (t, *J* = 6.2 Hz, 2 H), 1.42 (s, 9 H), 1.22 (t, 7.2 Hz, 3 H); ¹³C NMR (100.6 MHz, CDCl₃): δ = 172.5, 171.4, 156.1, 79.2, 60.7, 36.7, 36.2, 34.8, 34.0, 28.4 (3 C), 14.1; IR (Microscope, cm⁻¹) 3323, 3082, 2979, 2935, 1735, 1716, 1653, 1527, 1449; HRMS (ESI) for C₁₃H₂₅N₂O₅ (M+H)⁺: calcd. 289.1758; found, 289.1760.

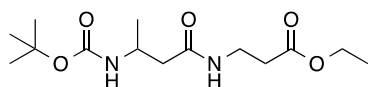
3.8.6.15 Preparation and Characterization Data of Ethyl 3-((*t*-Butoxycarbonyl)amino)propanamido)butanoate (**3-30**)



The title compound was prepared using the general procedure for dipeptide synthesis and toluene as a solvent yielded **3-30** (52%). M.p. 64-66 °C. ¹H NMR

(CDCl₃, 400 MHz): δ = 6.20 (br. s, 1 H), 5.20 (br. s, 1 H), 4.38 (m, 1 H), 4.22 (q, *J* = 6.1 Hz, 2 H), 3.38 (dt, *J* = 6.2, 6.2 Hz 2 H), 2.44 (d, *J* = 5.4 Hz, 2 H), 2.31 (t, *J* = 6.2 Hz, 2 H), 1.40 (s, 9 H), 1.25 (t, *J* = 6.6 Hz, 3 H), 1.20 (d, *J* = 6.7 Hz, 3 H); ¹³C NMR (100.6 MHz, CDCl₃): δ = 171.5, 170.4, 155.6, 78.7, 60.1, 41.5, 40.0, 36.1, 35.8, 27.9 (3 C), 19.5, 13.6; IR (Microscope, cm⁻¹) 3311, 3078, 2935, 1736, 1716, 1648, 1529, 1454; HRMS (ESI) for C₁₄H₂₇N₂O₅ (M+H)⁺: calcd. 303.1914; found, 303.1915.

3.8.6.16 Preparation and Characterization Data of ethyl 3-((*t*-Butoxycarbonyl)amino)butanamido)propanoate (**3-31**)

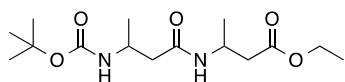


The title compound was prepared using the general procedure for dipeptide synthesis and toluene as a solvent yielded **3-31** (48%). M.p. 65-67 °C; ¹H NMR

(CDCl₃, 400 MHz): δ = 6.40 (br. s, 1 H), 5.30 (br. s, 1 H), 4.25 (q, *J* = 7.3 Hz, 2 H), 3.94 (m, 1 H), 3.50 (td, *J* = 6.2, 6.2 Hz, 2 H), 2.54 (t, *J* = 6.2 Hz, 2 H), 2.38 (d, *J* = 5.7 Hz, 2

H), 1.40 (s, 9 H), 1.25 (t, $J = 7.2$ Hz, 3 H), 1.20 (d, $J = 6.8$ Hz, 3 H); ^{13}C NMR (100.6 MHz, CDCl_3): $\delta = 172.5, 170.9, 155.4, 79.2, 60.7, 44.1, 42.6, 34.8, 34.0, 28.4, (3\text{ C}), 20.5, 14.2$; IR (Microscope, cm^{-1}) 3317, 3084, 2979, 2934, 1737, 1714, 1690, 1649, 1526, 1453; HRMS (ESI) for $\text{C}_{14}\text{H}_{27}\text{N}_2\text{O}_5$ ($\text{M}+\text{H}$) $^+$: calcd. 303.1914; found, 303.1912.

3.8.6.17 Preparation and Characterization Data of Ethyl 3-(3-((*t*-Butoxycarbonyl)amino)butanamido)butanoate (**3-32**)



The title compound was prepared using the general procedure for dipeptide synthesis and toluene as a solvent yielded **3-32** (48%). M.p. 69-71 °C; ^1H NMR (CDCl_3 , 400 MHz): $\delta = 6.40$ (br. s, 1 H), 5.30 (br. s, 1 H), 4.18 (m, 1 H), 4.11 (q, $J = 7.2$ Hz, 2 H), 3.96 (m, 1 H), 2.58 (m, 2 H), 2.38 (m, 2 H), 1.40 (s, 9 H), 1.22 (t, $J = 7.1$ Hz, 3 H), 1.15-1.20 (m, 6 H); ^{13}C NMR (100.6 MHz, CDCl_3): $\delta = 171.6, 169.5, 154.9, 78.7, 60.6, 43.6, 42.3, 41.5, 39.5, 27.9$ (3 C), 20.5, 19.5, 13.7; IR (Microscope, cm^{-1}) 3305, 3071, 2978, 2934, 1737, 1715, 1689, 1649, 1525, 1454; HRMS (ESI) for $\text{C}_{15}\text{H}_{29}\text{N}_2\text{O}_5$ ($\text{M}+\text{H}$) $^+$: calcd. 317.2071; found, 317.2070.

3.8.7 General Procedure for Preparation of epimerization scope study in direct peptide synthesis methodology (Scheme 3-10)

Into a 25 ml round bottom flask equipped with a stir bar was added N-Boc proline or phenylacetic acid (0.55 mmol, 1.1 equiv), 5-methoxy-2-iodophenylboronic acid (**1-31**) (0.10 mmol, 20 mol%), and benzyl amine or phenylalanine methyl ester or Leucine ethyl ester hydrochloride (0.50 mmol, 1.0 equiv) pre-neutralized with *t*-Pr₂Net (0.50 mmol, 1.0 equiv) were stirred at 50 °C for 18 h in dry CH_2Cl_2 containing 1 g of activated 4A molecular sieves. The reaction mixture was filtered through a pad of Celite ® 545 with 15 mL of CH_2Cl_2 , the filtrate was washed with aqueous acidic solution (15 mL, 1 M), aqueous basic solution (15 mL, 1 M) and brine (15 mL). The organic layer was collected, dried over anhydrous Na_2SO_4 , filtered and evaporated to yield the pure amide product **3-**

36, 3-35 and **3-33**. Characterization data of the product matched that found in the literature.¹⁸

3.9 Reference

- (1) a) Mustata, G.; Dinh, S. M.; *Crit. Rev. Ther. Drug Carrier Syst.* **2006**, *23*, 111. b) Thayer, A. M. *Chem. Eng. News* **2011**, *89*, 13. c) Sato, A. K.; Viswanathan, M.; Kent, R. B.; Wood, C. R. *Curr. Opin. Biotechnol.* **2006**, *17*, 638. d) Chow, D.; Nunalee, M. L.; Lim, D. W.; Simnick, A. J.; Chilkoti, A. *Mater Sci Eng R Rep.* **2008**, *62*, 125.
- (2) Bodanszky, M.; Ondetti, A. M. *Peptide Synthesis*. **1965**, New York, Interscience.
- (3) Schwyzler, R.; Sieber, P. *Nature*, **1963**, *199*, 172.
- (4) Wiinsch, E. *Z. Naturforsch.* **1967**, *B 22*, 1269.
- (5) Wiinsch, E.; Wendlberger, G.; Jaeger, E.; Scharf, R. *Proc. 9th Eur. Peptide Symp. Orsay, ed. E. Bricas, Amsterdam*, **1968**, North-Holland, 229.
- (6) Merrifield, R. B. *J. Am. Chem. Soc.* **1963**, *85*, 2149.
- (7) Fridkin, M.; Patchornik, A.; Katchalski, E. *J. Am. Chem. Soc.* **1966**, *88*, 3164.
- (8) Wieland, T.; Birr, C. *Angew. Chem. Int. Ed.* **1966**, *5*, 310.
- (9) Bodanszky, M.; du Vigneaud, V. *Nature*, **1954**, *183*, 1324.
- (10) Bodanszky, M.; du Vigneaud, V. *J. Am. Chem. Soc.* **1959**, *81*, 5688.
- (11) Bodanszky, M.; Williams, N. J. *J. Am. Chem. Soc.* **1967**, *89*, 685.

- (12) Bodanszky, M.; Ondetti, M. A.; Levine, S. D.; Williams, N. J. *J. Am. Chem. Soc.* **1967**, 89, 6753.
- (13) Weygand, F.; Huber, P.; Weiss, K. *Z. Naturforsch.* **1967**, B 22, 1084.
- (14) Weygand, F.; DiBello, C. *Z. Naturforsch.* **1969**, B 24, 314.
- (15) Lande, S., Ed. *Peptides*, **1972**, Chemistry and Biochemistry. Proceedings of the 2nd American Peptide Symposium, Cleveland, **1970**, London: Gordon & Breach.
- (16) Tilak, M. A. *Tetrahedron Lett.* **1970**, 849.
- (17) a) Griehl, C.; Kolbe, A.; Merkel, S. *J. Chem. Soc. Perkin Trans. 2* **1996**, 2525; b) Han, S.-Y.; Kim, Y.-A. *Tetrahedron* **2004**, 60, 2447; c) El-Faham, A.; Albericio, F. *Chem. Rev.* **2011**, 111, 6557.
- (18) Liu, S.; Yang, Y.; Liu, X.; Ferdousi, F. K.; Batsanov, A. S.; Whiting, A. *Eur. J. Org. Chem.* **2013**, 5692.
- (19) a) Arnold, K.; Davies, B.; Giles, R. L.; Grosjean, C.; Smith, G. E.; Whiting, A. *Adv. Synth. Catal.* **2006**, 348, 813. b) Arnold, K.; Batsanov, A. S.; Davies, B.; Whiting, A. *Green Chem.* **2008**, 10, 124.
- (20) Arnold, K.; Davies, B.; Héroult, D.; Whiting, A. *Angew. Chem.* **2008**, 47, 2673.
- (21) Al-Zoubi, R. M.; Marion, O.; Hall, D. G. *Angew. Chem. Int. Ed.* **2008**, 47, 2876.
- (22) Gernigon, N.; Al-Zoubi, R. M.; Hall, D. G. *J. Org. Chem.* **2012**, 77, 8386.
- (23) Knochel, P.; Dohle, W.; Gommermann, N.; Kneisel, F. F.; Kopp, F.; Korn, T.; Sapountzis, I.; Vu, V. A. *Angew. Chem. Int. Ed.* **2003**, 42, 4302.

- (24) Wegner, H. A.; Reisch, H.; Rauch, K.; Demeter, A.; Zachariasse, K. A.; de Meijere, A.; Scott, L. T. *J. Org. Chem.* **2006**, *71*, 9080.
- (24) Al-Zoubi, R. M.; Hall, D. G. *Org. Lett.* **2010**, *12*, 2480.
- (25) Orska, A. G'; Hajmowicz, H.; Kli's, T.; Serwatowski, J.; Synoradzki, L. *Appl. Organometal. Chem.* **2011**, *25*, 294.
- (26) Al-Zoubi, R. M. PhD thesis **2011**, *Section 3.2.4*, p. 133.
- (27) Pande, S. V.; Utale, P. S.; Gholse, S. B.; Tekade, P. V.; Patil, S. G. *Pharm. Chem. J.* **2014**, *48*, 29.
- (28) Kim, H.; Cho, J. K.; Aimoto, S.; Lee, Y.S. *Org. Lett.* **2006**, *8*, 1149.
- (29) a) Brase, S.; Gil, C.; Knepper, K.; Zimmerman, V. *Angew. Chem. Int. Ed.* **2005**, *44*, 5188-5240. And all references therein. b) Borger, E. D. G.; Stick, R. V. *Org. Lett.* **2007**, *9*, 3797.

Conclusions and Future Directions

The formation of amide bonds plays an important role in organic chemistry and biochemistry. A plethora of peptides and proteins contain this bond and the synthesis of these products is increasingly important. These reactions often require the use of stoichiometric excesses of expensive and often toxic coupling reagents. These reagents generate large amounts of wasteful by-products that complicate the isolation of the desired amide product. Therefore, future studies in this field are necessary in order to expand the efficiency and the scope of these reactions.

To overcome the drawbacks of our current methodology in catalytic direct amide syntheses using the MIBA catalyst (**1-31**), improved conditions for large-scale industrial applications needed to be achieved. Therefore, the reactant concentrations and amount of molecular sieves were optimized to obtain amide products in large-scale and greener conditions. After systematic optimization of the solvent, temperature, reactant concentration and molecular sieves amount, toluene was chosen as the best solvent (depending on the substrate, solvent may vary), the temperature was raised up to 50 °C to further enhance the reaction yield at higher concentration (0.5-1.0 M) and lesser amount of 4A molecular sieves (0.5 g per mmol reactants, half of the quantity of molecular sieves prescribed in the original procedure). The synthetic usefulness of the reaction was demonstrated in a large-scale reaction (up to 5 g), for the two model amidation reactions between phenylacetic acid and benzylamine, pyrrolidine in 89% and 46% product yields respectively (Chapter Two, **Table 2-6**). These conditions allowed access to β -peptide products **3-30** using β -amino acids (5 g) and acquiring 58% yield at 55 °C after 72h. Subsequently, the catalyst loading was increased to 25 mol% (instead of 10 mol% used for more reactive amine partners) in the case of β -peptide syntheses.

Aiming to replace molecular sieves with a Staudinger reaction process to eliminate water, amide product yield improved only by 11% for the catalyzed reaction with MIBA catalyst (**1-31**), a difference that is probably not significant. Further improvements may

be achieved by designing intramolecular azide and phosphine partners to overcome the entropy energy barrier or to observe the precise assessment of catalyzed and uncatalyzed (control) reactions, the electronic factors of phosphine partners can be manipulated and less reactive substrates than phenylacetic acid and benzyl azide may be employed.

The effect of three classes of additives was investigated (Lewis acids, protic acids and nucleophilic additive) to further enhance the catalytic efficiency in direct amidation methodology. Weaker protic acids (higher pK_a) such as *p*TsOH and MsOH provided better results. On the other hand, Whiting and co-workers found that a cooperative boronic acid catalyst systems (binary arylboronic acid of both *o*-tolyl- and *o*-nitrophenyl-boronic acids) was beneficial in direct dipeptide synthesis especially with the least reactive amino acid combinations. Therefore, if a proton transfer plays a key role in the reaction mechanism of amide bond formation according to Marcelli's DFT studies, the use of more neutral protic acids such as cooperative boronic acids, in which do not deactivate the amine partner by protonation but activate carboxyl moiety, may enhance the reaction efficiency and acted as the dual activation of carboxylic acid moiety. In other words, a proper combination of binary arylboronic acid with the optimal MIBA catalyst (**1-31**), could be considered as a dual catalytic system approach for future studies.

One other direction associated with this project involved the development of a novel catalyst for direct amidation reactions which promotes direct amidation reaction with a wider range of substrates (such as less reactive amino acids) under mild conditions. For this purpose, different heterocyclic boronic acids such as FIBA (**2-3**) and 3-bromo-2-thienylboronic acid (**2-5**) were synthesized and evaluated towards amidation reaction but did not show any significant superior activity when compared to MIBA (**1-31**). The rationale of designing this class of catalyst was based on increasing the nucleophilicity of the iodo substituent without adversely affecting boron's Lewis acidity by changing the aromatic backbone of MIBA (**1-31**) that a stronger X-H bond might form in transition state. Consequently, obtaining a better understanding of the reaction mechanism is an urgent need in order to develop new boron-based catalysts. It is noteworthy that two catalysts developed by our group, IBA (**1-30**) and MIBA (**1-31**), operate through a different mechanism than other electron deficient boronic acids, for instance, they are not

efficient with aromatic carboxylic acid and amine combinations. Two factors may play a role: 1) The pK_a of these substrates is more favored to form a thermodynamically stable carboxylate-ammonium salt rather than reactive monoacyloxyboronate intermediate, 2) HSAB Theory, hard and soft (Lewis) acids, may determine the type of substrates bonded to boron Lewis acid center. For example, boric acid was more effective towards aromatic carboxylic acid and amine than aliphatic at high temperature. Electron deficient boronic acids catalysts [harder boron core than IBA (**1-30**) and MIBA (**1-31**)] are also effective for amidation of aromatic carboxylic acid and amine. Therefore, a careful analysis of the mechanism involved in each method is essential for the further catalyst development.

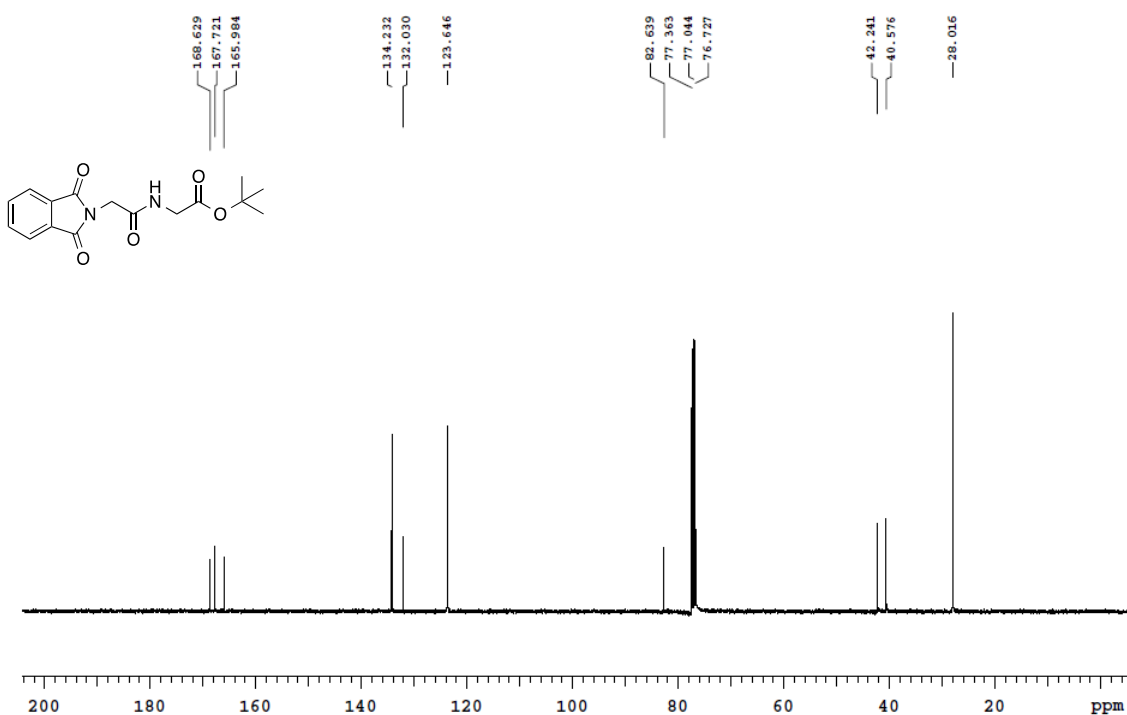
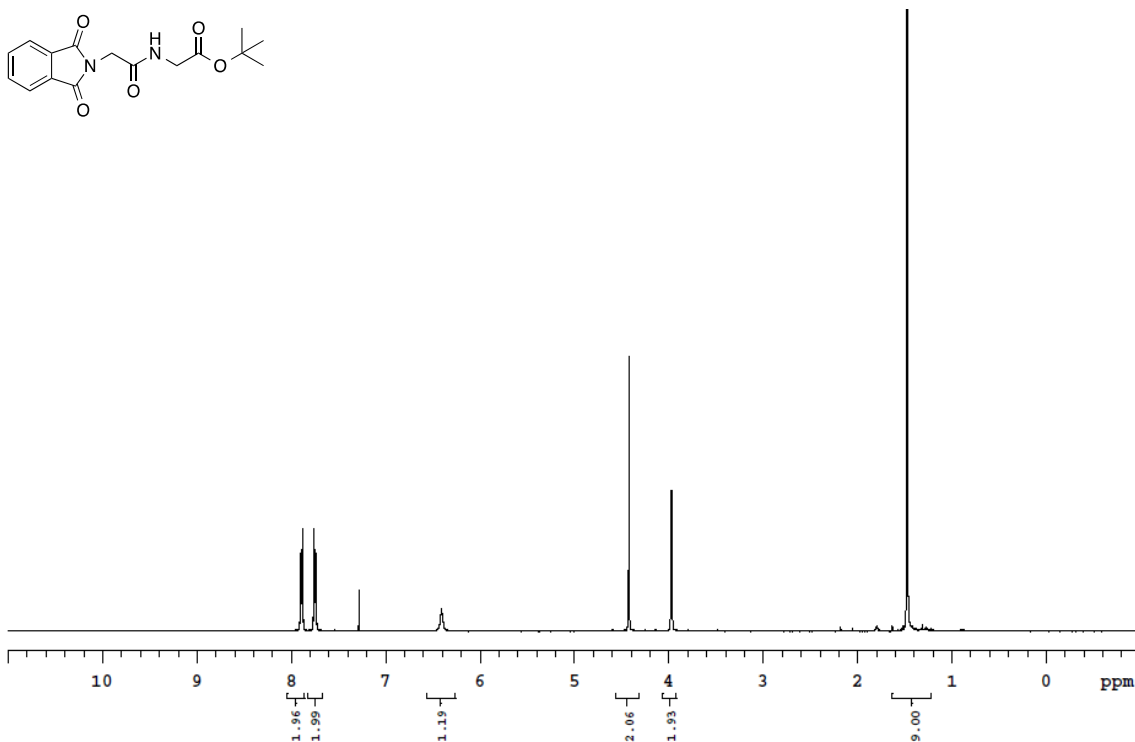
In order to develop a novel catalytic dipeptide synthesis methodology, systematic screening of potential catalysts and substrate modifications were examined. The research presented in this thesis addresses the development of a boron catalyst for an environmentally benign direct dipeptide synthesis at low temperature with high atom economy without any detected racemization. This novel catalytic approach represents a significant advance over the previous stoichiometric method reported by Whiting. The reaction procedure is operationally very simple. It employs equimolar amounts of acid and amine substrates, requires a little heating up to (50 °C), generates only water as a by-product, and affords pure dipeptide products after a simple filtration and acid–base extractions to remove any unreacted substrates and the catalyst without the need for chromatography. The examples compiled in **Figure 3-4, 3-5, 3-6** demonstrate the versatility and scope of our catalyst in promoting direct dipeptide synthesis using protected amino acids at low temperature, which avoid racemization under optimal reaction conditions. For more demanding substrates, more forcing conditions (higher catalyst loading up to 25 mol%, higher temperature up to 55 °C and longer time) were employed.

Bibliography of All Sources

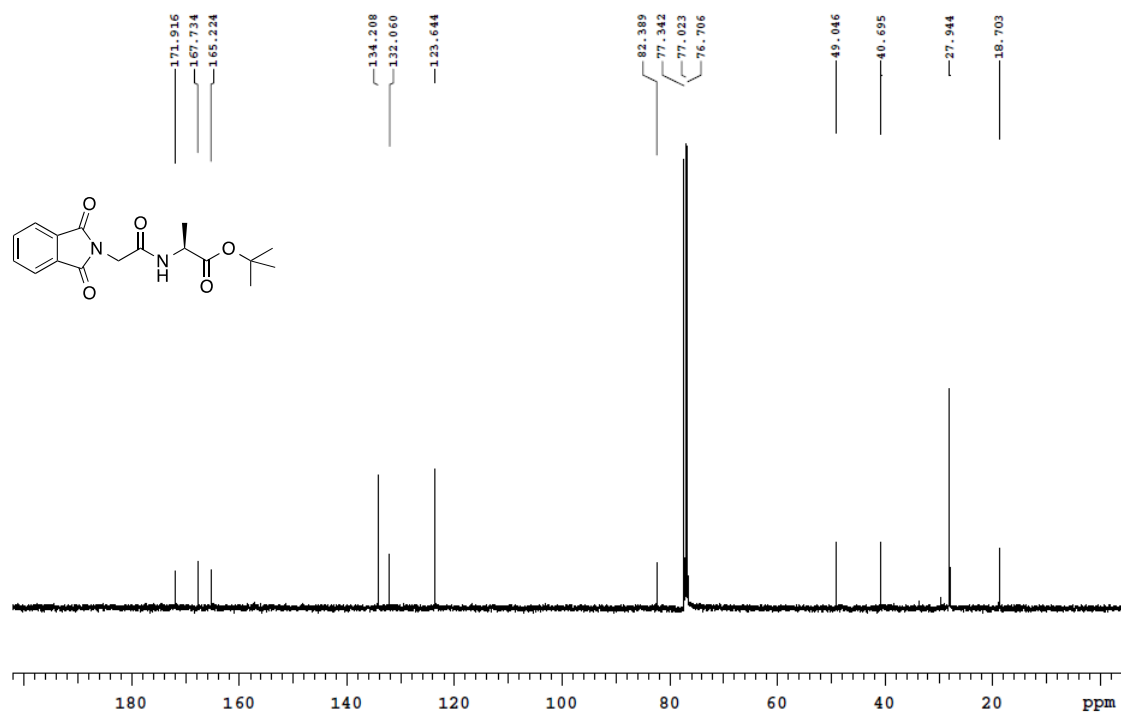
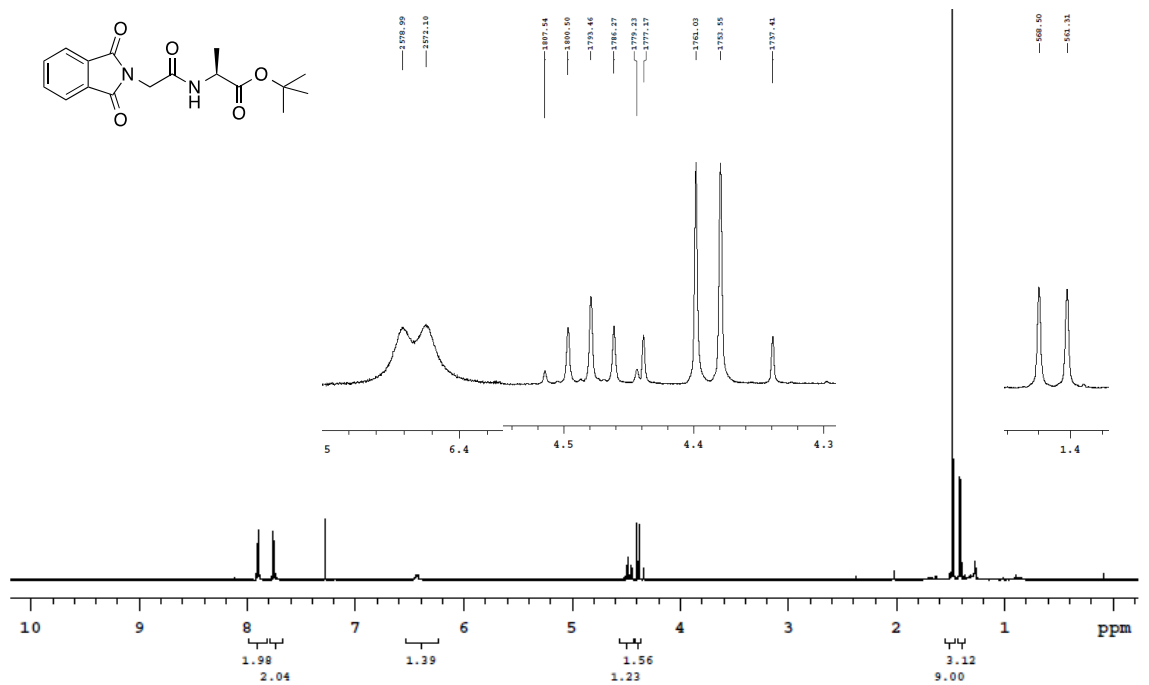
- (1) Al-Zoubi, R. M.; Marion, O.; Hall, D. G. *Angew. Chem. Int. Ed.* **2008**, *47*, 2876.
- (2) Al-Zoubi, R. M.; Hall, D. G. *Org. Lett.* **2010**, *12*, 2480
- (3) Al-Zoubi, R. M. PhD thesis **2011**.
- (4) Marcelli, T. *Angew. Chem. Int. Ed.* **2010**, *49*, 6840.
- (5) Gernigon, N.; Al-Zoubi, R. M.; Hall, D. G. *J. Org. Chem.* **2012**, *77*, 8386.
- (6) Gernigon, N.; Zheng, H.; Hall, D. G. *Tetrahedron Lett.* **2013**, *54*, 4475.

Appendix 1: Selected copies of NMR spectra

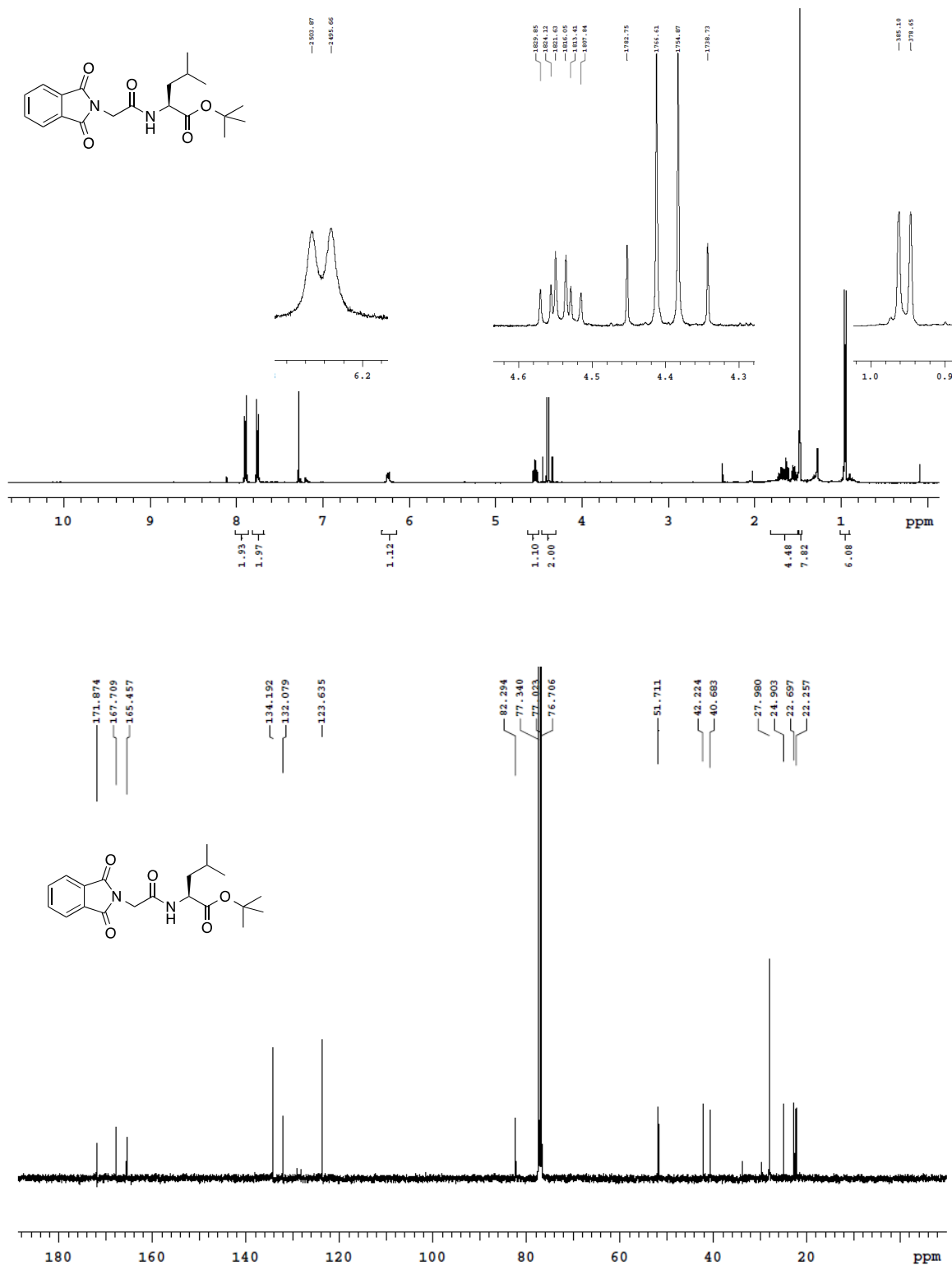
^1H -NMR (400 MHz), ^{13}C -NMR (100.6 MHz) of **3-14** in CDCl_3 at 27 °C



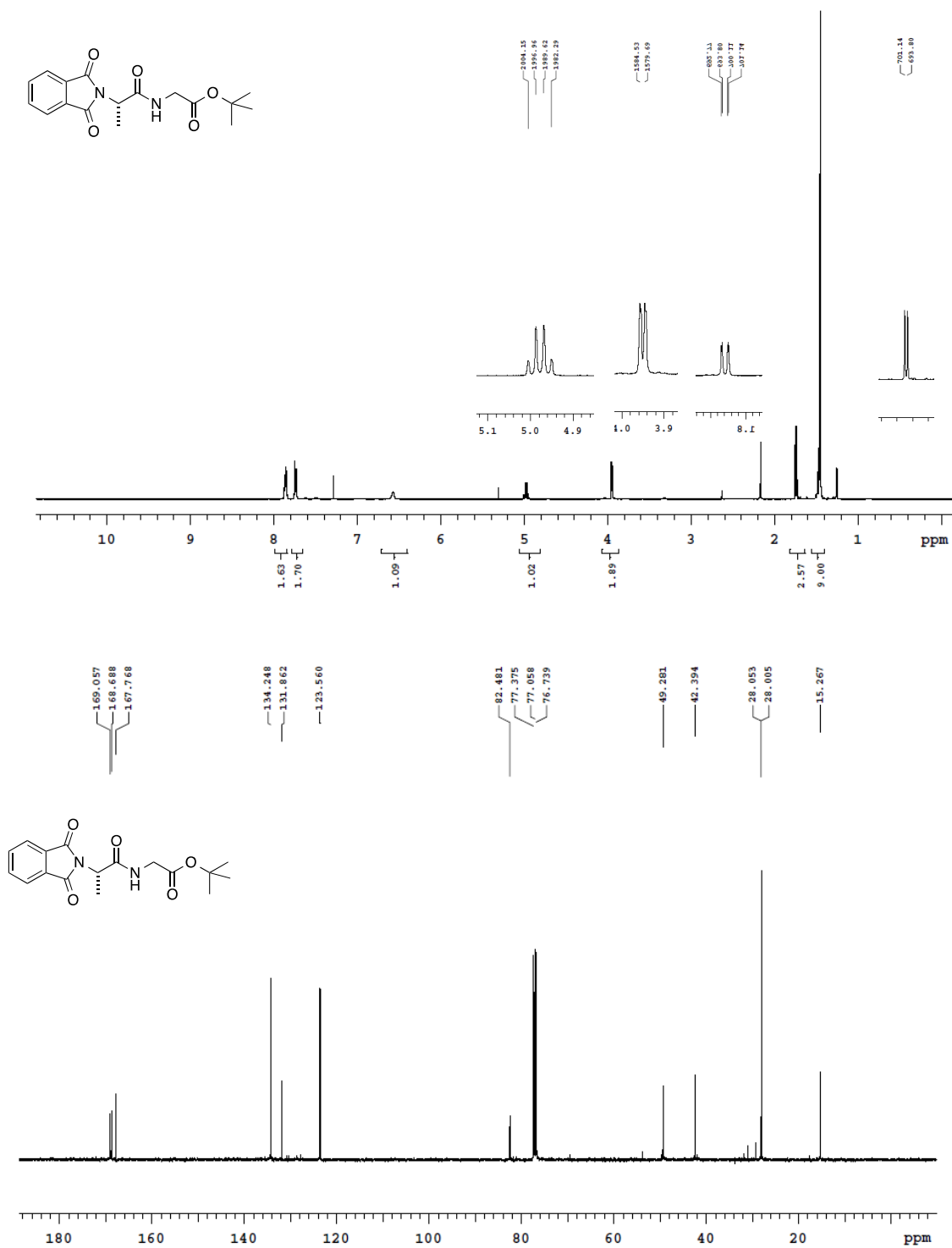
^1H -NMR (400 MHz), ^{13}C -NMR (100.6 MHz) of **3-15** in CDCl_3 at 27 °C



^1H -NMR (400 MHz), ^{13}C -NMR (100.6 MHz) of **3-16** in CDCl_3 at 27 °C

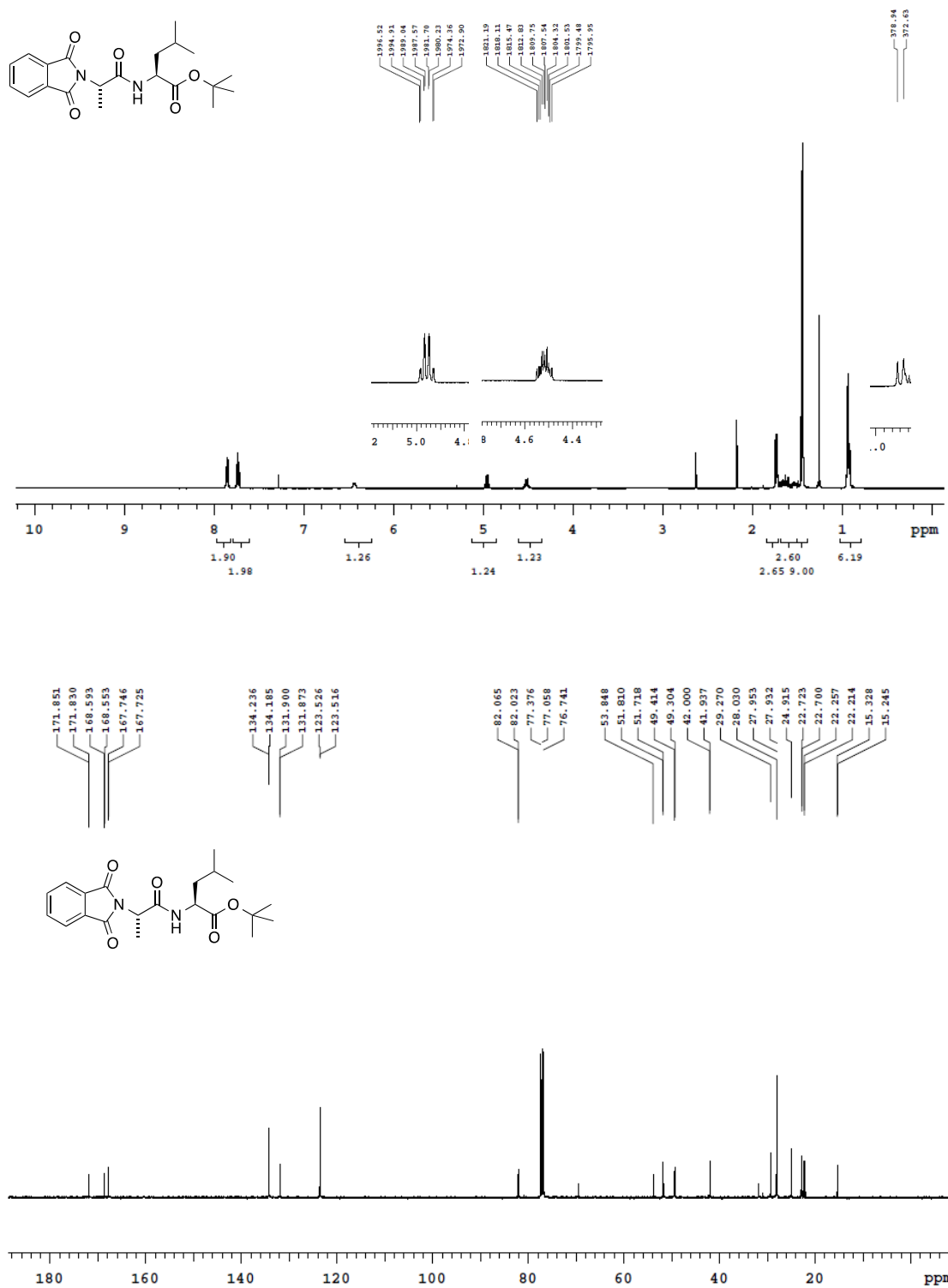


^1H -NMR (400 MHz), ^{13}C -NMR (100.6 MHz) of **3-17** in CDCl_3 at 27 °C

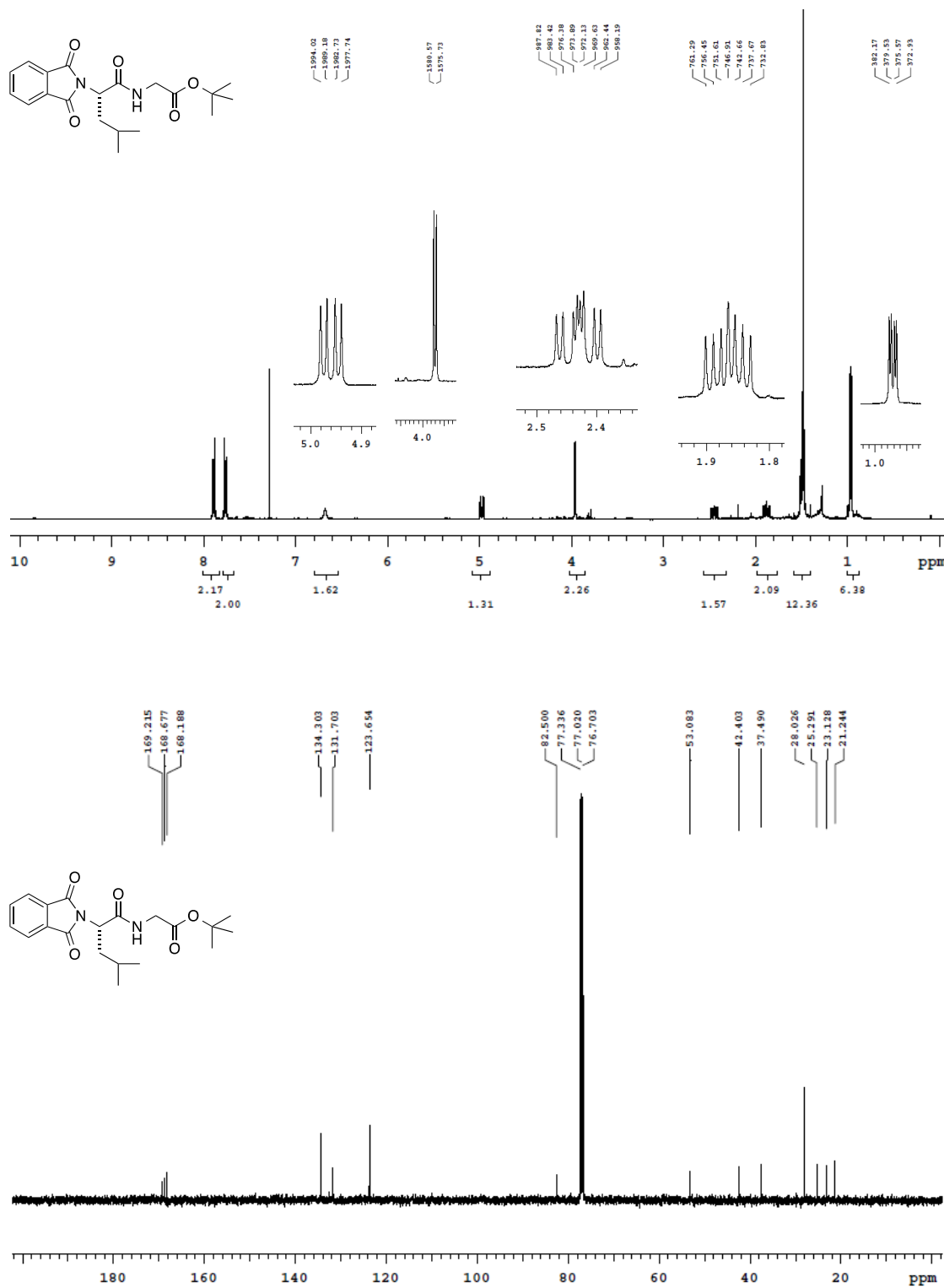


[illegible]

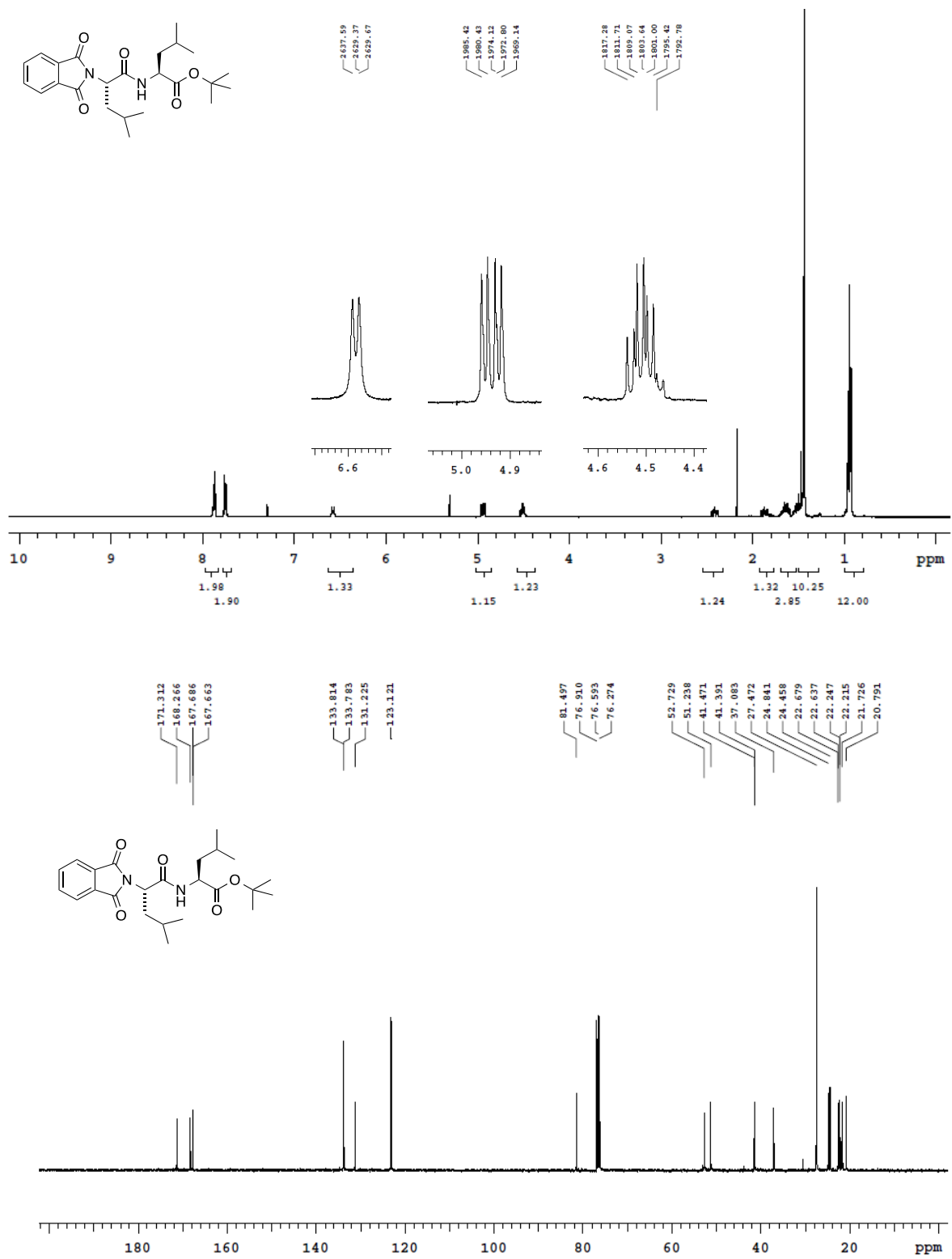
^1H -NMR (400 MHz), ^{13}C -NMR (100.6 MHz) of **3-19** in CDCl_3 at 27 °C



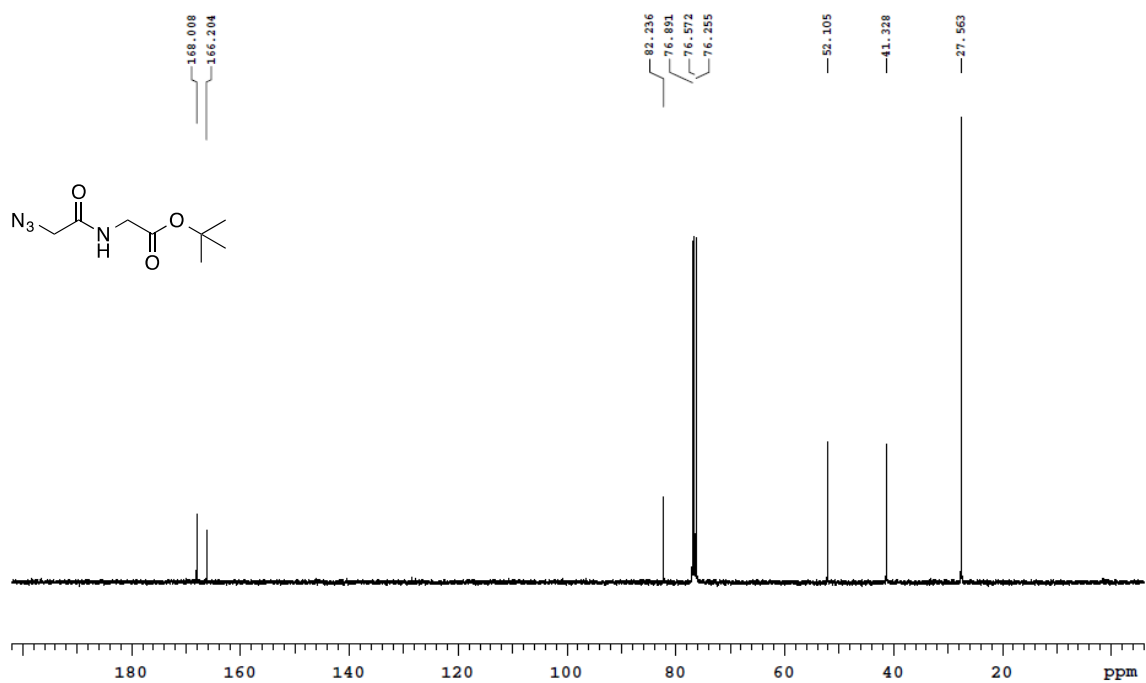
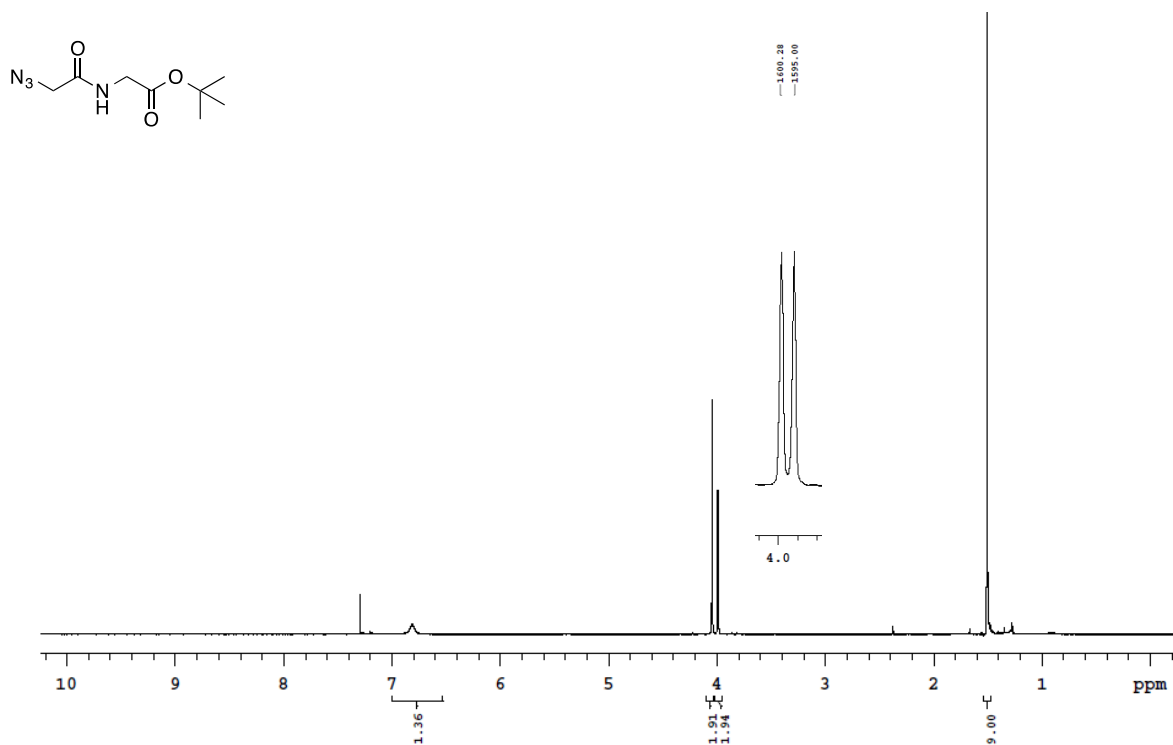
^1H -NMR (400 MHz), ^{13}C -NMR (100.6 MHz) of **3-20** in CDCl_3 at 27 °C



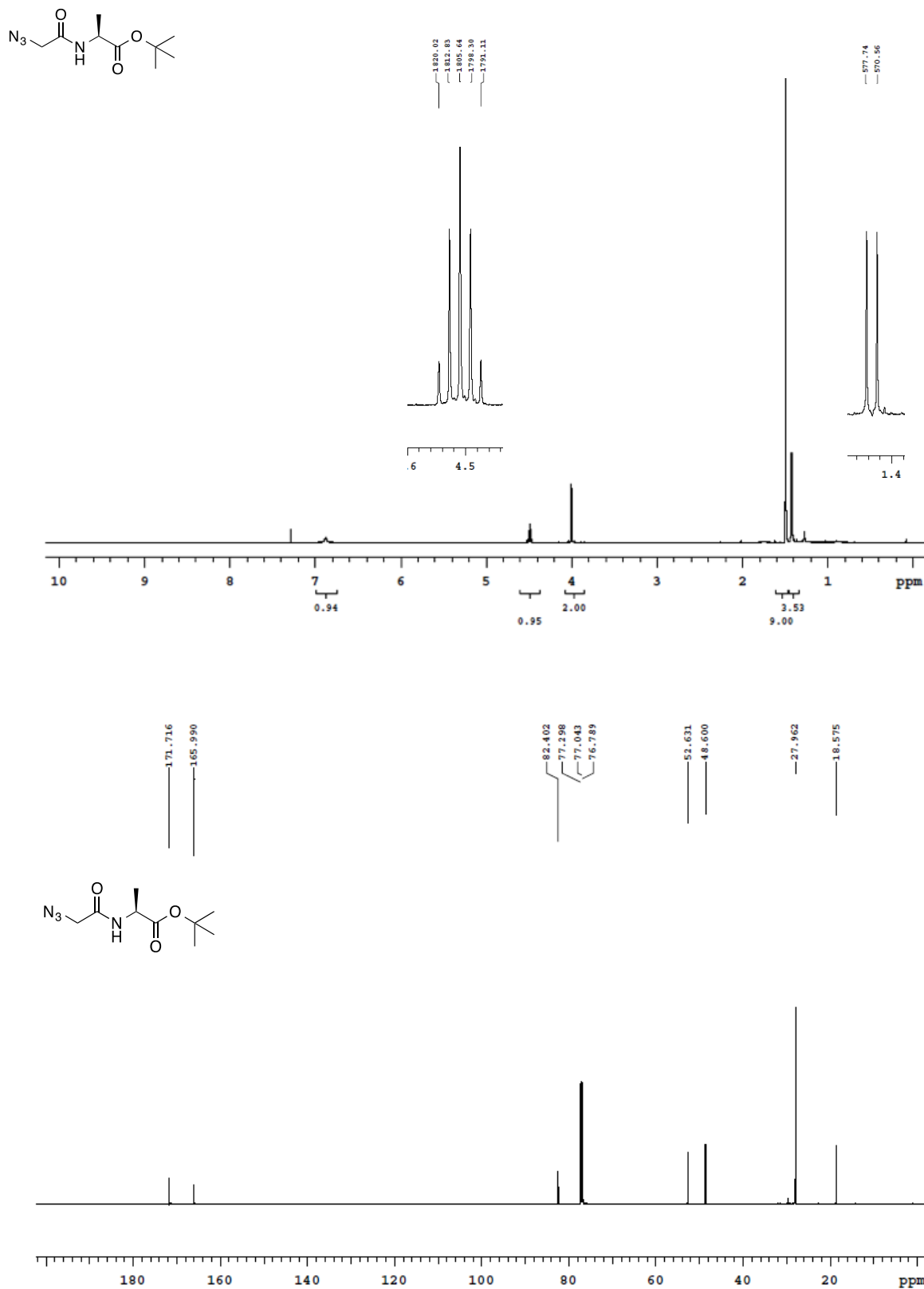
^1H -NMR (400 MHz), ^{13}C -NMR (100.6 MHz) of **3-21** in CDCl_3 at 27 °C



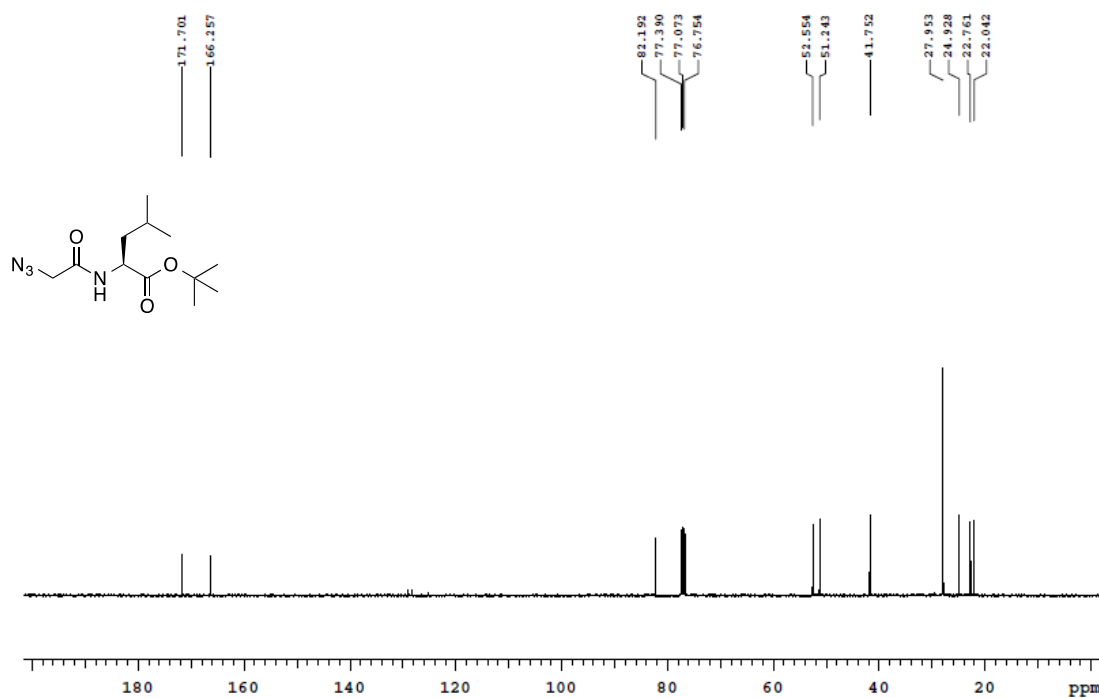
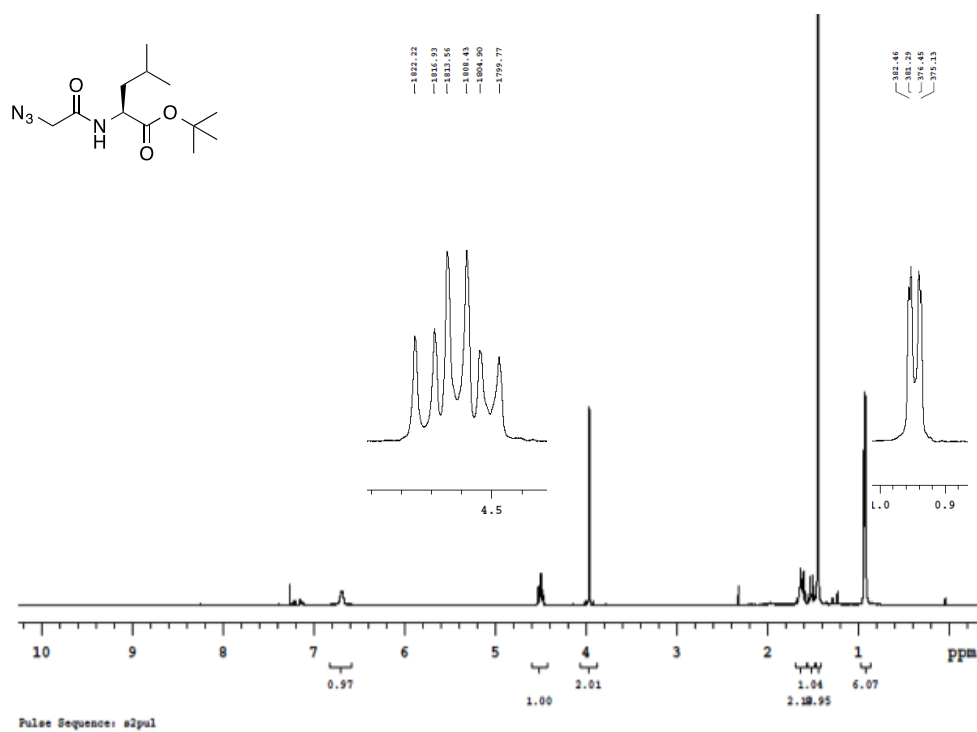
^1H -NMR (400 MHz), ^{13}C -NMR (100.6 MHz) of **3-24** in CDCl_3 at 27 °C



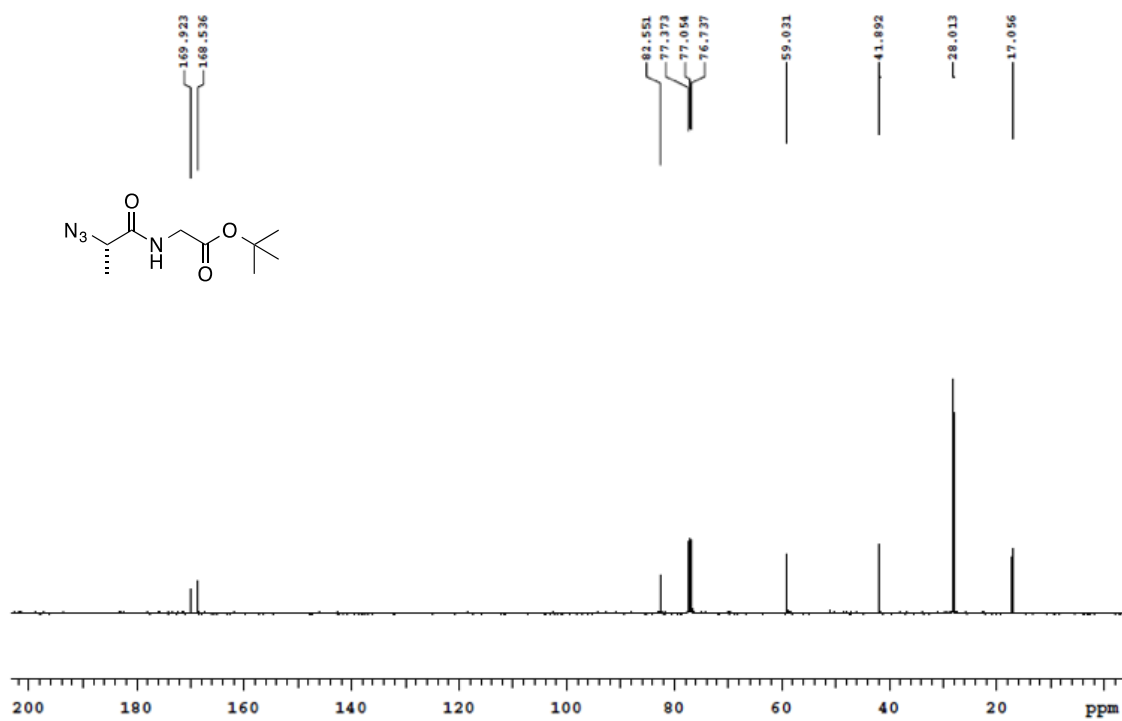
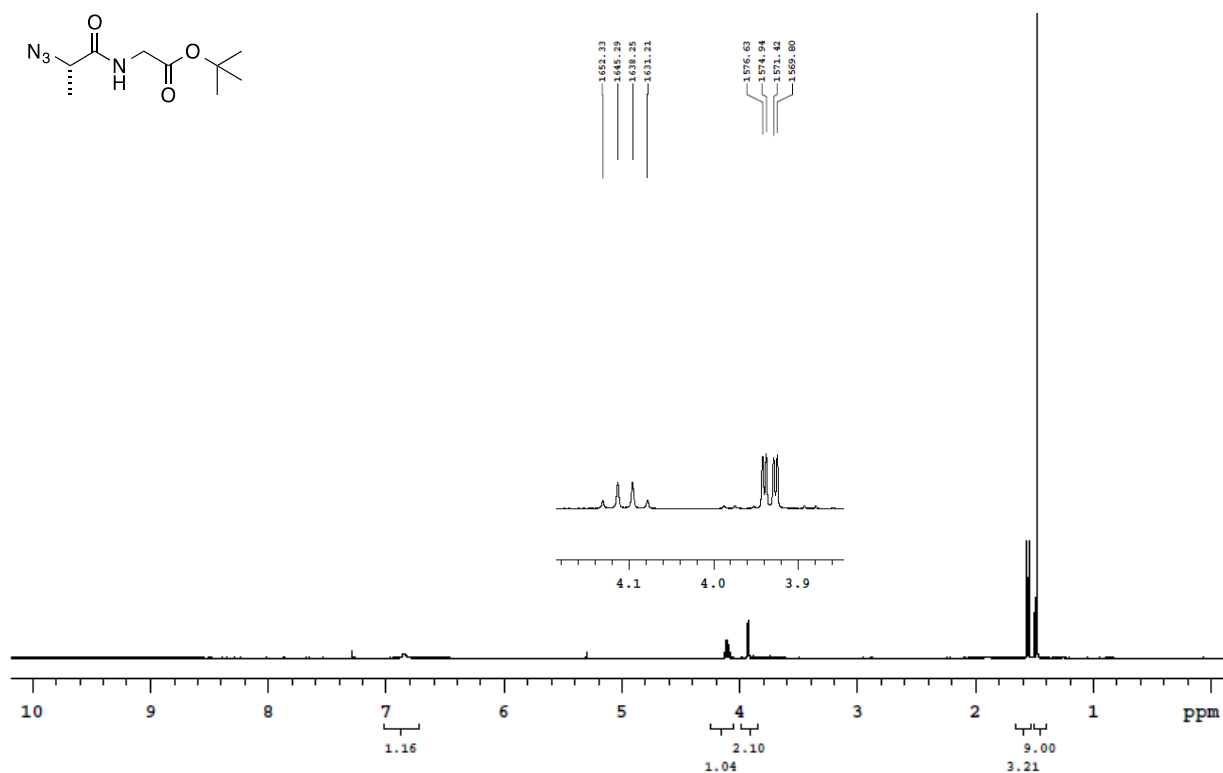
^1H -NMR (400 MHz), ^{13}C -NMR (100.6 MHz) of **3-25** in CDCl_3 at 27 °C



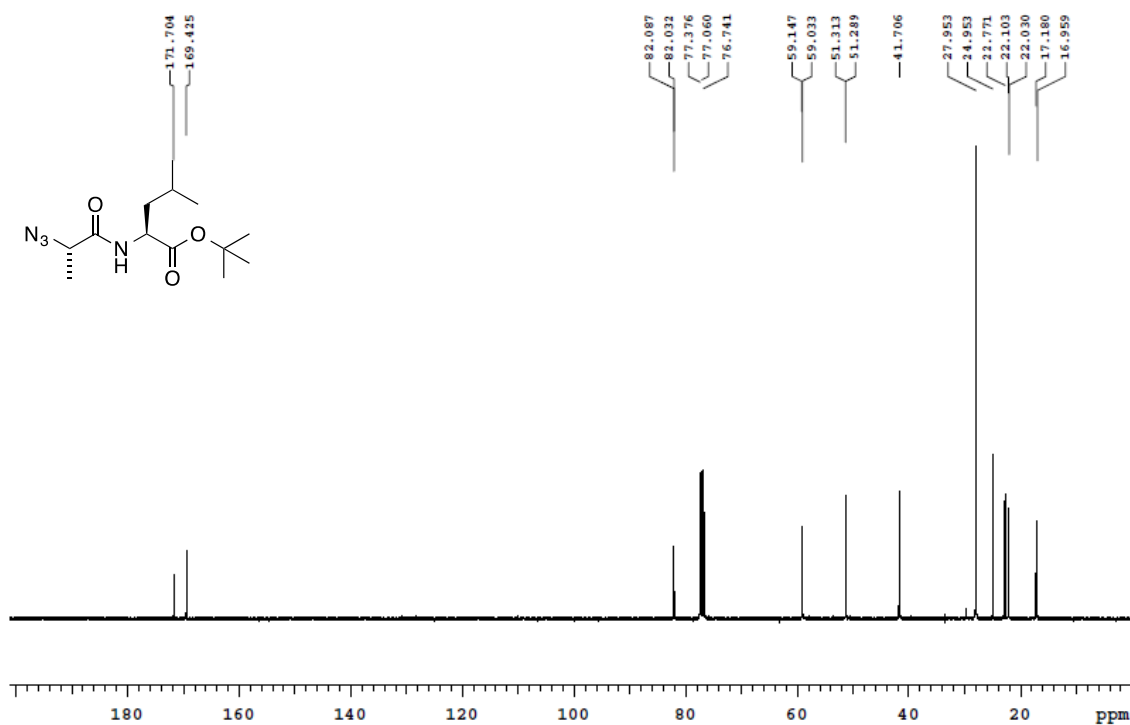
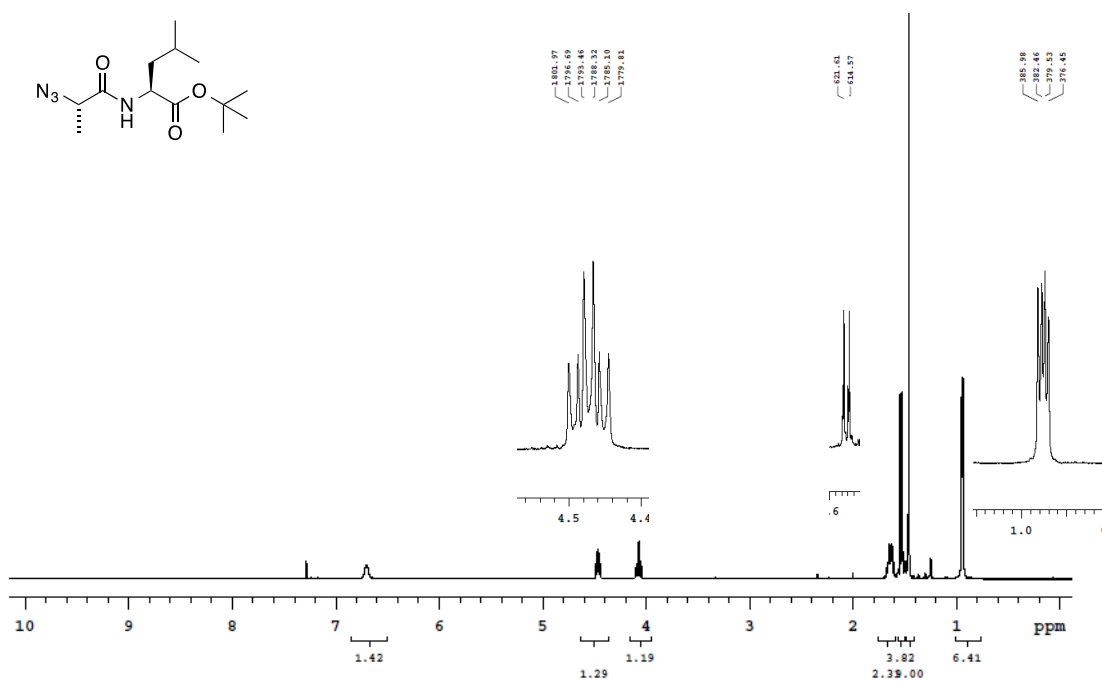
^1H -NMR (400 MHz), ^{13}C -NMR (100.6 MHz) of **3-26** in CDCl_3 at 27 °C



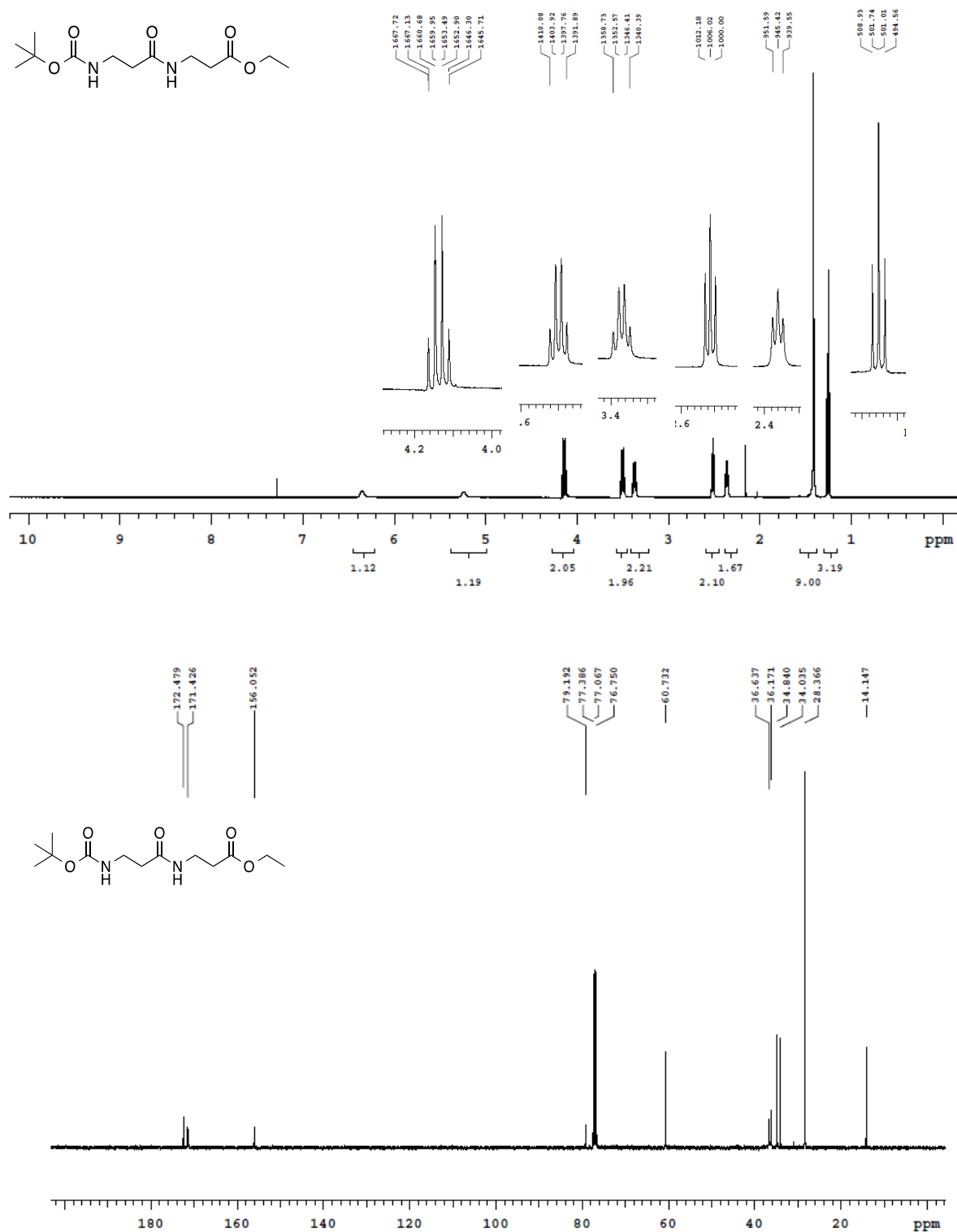
^1H -NMR (400 MHz), ^{13}C -NMR (100.6 MHz) of **3-27** in CDCl_3 at 27 °C



^1H -NMR (400 MHz), ^{13}C -NMR (100.6 MHz) of **3-28** in CDCl_3 at 27 °C



^1H -NMR (400 MHz), ^{13}C -NMR (100.6 MHz) of **3-29** in CDCl_3 at 27 °C



CCOC(=O)C[C@H](C)NC(=O)CCNC(=O)OC(C)(C)C

¹H NMR (400 MHz, CDCl₃)

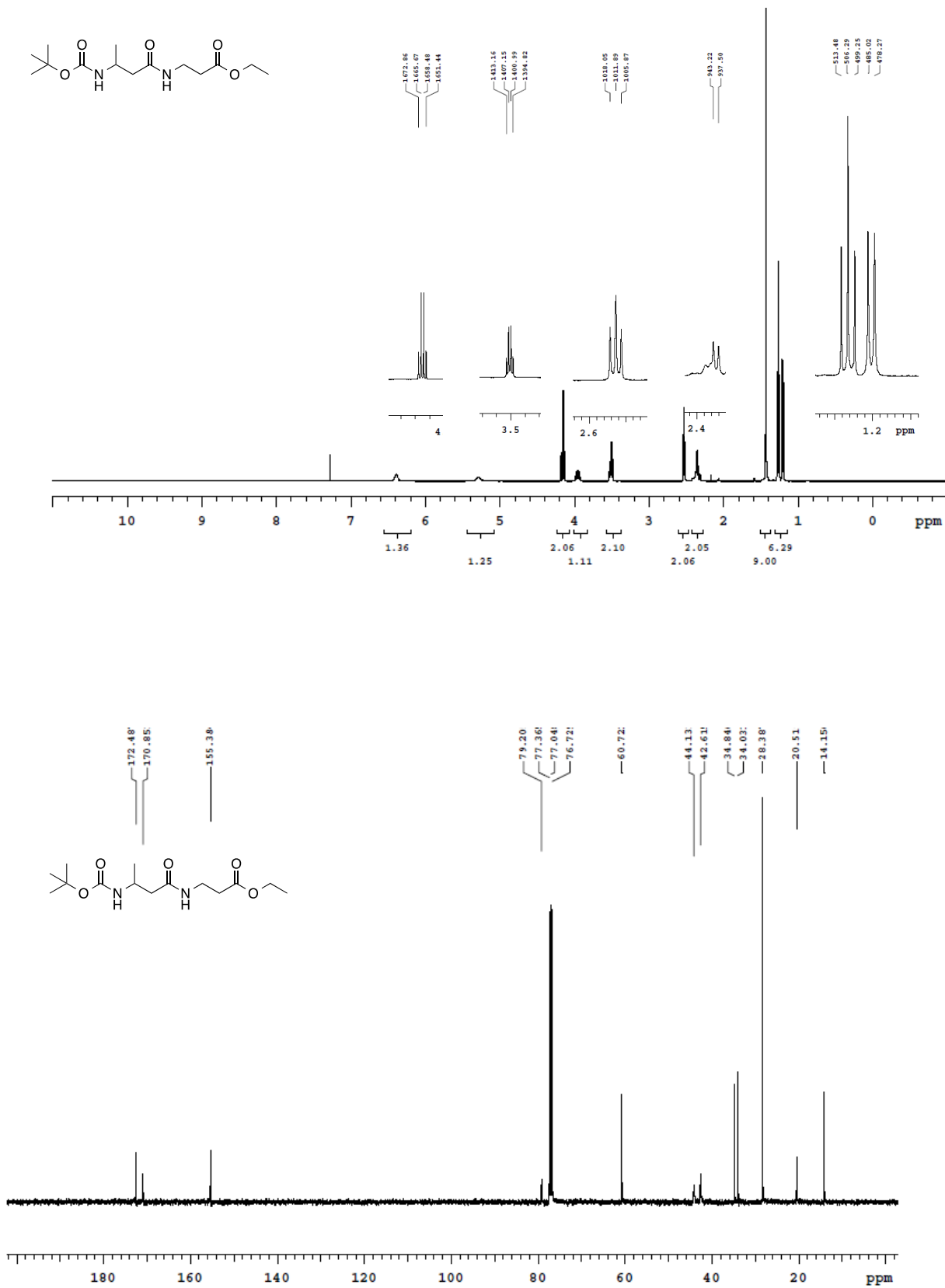
Chemical structure: CCOC(=O)C[C@H](C)NC(=O)CCNC(=O)OC(C)(C)C

Peak list (ppm): 7.26, 7.24, 7.22, 7.20, 7.18, 7.16, 7.14, 7.12, 7.10, 7.08, 7.06, 7.04, 7.02, 7.00, 6.98, 6.96, 6.94, 6.92, 6.90, 6.88, 6.86, 6.84, 6.82, 6.80, 6.78, 6.76, 6.74, 6.72, 6.70, 6.68, 6.66, 6.64, 6.62, 6.60, 6.58, 6.56, 6.54, 6.52, 6.50, 6.48, 6.46, 6.44, 6.42, 6.40, 6.38, 6.36, 6.34, 6.32, 6.30, 6.28, 6.26, 6.24, 6.22, 6.20, 6.18, 6.16, 6.14, 6.12, 6.10, 6.08, 6.06, 6.04, 6.02, 6.00, 5.98, 5.96, 5.94, 5.92, 5.90, 5.88, 5.86, 5.84, 5.82, 5.80, 5.78, 5.76, 5.74, 5.72, 5.70, 5.68, 5.66, 5.64, 5.62, 5.60, 5.58, 5.56, 5.54, 5.52, 5.50, 5.48, 5.46, 5.44, 5.42, 5.40, 5.38, 5.36, 5.34, 5.32, 5.30, 5.28, 5.26, 5.24, 5.22, 5.20, 5.18, 5.16, 5.14, 5.12, 5.10, 5.08, 5.06, 5.04, 5.02, 5.00, 4.98, 4.96, 4.94, 4.92, 4.90, 4.88, 4.86, 4.84, 4.82, 4.80, 4.78, 4.76, 4.74, 4.72, 4.70, 4.68, 4.66, 4.64, 4.62, 4.60, 4.58, 4.56, 4.54, 4.52, 4.50, 4.48, 4.46, 4.44, 4.42, 4.40, 4.38, 4.36, 4.34, 4.32, 4.30, 4.28, 4.26, 4.24, 4.22, 4.20, 4.18, 4.16, 4.14, 4.12, 4.10, 4.08, 4.06, 4.04, 4.02, 4.00, 3.98, 3.96, 3.94, 3.92, 3.90, 3.88, 3.86, 3.84, 3.82, 3.80, 3.78, 3.76, 3.74, 3.72, 3.70, 3.68, 3.66, 3.64, 3.62, 3.60, 3.58, 3.56, 3.54, 3.52, 3.50, 3.48, 3.46, 3.44, 3.42, 3.40, 3.38, 3.36, 3.34, 3.32, 3.30, 3.28, 3.26, 3.24, 3.22, 3.20, 3.18, 3.16, 3.14, 3.12, 3.10, 3.08, 3.06, 3.04, 3.02, 3.00, 2.98, 2.96, 2.94, 2.92, 2.90, 2.88, 2.86, 2.84, 2.82, 2.80, 2.78, 2.76, 2.74, 2.72, 2.70, 2.68, 2.66, 2.64, 2.62, 2.60, 2.58, 2.56, 2.54, 2.52, 2.50, 2.48, 2.46, 2.44, 2.42, 2.40, 2.38, 2.36, 2.34, 2.32, 2.30, 2.28, 2.26, 2.24, 2.22, 2.20, 2.18, 2.16, 2.14, 2.12, 2.10, 2.08, 2.06, 2.04, 2.02, 2.00, 1.98, 1.96, 1.94, 1.92, 1.90, 1.88, 1.86, 1.84, 1.82, 1.80, 1.78, 1.76, 1.74, 1.72, 1.70, 1.68, 1.66, 1.64, 1.62, 1.60, 1.58, 1.56, 1.54, 1.52, 1.50, 1.48, 1.46, 1.44, 1.42, 1.40, 1.38, 1.36, 1.34, 1.32, 1.30, 1.28, 1.26, 1.24, 1.22, 1.20, 1.18, 1.16, 1.14, 1.12, 1.10, 1.08, 1.06, 1.04, 1.02, 1.00, 0.98, 0.96, 0.94, 0.92, 0.90, 0.88, 0.86, 0.84, 0.82, 0.80, 0.78, 0.76, 0.74, 0.72, 0.70, 0.68, 0.66, 0.64, 0.62, 0.60, 0.58, 0.56, 0.54, 0.52, 0.50, 0.48, 0.46, 0.44, 0.42, 0.40, 0.38, 0.36, 0.34, 0.32, 0.30, 0.28, 0.26, 0.24, 0.22, 0.20, 0.18, 0.16, 0.14, 0.12, 0.10, 0.08, 0.06, 0.04, 0.02, 0.00.

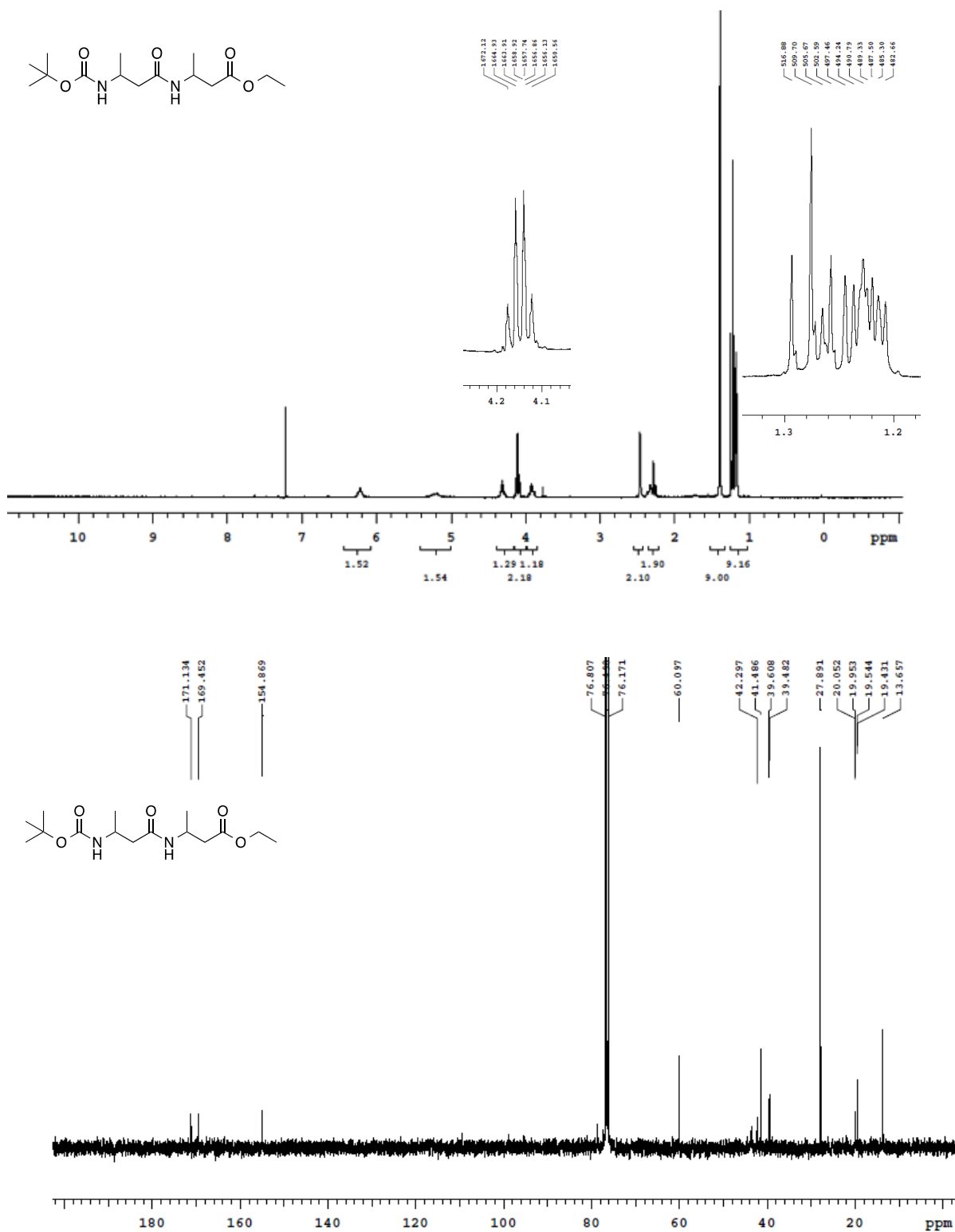
¹³C NMR (100 MHz, CDCl₃)

Chemical structure: CCOC(=O)C[C@H](C)NC(=O)CCNC(=O)OC(C)(C)C

Peak list (ppm): 171.080, 170.052, 155.556, 78.689, 76.826, 76.509, 76.190, 60.099, 41.505, 39.583, 36.149, 35.842, 27.865, 19.531, 13.650.

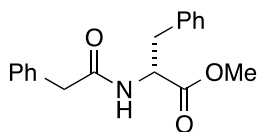
¹H-NMR (400 MHz), ¹³C-NMR (100.6 MHz) of **3-31** in CDCl₃ at 27 °C

^1H -NMR (400 MHz), ^{13}C -NMR (100.6 MHz) of **3-32** in CDCl_3 at 27 °C

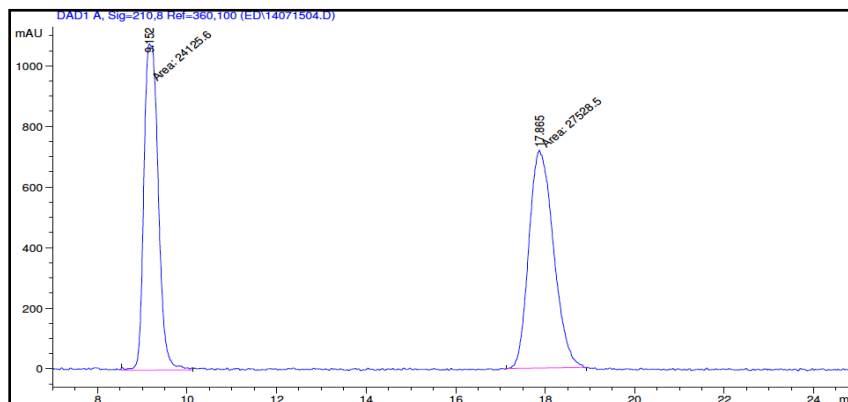


Appendix 2: Chromatograms for enantiomeric excess measurement

Racemic (top) and optically enriched (bottom) **3-35**

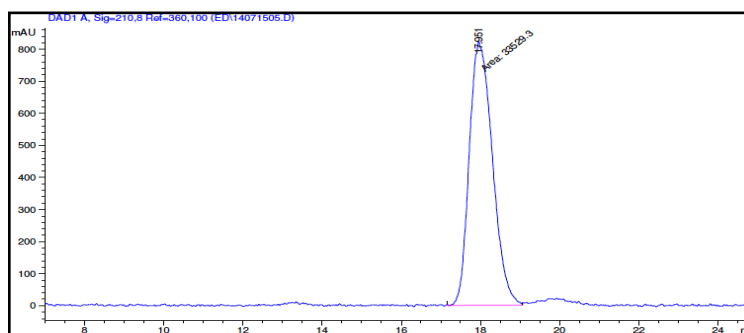


HPLC (Chiralcel IC): 50:50 *i*-PrOH/Hexanes, 0.5 mL/minute,
 $\lambda = 210$ nm, $T_{\text{major}} = 17.9$ min, $T_{\text{minor}} = 9.2$ min, ee =
 100%. No Other form was detected.



Peak #	RetTime [min]	Type	Width [min]	Area [mAU*s]	Height [mAU]	Area %
1	3.859	VV	0.0757	119.50421	21.87491	0.2211
2	4.094	VV	0.1696	525.76245	38.92090	0.9726
3	4.224	VV	0.1160	324.19495	35.02998	0.5997
4	4.722	VV	0.1381	1095.04370	113.95348	2.0257
5	4.921	VV	0.1111	339.92239	41.72220	0.6288
6	9.152	MM	0.3727	2.41256e4	1078.86792	44.6287
7	17.865	MM	0.6366	2.75285e4	720.66309	50.9235

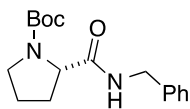
Totals : 5.40586e4 2051.03248



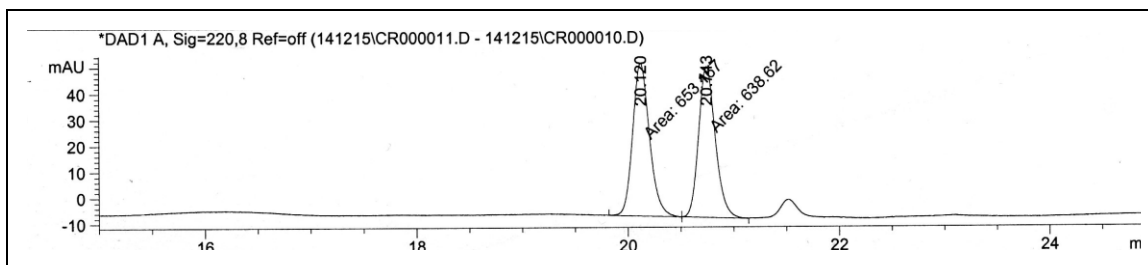
Peak #	RetTime [min]	Type	Width [min]	Area [mAU*s]	Height [mAU]	Area %
1	17.951	MM	0.6778	3.35293e4	824.52075	100.0000

Totals : 3.35293e4 824.52075

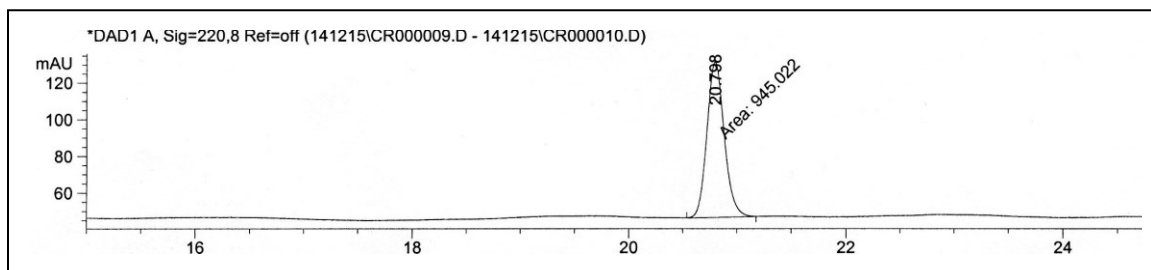
Racemic (top) and optically enriched (bottom) 3-36



HPLC (Chiralcel IB): 50:50 *i*-PrOH/Hexanes, 0.5 mL/minute, $\lambda = 210$ nm, $T_{\text{major}} = 20.8$ min, $T_{\text{minor}} = 20.1$ min, ee = 100%. No Other form was detected.

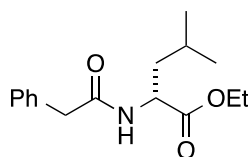


Peak #	RetTime [min]	Type	Width [min]	Area [mAU*s]	Height [mAU]	Area %
1	20.120	MF	0.1853	653.16650	58.76403	50.5630
2	20.743	FM	0.1832	638.61981	58.08435	49.4370
Totals :				1291.78632	116.84838	

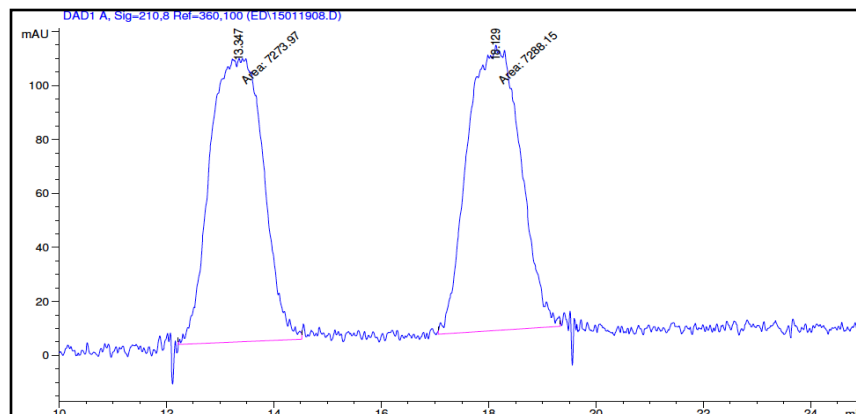


Peak #	RetTime [min]	Type	Width [min]	Area [mAU*s]	Height [mAU]	Area %
1	20.798	MM	0.1851	945.02228	85.07357	100.0000
Totals :				945.02228	85.07357	

Racemic (top) and optically enriched (bottom) 3-33

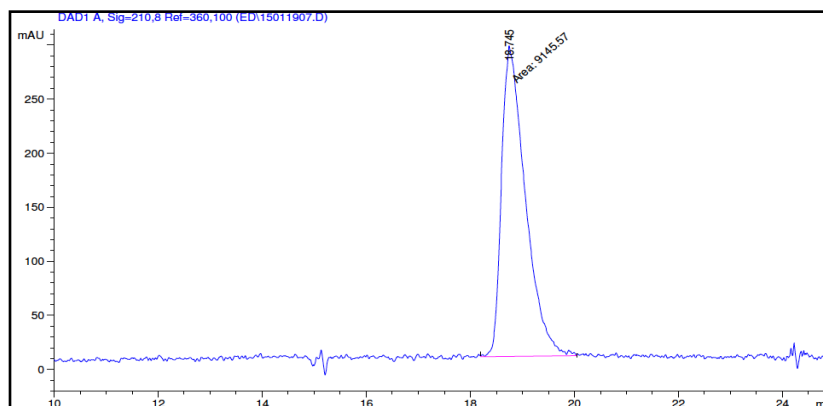


HPLC (Chiralcel OD): 5:95 *i*-PrOH/Hexanes, 0.5 mL/minute, λ = 210 nm, T_{major} = 18.4 min, T_{minor} = 13.3 min. ee = 100%. No Other form was detected.



Peak #	RetTime [min]	Type	Width [min]	Area [mAU*s]	Height [mAU]	Area %
1	13.347	MM	1.1523	7273.96826	105.20618	49.9513
2	18.129	MM	1.1463	7288.15430	105.96973	50.0487

Totals : 1.45621e4 211.17591



Signal 1: DAD1 A, Sig=210,8 Ref=360,100

Peak #	RetTime [min]	Type	Width [min]	Area [mAU*s]	Height [mAU]	Area %
1	18.745	MM	0.5325	9184.45215	287.44382	100.0000

Totals : 9184.45215 287.44382

